4-2020

Elucidation of the Mechanisms By Which Anesthetics Induce Blood-Brain Barrier Breakdown and Delirium in the Elderly

George A. Godsey II
Rowan University

ELUCIDATION OF THE MECHANISMS BY WHICH ANESTHETICS INDUCE BLOOD-BRAIN BARRIER BREAKDOWN AND DELIRIUM IN THE ELDERLY

George A. Godsey II, B.S.

A Dissertation submitted to the Graduate School of Biomedical Sciences, Rowan University in partial fulfillment of the requirements for the Ph.D. Degree.

Stratford, New Jersey 08084

April 2020

TABLE OF CONTENTS

ACKNOWLEDGEMENTS

Getting my doctorate has been quite an undertaking. I have been in school since I was around five (so basically my whole life up until now), and I cannot believe that that journey is finally over, and that I will finally be entering the workforce. The past seven years spent getting my doctorate have been both challenging and rewarding. I have learned a lot, and I am excited to finally get a job and apply what I have learned to that job.

First, I would particularly like to thank my mentor Dr. Nagele for allowing me to join his lab. Dr. Nagele's lab is the third lab I rotated in, and I really enjoyed both the research going on in the lab and the people working in the lab. Dr. Nagele pitched the idea of researching anesthesia and its effects on the brain to me, and I was very interested by the project, so much so that I asked to join the lab. Six and a half years later, I am happy to say that we made great progress in researching anesthesia, as readers will see as they read the rest of this dissertation. Dr. Nagele has always been so open and kind to me, and I have enjoyed that I can always walk into his office at any time with questions, to talk politics, or just to joke around. Well, as long as there is not a long line of other people already waiting to talk to him. We still need to buy Dr. Bob that deli ticket dispenser so we can all take a number and wait our turn…

Second, I would like to thank the Nagele lab family: Dr. Mary Kosciuk, Dr. Nimish Acharya, Dr. Cassandra DeMarshall, Dr. Abhirup Sarkar, Dr. Eric Goldwaser, Kimia Kheirkhah, and Hana Choi. You guys have always been here for me, and I would

never have been able to do this without all of you to lean upon. Being able to come to all of you with questions and concerns and know that one of you would have an answer for me was quite a relief. Working with all of you each day has made this a wonderful experience. We are a unique group: people of different ages and from different cultures, but we have come together and become a close family that works well together, and I have benefited from that greatly.

Third, I would like to thank the members of my thesis committee: Dr. Venkat Venkataraman, Dr. Kingsley Yin, Dr. Bernd Spur, and Dr. Forsberg. I greatly appreciate the advice and guidance that you gave me during my time here in the doctoral program.

Last but certainly not least, I would like to thank my family for supporting me during this long adventure. You have always stood by my side and encouraged me. You never doubted that one day I would finish this program and then go out and make something of myself. Well, that day is finally here! Thank you so much!

ABSTRACT

Delirium is a highly prevalent neuropsychiatric or neurocognitive disorder that presents a major problem to modern healthcare. Patients suffering from delirium normally have a worse prognosis, prolonged hospital stay, increased hospital cost, long-term cognitive impairment, and higher mortality rates. Many factors can predispose one to develop delirium, which makes treating this disorder a daunting task. Unfortunately, delirium is the most common psychiatric syndrome found in the hospital setting. In fact, a form of delirium known as postoperative delirium (POD) is one of the most common postoperative complications faced by elderly patients undergoing surgery.

POD is a major problem in modern healthcare, and it will only become worse because the world's older population (65+) is projected to triple between 2009 and 2050. This realization caused POD to emerge as an area of research interest. Many precipitating factors can cause one to develop POD, including exposure to anesthetics. Studies have indicated that many patients who were given general anesthesia have developed delirium; however, no studies have explained the mechanism by which anesthesia induces POD in patients. Unraveling this mechanism is the main goal of the research being presented here.

Our lab has hypothesized that POD is caused by a temporary, anesthesia- or drug-induced breakdown of the blood-brain barrier (BBB). The BBB, which is formed by the vascular endothelium in the brain, is a highly selective barrier that separates the

circulating blood from the brain and prevents a large number of substances from entering the brain. We believe that BBB breakdown after exposure to anesthetics allows an influx of plasma components into the brain tissue that disrupts brain homeostasis and causes neuronal misfiring. In the short-term, this culminates into the array of symptoms that hallmark POD. In the long-term, if not reversed or only partially reversed, this could trigger subsequent Postoperative Cognitive Decline (POCD) and Dementia.

A preliminary anesthesia study conducted in our lab revealed that exposure to the inhalation anesthetics (IAs) Sevoflurane and Isoflurane causes immediate structural changes in brain vascular endothelial cells (BVECs), including an overall flattening of surface membranes and loss of the tight junction ridge. These structural changes can lead to the formation of holes in the vascular endothelial lining. This study also revealed that exposure to Sevoflurane leads to an increase in BBB permeability.

A subsequent study revealed that Sevoflurane increases BBB permeability in pre-adolescent and elderly rats, age-dependent changes occur in the luminal surface topography of brain vascular endothelial cells associated with development and maintenance of the BBB, and Sevoflurane and Isoflurane induce changes in BVEC luminal surface topography that may be linked to increased BBB permeability.

In vitro experiments using a human brain endothelial cell line (hCMEC/D3) that can form a BBB-like barrier yielded the following results: (1) hCMEC/D3 cells express

tight junction proteins, (2) transendothelial electrical resistance (TEER) decreases and barrier permeability increases after hCMEC/D3 cells are exposed to anesthesia, (3) the distribution and expression of the tight junction protein ZO-1 in hCMEC/D3 cells is not effected by exposure to anesthesia, (4) addition of DMSO or floating cells to the cell culture medium does not aid the transfer of anesthetics from the air to the cell monolayer, and (5) Histamine and Acetaminophen induce contraction in hCMEC/D3 cells, which can compromise barrier functional integrity.

Finally, studies on the effects of the specialized pro-resolving lipid mediator (SPM) Lipoxin in resolving BBB insults revealed the following: (1) bacterial lipopolysaccharide (LPS) injections led to an increase in BBB permeability, as evidenced by detecting IgG, a serum component normally restricted to blood vessels, in rat brain tissue. (2) Lipoxin reduces LPS-induced BBB permeability, as evidenced by decreased levels of IgG in rat brain tissue. (3) LPS induces a number of luminal surface changes in rat BVECs, as shown by scanning electron microscopy. (4) Lipoxin helps restore key luminal surface features of rat BVECs to near normal, and most importantly, blocks the death of BVECs and the associated loss of barrier integrity.

CHAPTER I:

Introduction

Delirium

Delirium is a highly prevalent neuropsychiatric or neurocognitive disorder. In general, delirium refers to a cerebral dysfunction that causes a major disturbance in a person's mental abilities and leaves them in a severe state of mental confusion. Delirium is characterized by disturbances of consciousness, attention, cognition, perception, emotion, motor behavior, and the sleep-wake cycle. These symptoms tend to fluctuate throughout the day, and patients will often experience long periods of lucidity [1]. Patients suffering from delirium experience greater cognitive deterioration following hospitalization than non-delirious patients [2]. In fact, patients with delirium are believed to be predisposed to subsequently acquiring a long-term dementia-like disability [3]. Therefore, people suffering from delirium must get diagnosed and treated quickly in order to prevent this increased trajectory of cognitive decline and dementia.

There is no laboratory test for the detection of delirium; therefore, delirium can only be diagnosed clinically. Doctors often consult the *Diagnostic and Statistical Manual of Mental Disorders, 5th edition* (DSM–5), when diagnosing delirium. The DSM-5 is a widely accepted handbook used by clinicians and researchers in the United States and much of the world as a guide for the classification and diagnosis of mental

disorders [4]. The DSM-5 outlines five diagnostic criteria for delirium:

1) A disturbance in attention (i.e., reduced ability to direct, focus, sustain, and shift attention) and awareness (reduced orientation to the environment).
2) The disturbance develops over a short period of time (usually hours to a few days) and tends to fluctuate in severity during the course of the day.
3) A disturbance in cognition (e.g., memory deficit, disorientation, language, visuospatial ability, or perception).
4) These disturbances are not better explained by another preexisting, established, or evolving neurocognitive disorder.
5) Evidence from the history, physical examination, or laboratory findings that the disturbance is caused by another medical condition, an intoxicating substance or medication use, exposure to a toxin, or is due to multiple etiologies [4].

Delirium is the most common psychiatric syndrome found in the hospital setting [1]. Studies have shown that delirium develops in 10-15% of general hospitalized surgical patients, in 25-45% of hospitalized cancer patients, and in 80-90% of terminally ill intensive care unit (ICU) patients [5]. Unfortunately, delirium is frequently misdiagnosed [1]; it is estimated that doctors misdiagnose delirium in 80% of cases [6]. This is a major problem, as patients suffering from delirium normally have a worse prognosis, prolonged hospital stay, increased hospital costs, long-term cognitive impairment, increased risk of Alzheimer's disease, and higher mortality rates [7].

Risk Factors for Delirium

Many risk factors have been identified that predispose one to develop delirium, including age, prior cognitive impairment, comorbid illnesses, head trauma, infection, sensory impairment (particularly vision), malnutrition, exposure to certain medications, and a history of alcohol and other substance abuse [1]. The integrity of the blood-brain barrier (BBB) has also been identified as a predisposing factor of delirium [1, 8]. Studies have also shown that people suffering from delirium experience changes in their neurotransmitter levels, specifically acetylcholine and dopamine [1]. All of these risk factors or causes of delirium have led researchers to conclude that delirium is really a disorder with many potential causes that all result in a similar display of symptoms [1, 6].

Testing for Delirium

Since delirium is a common occurrence in the surgical setting, several screening tests have been designed to screen for patients that are at high risk for developing delirium. These screening tests include the Delirium Observation Screening Scale (DOSS), the NEECHAM Confusion Scale, and the Nursing Delirium Screening Scale (Nu-DESC) [9]. The results of the screening tests are used to determine if a diagnostic test should be performed. Over the years, various diagnostic tests based on DSM criteria have been developed; these diagnostic tests provide a definitive diagnosis of Ddelirium. Diagnostic tests include the Confusion Assessment Method (CAM), the Confusion Assessment Method for the Intensive Care Unit (CAM-ICU), the Delirium Rating Scale-revised version (DRS-R-98), the Delirium Symptom Interview (DSI), the

Intensive Care Delirium Screening Checklist (ICDSC), and the Memorial Delirium Assessment Scale (MDAS) [9-11]. Once a patient is diagnosed with delirium, the severity of the patient's delirium can be assessed using tests such as the Delirium Detection Score (DDS), the DRS-R-98, and the MDAS [9].

Managing and Treating Delirium

Much effort has been put into the management and/or treatment of delirium. The many different causes of delirium make treating this disorder a daunting task. The first step is to find and treat the underlying cause of the delirium. After discovering that a patient is delirious, stopping or reducing the dosage of any delirifacient (delirium-inducing) medications is the first thing that doctors do [1]. Then, proper medication may be given to the patient to reverse the effects of the delirifacient medications. Antipsychotics (such as Haloperidol) seem to be the most effective way to control the symptoms of delirium, particularly Postoperative Delirium [1, 12]. Dopamine is a neurotransmitter that is elevated in certain instances of delirium. Doctors decided to treat these patients with Haloperidol, as Haloperidol is a dopamine receptor antagonist that binds with high affinity to the dopamine receptors in place of dopamine itself. This prevents dopamine from inducing delirium in these patients. Recent studies also show that preoperative use of statins reduces the incidence of Postoperative Delirium. Statins are cholesterol-lowering drugs that also have anti-inflammatory and endothelial function-enhancing effects. The beneficial effects of statins support the possibility that inflammation may be involved in Postoperative Delirium. [13-15].

Postoperative Delirium

Postoperative Delirium (POD) is a very prevalent form of delirium. In fact, POD is one of the most common postoperative complications faced by elderly patients undergoing surgery [6, 16]. POD has become a serious problem in modern healthcare, and the problem will only become worse, as people that are 65 years of age and older comprise the most rapidly growing segment of the U.S. population [6]. In fact, it is projected that the world's older population (65+) will triple between 2009 and 2050, going from 516 million to 1.53 billion [6, 17]. This realization caused POD to emerge as an area of research interest, since it is the elderly who commonly suffer from POD. Patients suffering from POD face a prolonged hospital stay, increased hospital costs, and higher morbidity and mortality rates [6]. The total cost of caring for a hospitalized patient suffering from Delirium ranges anywhere from $15,000 to $65,000 per visit; it is estimated that the U.S. healthcare system spends between $143 billion to $152 billion annually caring for patients with delirium [6, 18].

Risk Factors and Mechanism for POD

There are many precipitating factors that can cause one to develop POD, including exposure to certain drugs and anesthetics [1, 6]. While studies have indicated that many patients who were given general anesthesia have developed delirium, no studies have explained the mechanism by which anesthesia induces POD in patients. Unraveling this mechanism is the main goal of the research being presented here. Our lab has hypothesized that POD is caused by a temporary, anesthesia or drug-induced breakdown of the BBB. Before we look further into this link between delirium and

the BBB, let us first discuss the BBB.

Introduction to the Blood-Brain Barrier (BBB)

The Blood-Brain Barrier (BBB) is a dynamic structure formed by the vascular endothelium in the brain (**Fig. 1; Fig. 2**). It is a highly selective barrier that separates the circulating blood from the brain parenchyma and prevents a large number of substances (like IgG) from entering the brain parenchyma. Therefore, the BBB plays a key role in maintaining brain homeostasis and the normal functioning of neurons in the CNS. The two major functions of the BBB are the protection of the brain from harmful substances and the regulation of nutrient uptake and waste efflux between the brain and the circulating blood.

Cellular Composition of the Blood-Brain Barrier

The main cellular components of the BBB are endothelial cells, astrocytes, and pericytes (**Fig. 1; Fig. 3**). Brain vascular endothelial cells (BVECs) are the major structural component of the BBB. Endothelial cells can be found on the inner surface of all blood vessels in the body. This thin layer of endothelial cells lining the blood vessels is also referred to as the endothelium [8]. The brain endothelium differs from the peripheral endothelium in several unique ways: first, whereas peripheral endothelial cells are highly fenestrated in order to allow the rapid exchange of molecules between the blood vessels and the surrounding tissue, brain endothelial cells lack fenestrations [8, 19]. Second, brain endothelial cells have lower rates of transcytosis than peripheral endothelial cells (**Fig. 4**). The peripheral endothelium

uses vesicular transport to deliver nutrients to peripheral tissues, whereas the brain endothelium expresses transporters to selectively transport nutrients across the BBB [20, 21]. Third, the junctional complexes between adjacent brain endothelial cells are much stronger and more restrictive than those found in the peripheral endothelium ([8, 19]. Fourth, the brain endothelium contains a number of membrane transport channels and proteins that are not found in the peripheral endothelium. Finally, the brain endothelium contains a large quantity of mitochondria, which suggests that the brain endothelium requires a large amount of energy in order to function [8]. These differences between the brain and peripheral endothelium allow the brain endothelium to form the highly selective BBB [8]. The presence of the other aforementioned cells of the BBB, particularly astrocytes, stimulates and maintains the BBB characteristics of BVECs [8].

Astrocytes are the most abundant glial cells in the CNS. Perivascular astrocytic endfeet cover the majority (>99%) of the abluminal/basolateral surface of BVECs. While astrocytes are not a major component of the physical BBB, they do play an essential role in BBB formation and maintenance by secreting a plethora of factors and active molecules which, among other things, influence the brain endothelium to develop BBB characteristics [22, 23]. In particular, astrocytes induce the BVEC expression of certain tight junction proteins, enzyme systems, and transporters [24, 25].

Pericytes are vascular contractile cells found on the abluminal side of the BVEC capillary wall and luminal to the astrocytic endfeet [19, 26]. Pericytes are embedded in the endothelial basement membrane [26]. They produce long cytoplasmic processes which encircle around 20-30% of the BVECs forming the capillaries [19, 25]. Pericyte recruitment to the capillary wall is essential for the formation, maturation, and maintenance of normal vascular structure and function [25]. Pericytes secrete factors and signals which are needed for BVEC differentiation; furthermore, the contractile properties of pericytes are vital for capillary blood flow regulation in response to neural activity and vasoactive agents [19, 27]. The loss of pericyte coverage of the capillaries causes abnormal vasculogenesis, endothelial hyperplasia, and ultimately increased BBB permeability [22, 26].

Functions of the Blood-Brain Barrier

The BBB serves dual barrier and carrier functions [22]. First, it serves as a highly selective barrier that protects the brain from toxins, infectious agents, and buffer variations in blood composition [28]. This barrier function is due to the extensive junctional complexes that exist between adjacent endothelial cells. The junctional complexes force most substances to take a transcellular route across the BBB instead of travelling paracellularly between the endothelial cells, which occurs in the peripheral endothelia [29]. Under normal circumstances, the BBB also regulates the entry of red blood cells and immune cells into the brain parenchyma [19].

While protecting the brain from harmful blood-borne substances, the BBB must also regulate nutrient and hormone uptake and waste efflux between the brain and circulating blood [26]. Many lipid-soluble compounds as well as small gaseous compounds like O_2 and CO_2 can passively diffuse across the BBB [22]. On the other hand, water-soluble compounds are unable to passively diffuse across the BBB, and the BBB-associated tight junctions prevent the paracellular passage of water-soluble compounds across the BBB [20, 22]. Many nutrients such as amino acids, glucose, and salts are small water-soluble compounds; therefore, the BBB contains a variety of transport proteins and channels to facilitate the transport of these essential nutrients across the blood brain barrier and into the brain [8, 20, 22]. Also, these transport systems can export dangerous or harmful compounds from the brain into the blood [19]. The BBB prevents most large water-soluble compounds such as peptides and proteins from entering the brain parenchyma unless they can be transferred by transcytosis [20]. However, as mentioned above, the brain endothelium has a much lower rate of transcytosis than the peripheral endothelium [20, 21]. Lastly, the BBB is an effective enzymatic or metabolic barrier due to BVEC expression of an extensive set of intracellular and extracellular enzymes that are capable of degrading drugs and various other chemical compounds [8, 20, 22]. It is for this reason that many drugs are unable to reach the CNS in therapeutically relevant concentrations [8, 20, 22]. **Figure 5** sums up various pathways across the BBB.

Blood-Brain Barrier Interendothelial Junctional Complexes

Together, tight junctions (TJs) and adherens junctions (AJs) compose the junctional

complex found between adjacent endothelial cells [30]. Endothelial TJs and AJs intercalate along the entire length of the junctional area, which effectively prevents paracellular passage across the BBB [30]. The tight junctions regulate the passage of ions and small molecules between cells and establish cell polarity, while the adherens junctions primarily control cell-cell adhesion [31]. **Figure 6** shows both electron micrographs and a schematic drawing of the BBB tight junctions between two endothelial cells. **Figure 7** is a schematic drawing of the junctional complexes of the BBB.

BBB Tight Junctions

Tight junctions (also known as *Zonula Occludens*) are a network of intramembranous protein strands that are responsible for sealing the intercellular cleft found between adjacent BVECs (**Fig. 6; Fig. 7**) [32, 33]. The extracellular regions of transmembrane TJ proteins form the TJ protein strands; the TJ protein strands on adjacent BVECs are able to associate and bind to one another, sealing the intercellular cleft and giving the BBB its barrier properties [32-34]. BBB TJs are composed of a combination of transmembrane and cytoplasmic proteins that are linked to the actin cytoskeleton [30, 35].

The three main transmembrane TJ proteins are the Claudins, Occludin, and Junctional Adhesion Molecule (JAM). The Claudins are a family of tetraspan transmembrane proteins whose N-terminus and C-terminus are both located in the cytoplasm. There are twenty-four members of the Claudin family; they have molecular weights ranging

from 20-27kDa. Claudin-5, which is the most abundant Claudin in BVECs, is a critical component of the BBB [30, 33, 35, 36]. Claudin-5 strands on adjacent BVECs bind to one another and prevent molecules smaller than 800 Da from crossing the BBB [33, 35]. Claudin-1, Claudin-3, and Claudin-12 have also been detected in BVECs [33]. Occludin is a 60-65kDa tetraspan transmembrane protein whose N-terminus and C-terminus are both located in the cytoplasm [30, 35]. Occludin expression helps to seal the TJs and is associated with increased electrical resistance and decreased paracellular movement across the BBB [30, 32, 35]. It has been shown that the phosphorylation of Occludin regulates TJ permeability [32]. BVECs need Occludin in order to transduce the signals of cytokines such as TNFα, IFNγ, and VEGF [37]. Occludin and Claudin-5 are the most important components of BBB TJs [35]. JAM is a 40kDa single-span transmembrane protein that is a member of the immunoglobulin superfamily [30]. JAM is involved in cell-cell adhesion through homophilic and heterophilic interactions in the TJs [32]. Furthermore, JAM contributes to both permeability control and leukocyte extravasation, and its expression leads to increased electrical resistance [30, 32, 37].

TJs are also comprised of cytoplasmic TJ proteins such as the Zonula Occludens (ZO) proteins and Cingulin. These cytoplasmic TJ proteins bind to both transmembrane TJ proteins (Claudin-5 and Occludin) and the actin cytoskeleton, linking them together and forming a large protein complex known as the cytoplasmic plaque [32]. Thus, tight junctions join together the cytoskeletons of adjacent cells. Furthermore, the ZO proteins also bind the adherens junction proteins, meaning the adherens junctions and

tight junctions are physically linked [31]. Refer back to **Figure 7** for a schematic drawing of the TJ proteins and their interactions with one another.

BBB Adherens Junctions

Adherens Junctions (also known as *Zonula Adherens*) are necessary for the primary contact between adjacent endothelial cells. The two main transmembrane AJ proteins are the Cadherins and the Nectins [38]. The extracellular regions of these two proteins mediate the adhesion of adjacent endothelial cells, while the intracellular regions of these proteins interact with a number of proteins [31]. Refer back to **Figure 7** for a schematic drawing of the Adherens Junction proteins and their interactions with one another.

Cadherins are single-pass transmembrane proteins with their N-terminus located in the extracellular domain and the C-terminus located in the cytoplasm [38, 39]. The N-terminus of one cadherin binds to the N-terminus of the same cadherin on an adjacent cell in a form of adhesion known as homophilic adhesion (**Fig. 8**) [39]. The Cadherin C-terminus associates with a family of cytoplasmic proteins known as the Catenin family, which includes β-catenin, p120-catenin, and γ-catenin (also named plakoglobin) [39, 40]. β-catenin binds to α-catenin, which also binds to the actin cytoskeleton. Therefore, Adherens Junctions are also linked to the actin cytoskeleton[39]. While there are many members of the Cadherin family, two are of special importance to brain endothelial cells. These are Vascular Endothelial Cadherin (VE-Cadherin) and Neuronal Cadherin (N-Cadherin) [41].

Nectins are also single-pass transmembrane proteins with their N-terminus located in the extracellular domain and the C-terminus located in the cytoplasm [38, 42]. The N-terminus of one Nectin binds to the N-terminus of another Nectin on an adjacent cell. There are four members of the Nectin family: Nectin-1, Nectin-2, Nectin-3, and Nectin-4. If the same Nectins bind to one another, it is known as homophilic adhesion, while if different Nectins bind together, it is known as heterophilic adhesion (**Fig. 8**) [42]. The Nectin C-terminus associates with the scaffold protein Afadin (also known as AF6), which is an actin binding protein that anchors the Nectins to the actin cytoskeleton [31, 42, 43].

The Blood-Brain Barrier and Delirium

In a large number of neurological disorders, including cerebral ischemia, brain trauma, tumors, and neurodegenerative disorders, the BBB is disrupted, which leads to an increase in BBB permeability [22]. Researchers have speculated that BBB disruption is also associated with the presence of delirium in postoperative patients, which is better known as POD. In particular, it has been speculated that inflammation of the BBB may be a mechanism of POD, as inflammatory conditions such as sepsis and wound infection are major causes of delirium [44]. Other research has speculated that anesthesia and surgery are responsible for BBB disruption and consequent delirium [45, 46]. Our lab has hypothesized that POD is caused by a temporary, anesthesia- or drug-induced breakdown of the BBB. We believe that BBB breakdown after exposure to anesthetics allows an influx of plasma components such as soluble

amyloid-β (Aβ) peptides, complement components, serum albumin, and immunoglobulins (Igs) into the brain tissue. This influx of plasma components disrupts brain homeostasis and causes neuronal misfiring as plasma proteins like IgG that were once in the blood now enter the brain parenchyma and bind to neurons. This all culminates into the array of symptoms that hallmark delirium, and if left untreated, could serve as a trigger for subsequent postoperative cognitive decline (POCD) and even dementia (**Fig. 9**) [45].

FIGURES

Figure 1: The Blood-Brain Barrier

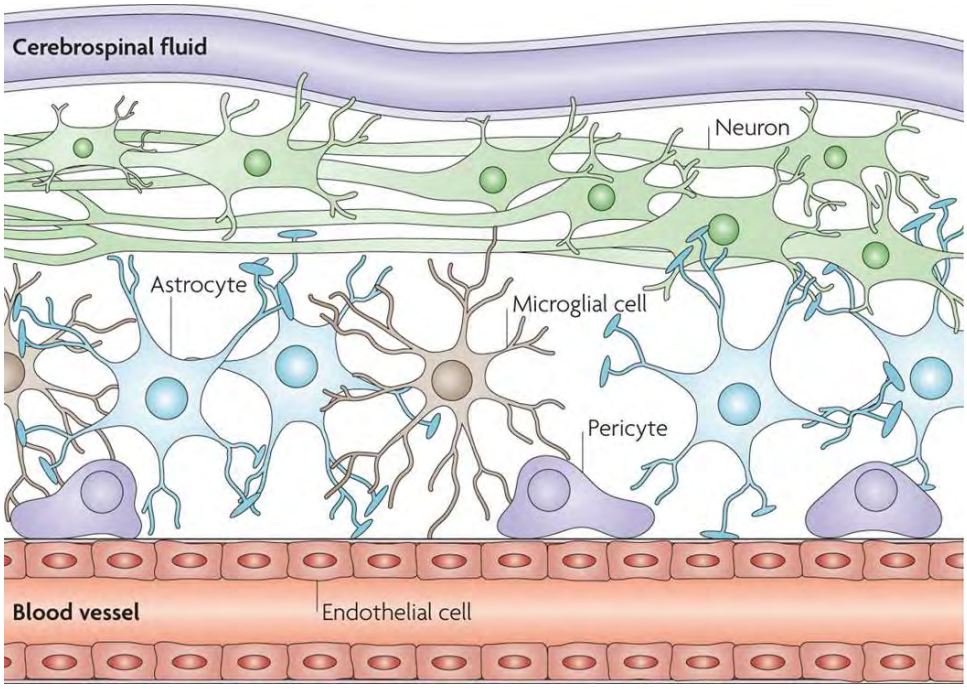

The blood-brain barrier is formed by brain vascular endothelial cells, in conjunction with surrounding astrocytes and pericytes. It maintains the neural microenvironment by regulating the passage of molecules into and out of the brain, and it protects the brain from any microorganisms and toxins that are circulating in the blood. This was taken from [47].

Figure 2: Visualizing the Blood-Brain Barrier (BBB) using Scanning Electron Microscopy (SEM)

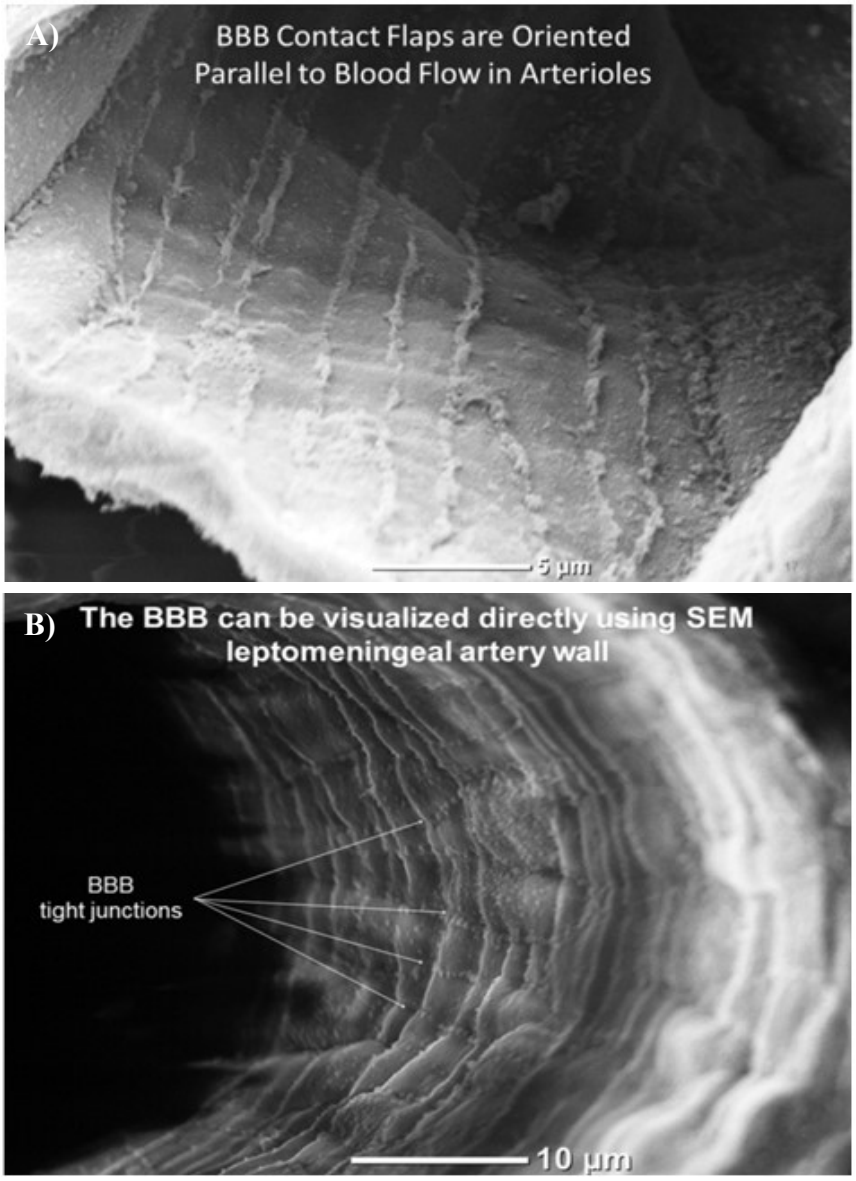

A) View looking down the barrel of an arteriole showing BBB-associated junctional ridges oriented parallel to the long axis of the vessel in the direction of blood flow. **B**) SEM image showing a leptomeningeal artery in a rat with an inner lining of brain vascular endothelial cells (BVECs) (arrows point to the BBB; it looks like a row of dots). The site of the tight junctions associated with the BBB is evident as a linear ridge of globular surface projections present at the cell perimeter.

Figure 3: Cellular Constituents of the Blood-Brain Barrier

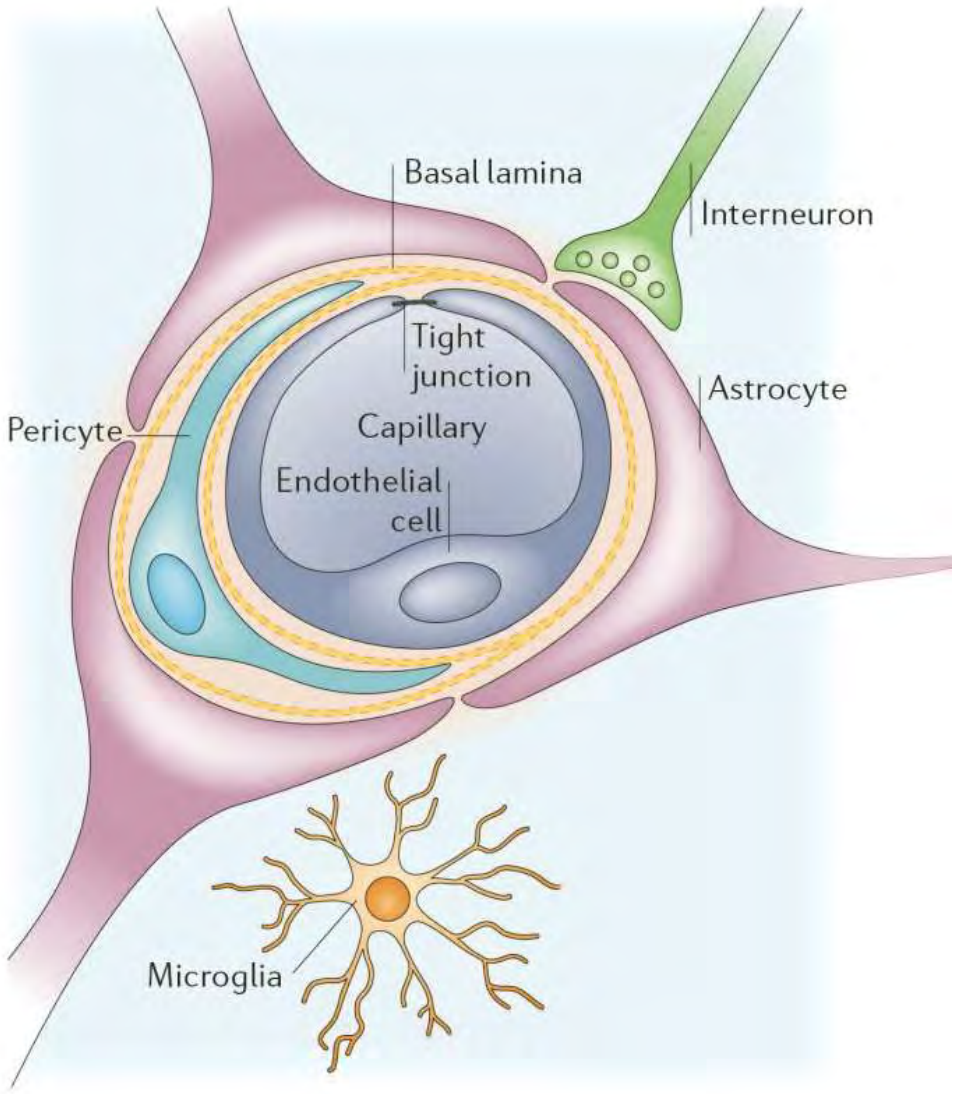

The Blood-Brain Barrier is formed by brain vascular endothelial cells, surrounded by basal lamina and astrocytic perivascular endfeet, pericytes, and microglia. This was taken from [29] and [48].

Figure 4: Diagram Illustrating Two Unique BBB Properties of CNS Endothelial Cells

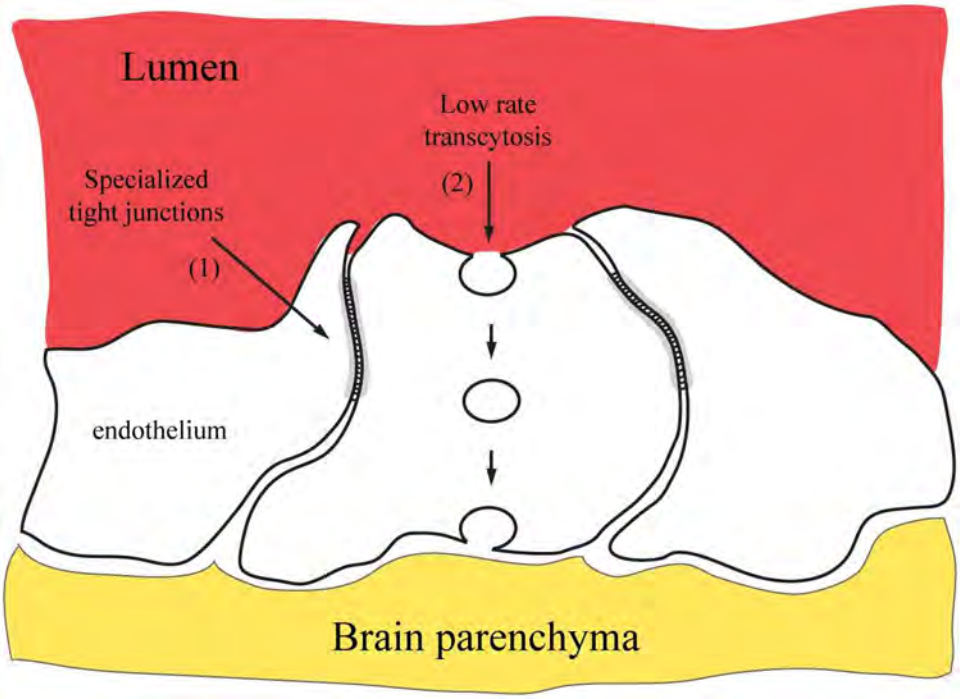

Compared to the endothelial cells from the rest of the body, CNS endothelial cells that possess a BBB are characterized by highly specialized tight junctions sealing the space between adjacent cells (1), and an unusually low rate of transcytosis from the vessel lumen to the brain parenchyma (2). This was taken from [21].

Figure 5: Pathways across the Blood-Brain Barrier

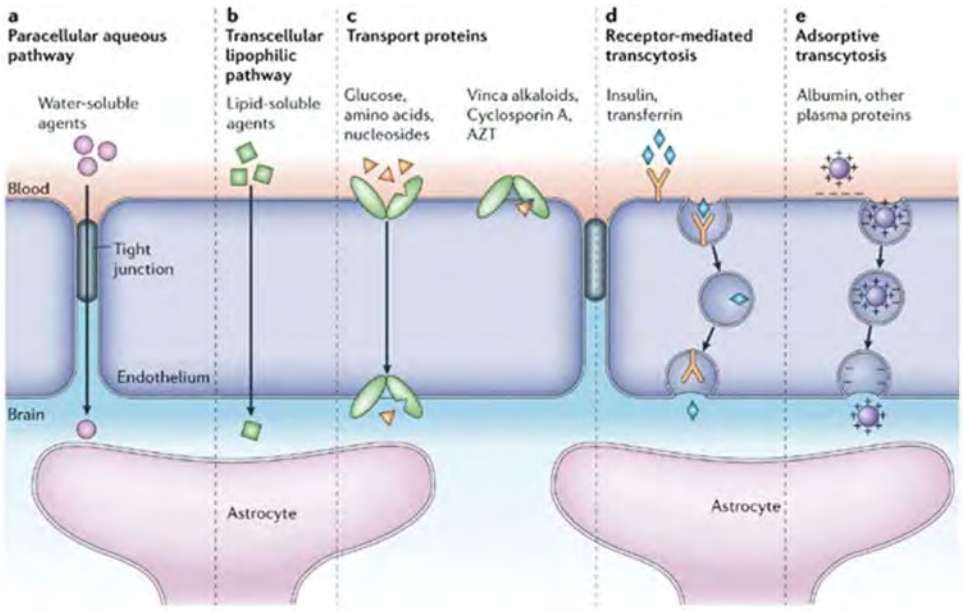

A schematic diagram of the endothelial cells that form the blood-brain barrier (BBB) and their associations with the perivascular endfeet of astrocytes. The main routes for molecular traffic across the BBB are shown. **A)** Normally, the tight junctions severely restrict penetration of water-soluble compounds, including polar drugs. **B)** However, the large surface area of the lipid membranes of the endothelium offers an effective diffusive route for lipid-soluble agents. **C)** The endothelium contains transport proteins (carriers) for glucose, amino acids, purine bases, nucleosides, choline, and other substances. Some transporters are energy-dependent (for example, P-glycoprotein) and act as efflux transporters. **D)** Certain proteins, such as insulin and transferrin, are taken up by specific receptor-mediated endocytosis and transcytosis. **E)** Native plasma proteins such as albumin are poorly transported, but cationization can increase their uptake by adsorptive-mediated endocytosis and transcytosis. Drug delivery across the brain endothelium depends on making use of pathways **B-E**; most CNS drugs enter via route **B**. AZT - azidothymidine. This was taken from [29].

Figure 6: The Anatomical Structure of the Blood-Brain Barrier

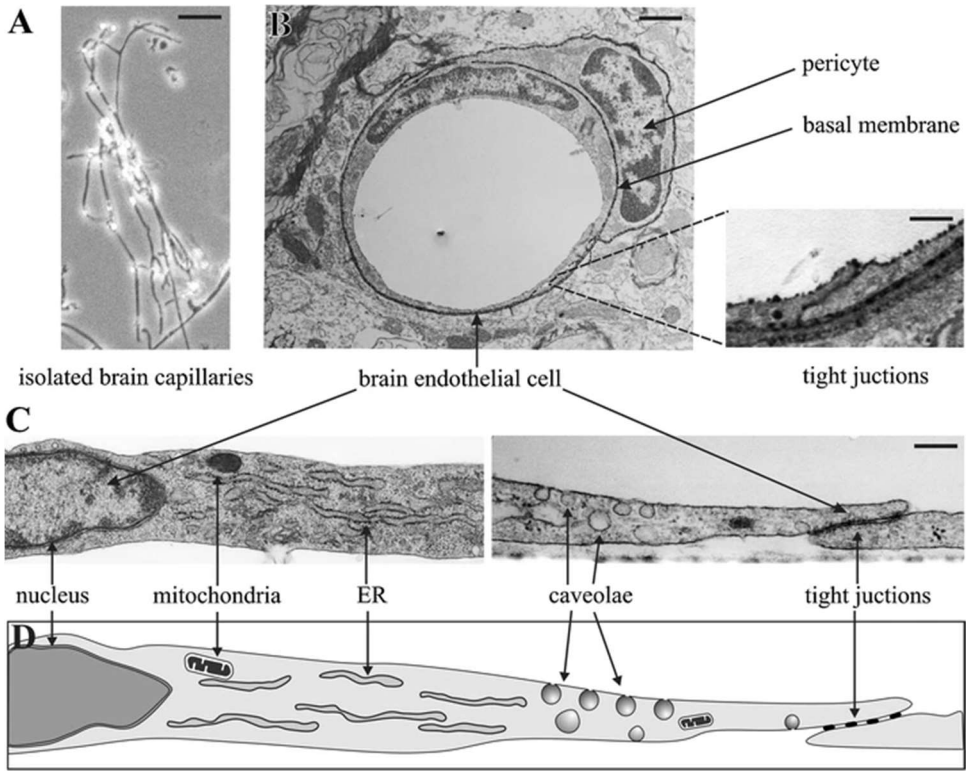

A) Isolated rat brain capillaries viewed by phase contrast microscopy. **B)** A rat brain capillary cross-section viewed by transmission electron microscopy. **C)** Ultrastructure of primary rat brain endothelial cells in culture by electron microscopy. **D)** A schematic drawing of the morphological details. ER - endoplasmic reticulum. Scale bars: **A)** 20µm, **B)** 1µm, insert 500nm, **C)** 500nm. This was taken from [19].

Figure 7: Schematic Representation of the Junctional Complexes of the BBB

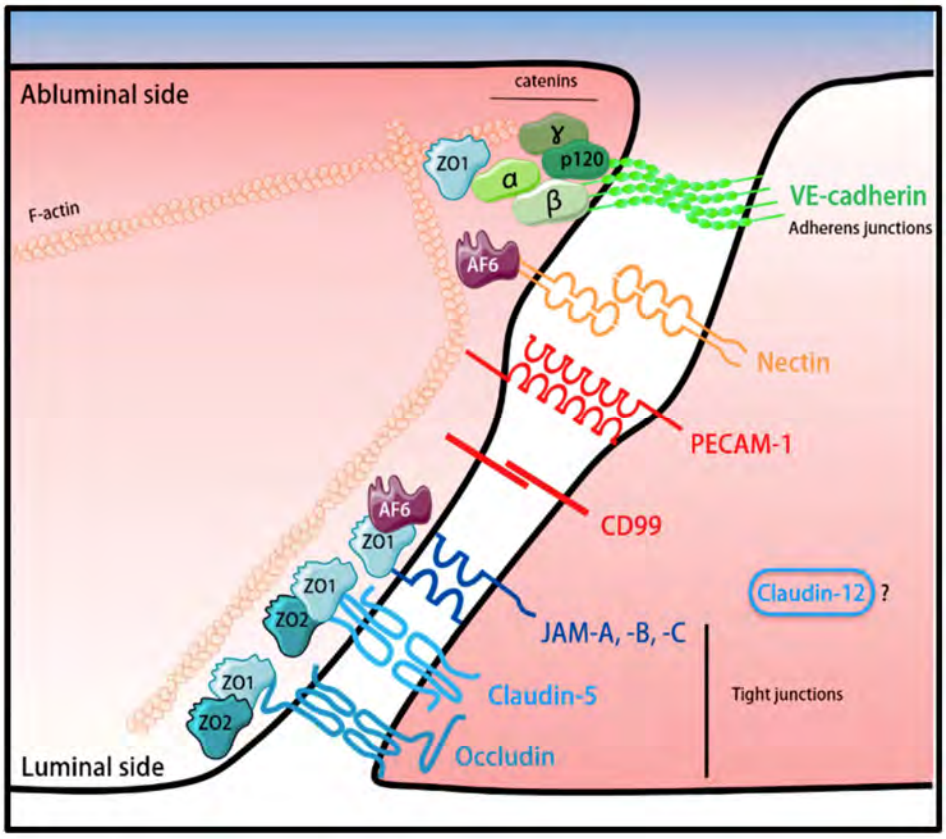

The proteins that compose the tight and adherens junctions are connected to the cytoskeleton via intracellular scaffolding proteins, ZO-1, ZO-2, and AF-6. Despite being expressed at low levels by the BBB endothelial cells, the subcellular location and function of claudin-12 remains to be defined. This was taken from [43].

Figure 8: Types of Cell-Cell Adhesion and Interactions between Cell Adhesion Molecules

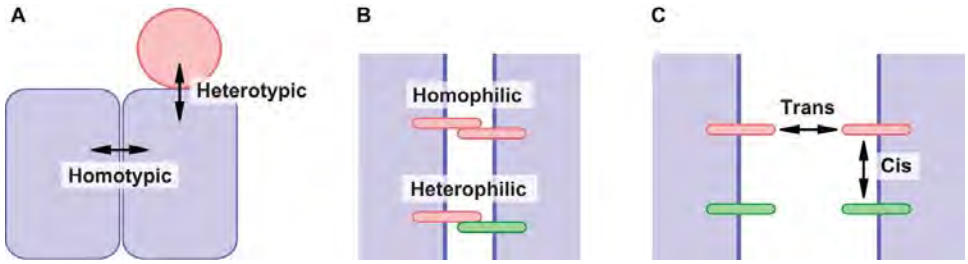

(**A**) Cell adhesion can occur homotypically (i.e. between the same cell types) or heterotypically (i.e. between two different cell types). (**B**) Along similar lines, cell adhesion molecules can interact with each other in a number of different ways. They can interact homophilically (i.e. forming interactions between molecules of the same type) or heterophilically (i.e. forming interactions between two different molecules). (**C**) Additionally, cell adhesion molecules can form interactions in cis (i.e. cell adhesion molecules on the surface of one cell interact) or in trans (i.e. cell adhesion molecules on the surface of one cell interact with adhesion molecules on the surface of an opposing cell). This was taken from [42].

Figure 9: Proposed Mechanism of Anesthetic-Induced Blood-Brain Barrier Breakdown and Its Mechanistic Relationship to Postoperative Delirium, Postoperative Cognitive Decline, and Dementia

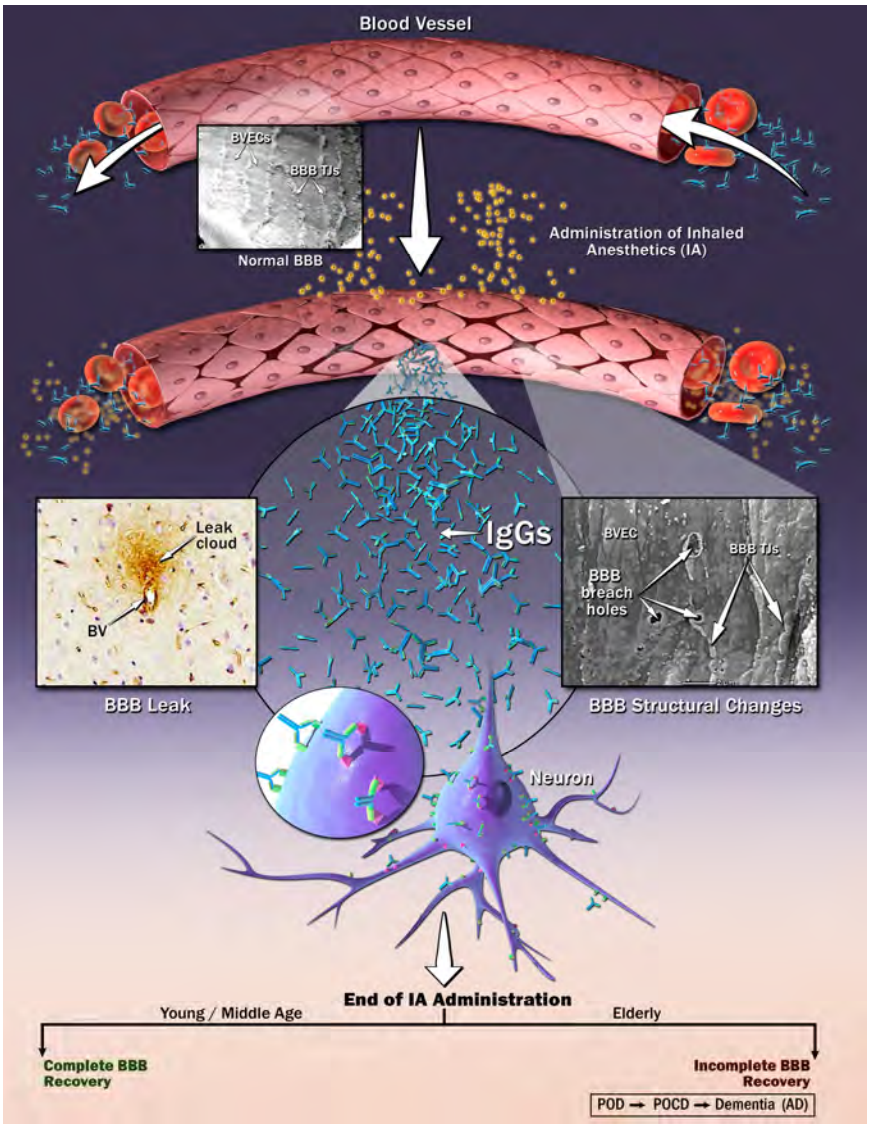

We propose that the combination of anesthesia-induced BBB breakdown and entry of plasma components (like IgG) into the brain tissue followed by selective binding of plasma components to pyramidal neurons act together to contribute to the disruption of normal neuronal activity and collectively elicit the symptoms that define POD. Failure to restore BBB function and resolve POD could lead to the development of POCD and even Dementia in the long term. This was taken from [45].

CHAPTER II:
Rationale

Delirium

As stated previously, Delirium is a highly prevalent neuropsychiatric or neurocognitive disorder. In general, Delirium refers to a cerebral dysfunction that causes a major disturbance in a person's mental abilities and leaves them in a severe state of mental confusion. Delirium is characterized by disturbances of consciousness, attention, cognition, perception, emotion, motor behavior, and the sleep-wake cycle. These symptoms tend to fluctuate throughout the day, and patients will often experience long periods of lucidity [1]. Patients suffering from delirium experience greater cognitive deterioration following hospitalization than non-delirious patients [2]. In fact, patients with delirium are believed to be predisposed to subsequently acquiring a long-term dementia-like disability [3]. Therefore, people suffering from delirium must get diagnosed and treated quickly in order to prevent this increased trajectory of cognitive decline and dementia.

Delirium is the most common psychiatric syndrome found in the hospital setting [1]. Studies have shown that delirium develops in 10-15% of general hospitalized surgical patients, in 25-45% of hospitalized cancer patients, and in 80-90% of terminally ill intensive care unit (ICU) patients [5]. Unfortunately, delirium is frequently misdiagnosed [1]; it is estimated that doctors misdiagnose delirium in 80% of cases [6]. This is a major problem, as patients suffering from delirium normally have a

worse prognosis, prolonged hospital stay, increased hospital costs, long-term cognitive impairment, increased risk of Alzheimer's disease, and higher mortality rates [7].

Postoperative Delirium

Postoperative Delirium (POD) is a very prevalent form of delirium. In fact, POD is one of the most common postoperative complications faced by elderly patients undergoing surgery [6, 16]. POD has become a serious problem in modern healthcare, and the problem will only become worse, as people that are 65 years of age and older comprise the most rapidly growing segment of the U.S. population [6]. In fact, it is projected that the world's older population (65+) will triple between 2009 and 2050, going from 516 million to 1.53 billion [6, 17]. This realization caused POD to emerge as an area of research interest, since it is the elderly who commonly suffer from POD. Patients suffering from POD face a prolonged hospital stay, increased hospital costs, and higher morbidity and mortality rates [6]. The total cost of caring for a hospitalized patient suffering from Delirium ranges anywhere from $15,000 to $65,000 per visit; it is estimated that the U.S. healthcare system spends between $143 billion to $152 billion annually caring for patients with delirium [6, 18].

Risk Factors and Mechanism for POD

There are many precipitating factors that can cause one to develop POD, including exposure to certain drugs and anesthetics [1, 6]. While studies have indicated that many patients who were given general anesthesia developed delirium, no studies have

explained the mechanism by which anesthesia induces POD in patients. Unraveling this mechanism is the main goal of the research presented here. Our lab has hypothesized that POD is caused by a temporary, anesthesia or drug-induced breakdown of the BBB, and that this event can serve as a trigger for subsequent postoperative cognitive decline (POCD) and even Dementia.

Rationale for Researching Delirium and POD

The prevalence of delirium and POD in the elderly population and the toll that they take in the hospital setting and afterwards have made both areas of intense research interest. There are many reasons to research delirium and POD, including: (1) they are prevalent in a portion of the population that is set to triple in number over the next several decades, (2) people suffering from delirium and POD have increased morbidity and mortality rates, (3) people suffering from delirium and POD are prone to suffer worse cognitive decline and even dementia, and (4) there are huge medical care costs associated with delirium. Hopefully, the research presented here will provide the delirium and POD fields with data that helps in the diagnosis and treatment of delirium and POD and lessens the burden created by these disorders.

CHAPTER III:

Sevoflurane and Isoflurane Induce Structural Changes in Brain Vascular Endothelial Cells and Increase Blood-Brain Barrier Permeability: Possible Link to Postoperative Delirium and Cognitive Decline

ABSTRACT

A large percentage of patients subjected to general anesthesia at 65 years and older exhibit postoperative delirium (POD). Here, we test the hypothesis that inhaled anesthetics (IAs), such as Sevoflurane and Isoflurane, act directly on brain vascular endothelial cells (BVECs) to increase blood-brain barrier (BBB) permeability, thereby contributing to POD. Rats of young (3-5 months), middle (10-12 months), and old (17-19 months) ages were anesthetized with Sevoflurane or Isoflurane for 3 hours. After exposure, some were euthanized immediately; others were allowed to recover for 24 hours before sacrifice. Immunohistochemistry (IHC) was employed to monitor the extent of BBB breach, and scanning electron microscopy (SEM) was used to examine changes in the luminal surfaces of BVECs. Quantitative IHC revealed increased BBB permeability in older animals treated with Sevoflurane, but not Isoflurane. Extravasated immunoglobulin G (IgG) showed selective affinity for pyramidal neurons. SEM demonstrated marked flattening of the luminal surfaces of BVECs in anesthetic-treated rats. Results suggest an aging-linked BBB compromise

resulting from exposure to Sevoflurane. Changes in the luminal surfaces of BVECs indicate a direct effect on the plasma membrane, which may weaken or disrupt their BBB-associated tight junctions. Disruption of brain homeostasis due to plasma influx into the brain parenchyma and binding of plasma components (such as IgG) to neurons may contribute to POD. We propose that, in the elderly, exposure to some IAs can cause BBB compromise that disrupts brain homeostasis, perturbs neuronal function, and thereby contributes to POD. If unresolved, this may progress to postoperative cognitive decline (POCD) and later dementia.

INTRODUCTION

Nearly 60,000 patients undergo general anesthesia every day with the hope of alleviating chronic diseases and improving their quality of life [49, 50]. Unfortunately, after exposure to anesthetics, a large percentage of elderly patients at age 65 and older exhibit postoperative delirium (POD), and many subsequently develop postoperative cognitive decline (POCD), which may be linked to later dementia [51-54]. In the US, the number of affected individuals continues to rise because the elderly are the fastest growing segment of our population [18, 55-57]. POD is characterized by an acute, fluctuating onset of attention disturbance and cognitive change in patients who may otherwise lack a history of neurocognitive manifestations [58-60]. As multifactorial disorders, POD and POCD have been associated with a variety of somatic factors as well as medication intoxication or withdrawal [60, 61]. Advanced age and exposure to inhaled anesthetics have been widely implicated as risk factors [53, 56, 58, 60].

Although the underlying mechanisms of POD and POCD are unknown [62], emerging evidence suggests a common mechanistic link. Aging is a known predisposing factor in a number of vascular pathologies, including chronic vascular inflammation, atherosclerosis, amyloid angiopathy, hyalinosis, and hypertension [63-66]. The blood vessels in the brain are not spared from these anomalies. Brain vascular endothelial cells (BVECs) line the luminal surfaces of these vessels and contribute both structurally and functionally to the blood-brain barrier (BBB). These cells are held together at their margins by extensive tight junctions associated with

prominent tight junctional folds or ridges. The BBB is thought to be further supported by the basement membrane of BVECs, pericytes, and the end-feet of astrocytes [20, 67]. The BBB regulates the movement of various molecules into and out of the brain, which is crucial for establishing and maintaining brain homeostasis and enabling the normal functioning of the neurons and glia within their microenvironment in the brain. Factors or conditions that disrupt BBB function can trigger a transient or chronic leakage of plasma components into the brain tissue, thereby disrupting brain homeostasis and triggering disease states [20, 67]. Several neurodegenerative diseases, most notably Alzheimer's disease (AD), exhibit BBB breakdown as a consistent pathological feature that likely contributes to both disease initiation and progression [68].

In the present study, we tested the hypothesis that exposure to commonly used inhalation anesthetics disrupts BBB integrity, causing an influx of plasma components into the brain that locally disrupts brain homeostasis. To investigate this, young (3-5 months), middle-aged (10-12 months), and old (17-19 months) rats were subjected to either Sevoflurane or Isoflurane anesthesia for 3 hours and then were sacrificed immediately or allowed to recover for 24 hours prior to sacrifice. Using immunohistochemistry (IHC) and immunoglobulin G (IgG) as a tissue biomarker of BBB leak, we compared the functional integrity of the BBB between control animals and those exposed to anesthesia with or without 24 hours of recovery. Results showed an increase in BBB permeability as evidenced by an influx of plasma components into the brain tissue in Sevoflurane-treated animals, but not in those exposed to

Isoflurane, as compared to controls. Extravasated IgG showed selective affinity for the surfaces of pyramidal neurons. Scanning electron microscopy (SEM) revealed an increased incidence of BVEC degeneration and death within the walls of brain blood vessels along with a marked flattening of their luminal surfaces and stretching of tight junctional ridges at their margins. The BBB of older and anesthetic-treated older rats appeared to be most sensitive to disruption, and Sevoflurane was more effective than Isoflurane in promoting BBB compromise and luminal surface changes in BVECs. These data link aging-associated decline in BBB functional integrity to the increased vulnerability of brain blood vessels in older animals to the effects of anesthesia. Extrapolation of this data to humans leads us to suggest that, particularly in the elderly, exposure to certain types of anesthetics causes a rapid, transient breakdown of the BBB which results in a critical loss of brain homeostasis and disruption of neuronal function that could, at least in part, account for the expression of symptoms that characterize delirium. Furthermore, if BBB function is not completely restored in elderly patients suffering from POD, we suggest that they are at an increased risk for subsequently developing POCD and perhaps even dementia.

MATERIALS AND METHODS

Rodents

Seventy-seven wild-type Sprague Dawley rats (Harlan Laboratories, Inc.) were maintained on *ad libitum* food and water in an AAALAC-accredited vivarium with a 12-hour light/dark cycle. Animal use was approved by the RowanSOM IACUC.

Animal Treatment

Young (3-5 months), middle-aged (10-12 months), and older (17-19 months) rats were subjected to Sevoflurane (1-3%) or Isoflurane (1-3%) for 3 hours. Anesthesia was first induced by exposing rats in an induction chamber to 3% Sevoflurane or Isoflurane. Once surgical plane anesthesia was attained, they were removed from the induction chamber and put on a heat pad (T/Pump by Stryker, Kalamazoo, MI). Surgical plane anesthesia was maintained by supplying the anesthetics via nose cones. The concentration of the anesthetics was gradually lowered but the animal was not allowed to either progress to deeper sleep or to regress to a wakeful state. The state of anesthesia was constantly monitored by testing for the pedal withdrawal reflex (toe pinch) and by pinching the tail. In addition, animal vital signs such as rate and depth of respiration were monitored and maintained (at 32±3 respirations per minute) by regulating the mixture of anesthetic and oxygen. Body temperature was maintained by a heated pad and by covering the body. A calibrated Midmark Matrx VMR tabletop anesthesia machine with a VIP 3000 well-fill style vaporizer was used to supply Sevoflurane (Sevothesia™; Butler Schein™ Dublin, OH; NDC: 11695-0501-2) and Isoflurane (Isothesia™; Butler Schein™; Dublin, OH; NDC 11695-6776-2),

with oxygen as the carrier gas. Separate vaporizers for Sevoflurane and Isoflurane were acquired and used as each rodent received only one type of anesthetic. The concentration of anesthetic required for maintaining surgical plane anesthesia varied between the age-groups and individuals. Non-recovery rats were euthanized at the end of the third hour by exsanguination: the animal was perfused with phosphate-buffered saline (PBS) followed by freshly prepared 4% paraformaldehyde (PFA) in PBS. Recovery rats were first allowed to recover for 24 hours after the 3 hour exposure to anesthesia and were euthanized by CO_2 asphyxiation. The control group included rats of all three age-groups that were not exposed to either anesthetic and were euthanized by CO_2 asphyxiation. To achieve the best preservation of the brain tissue, all animals were fixed by perfusion using freshly prepared 4% PFA in PBS. Brains were quickly removed and, using a brain block, coronal sections were cut anteroposteriorly for bright-field microscopy, IHC, and SEM. Left hemispheres were sliced into 4mm thick sections for IHC; right hemispheres were sliced into 2mm thick sections for SEM. From the left hemispheres a total of four tissue blocks were generated - anterior, middle, posterior, and cerebellar. Anterior, middle, and posterior tissue blocks comprising different regions of cerebral cortex were the primary focus of this study.

Tissue Preparation, Immunohistochemistry, and Scanning Electron Microscopy

Brain tissues for IHC were fixed in 4% PFA and prepared for routine embedding in paraffin and sectioning as described previously [68]. Sections representing each brain region (anterior, middle, and posterior) were randomly selected for detection of

extravasated IgG using IHC. IHC was performed using the protocol and reagents described previously [68]. To detect IgG, biotinylated anti-rat IgG (Vector Laboratories, BA-9400, 1:20 in Dako antibody diluent) was used as the primary antibody [68, 69]. Cortical regions from each section were photographed using a Nikon Microphot-FXA microscope, and images were analyzed using NIS-Elements Imaging Software (Nikon Instruments Inc., USA). For SEM, the brain tissue was fixed in 4% PFA, rinsed in PBS, and post-fixed with 1% osmium tetroxide. After washing in buffer, tissues were first dehydrated in ethanol followed by amyl acetate. Samples were then dried with carbon dioxide in an E3100 critical point dryer (Quorum Technologies, USA) and rendered conductive by coating with a thin (~40Å) layer of gold using an EMS 150RS sputter coater (Quorum Technologies, USA). Tissues were examined using a JEOL NeoScope JCM-5000 scanning electron microscope.

Determination of the Density of Leaking Cortical Blood Vessels

The effects of age and inhalation anesthetics on the functional integrity of the BBB were assessed by counting blood vessels (arteries, veins, and capillaries) with associated perivascular IgG leak clouds and measuring the extent of the leak in the cerebral cortex (**Fig. 1; Fig. 2**). Extravasation of IgG has been widely used as a biomarker of BBB breach [68-71]. For each image, the area of the cerebral cortex and the number of cortical blood vessels exhibiting perivascular leak clouds were quantified. For each animal, the total number of leaking blood vessels per unit area of cortex was determined. Data from individual animals of the same age and treatment

groups were averaged and used for comparison. Only perivascular leak clouds displaying the source blood vessel were included in the analysis.

Determination of the Extent of BBB Breach in Cortical Blood Vessels

A relative scoring system based on the area of IgG extravasation was used to quantify the extent of BBB breach (**Fig. 2**) [69]. Normally, IgG in the cerebral cortex is contained within local blood vessels (**Figs. 1A-B; Fig. 2A**). Under conditions of BBB breakdown, IgG is able to extravasate and form perivascular leak clouds which take on a brown color in IHC preparations. The interaction of IgG with cognate epitopes present on the exposed surfaces of brain tissue components also causes immunostaining of pyramidal neurons, axons, dendrites, and synapses within tissue sections (**Fig. 2C-F**). The area and intensity of each perivascular leak cloud were considered to be directly proportional to the extent of BBB breach (**Fig. 2**). Investigators were blinded as to the identity of the specimens during image analysis.

Statistics

Using Student's t-test, statistical significance was calculated and a $p<0.05$ was considered statistically significant. Variation within each treatment group was represented by standard error.

EXPERIMENTAL RESULTS

Inhalation Anesthetics Increase BBB Permeability in the Rat

To assess the effects of anesthetics on the functional integrity of the BBB, IHC was used to detect the leak of plasma components from blood vessels into the cerebral cortex of anesthetic-treated and control rats (**Fig. 1**). IgG, which is normally absent in the brain interstitial space, was used as a biomarker of plasma leak and therefore BBB compromise. Results revealed the leakage of plasma components from cortical blood vessels (mostly small arterioles) in both Sevoflurane-treated and Isoflurane-treated animals, with extravasated IgG highlighting the presence of perivascular leak clouds (**Fig. 1C** and **E-H**). Perivascular leak clouds were clearly more prominent in the cerebral cortex of older rodents (**Fig. 1G-H**) than in young and middle-aged animals (**Fig. 1A-F**), suggesting that the BBB of older animals is more sensitive to the disruptive effects of anesthetics. In addition, perivascular leak clouds in the cerebral cortex of Sevoflurane-treated rats (**Fig. 1E, G,** and **H**) were more extensive than those in Isoflurane-treated rats (**Fig. 1C** and **F**). These findings imply that Sevoflurane is more disruptive than Isoflurane to BBB functional integrity. Immunohistochemical controls were used to confirm the specificity of the anti-IgG antibody staining reaction (**Fig. 1I**).

Synergistic Effect of Anesthetic Exposure and Aging on Increasing BBB Permeability

We next sought to quantify the separate effects of Sevoflurane and Isoflurane on the density of vessels exhibiting BBB compromise in the cerebral cortex and the extent of

the plasma leak emanating from these vessels. To accomplish this, we first established a scoring system that could be used to measure the relative extent of BBB leak from cortical blood vessels based on specific features of perivascular leak clouds as shown in **Fig. 2**. Using this system, a score of 0 corresponds to no detectable leak (**Fig. 2A**), whereas scores of 1-3 reflect a progressive increase in the size (and thus extent) of the perivascular leak cloud (**Fig. 2B-F**). A maximum score of three reflects the largest IgG-positive perivascular leak clouds, with IgG-labeled neurons either within it or in its immediate vicinity (**Fig. 2E-F**). Selective binding of IgG to neurons was consistently observed in the brains of both control animals and those subjected to Sevoflurane and Isoflurane anesthesia. Interestingly, non-neuronal cells were IgG-negative, suggesting that brain-reactive autoantibodies in the blood primarily target the pyramidal neurons that are dominant in the cerebral cortex (**Fig. 2E-F**). Quantification revealed an age-dependent increase in BBB permeability in control animals that were not exposed to anesthetics, as evidenced by increases in both the density of cerebrocortical blood vessels exhibiting BBB leaks and the extent or amount of material leaking from these vessels (**Fig. 3A-B**). Likewise, the older group of animals subjected to Sevoflurane anesthesia showed a dramatic and significant increase in the density and extent of vascular leak compared to controls (**Fig. 3A-B**). By contrast, older animals exposed to Isoflurane for 3 hours failed to show any significant age-related differences in either the density or extent of vascular leaks. Taken together, these data indicate that, in rodents, Sevoflurane is much more effective than Isoflurane in enhancing BBB permeability (**Fig. 3A-B**). In addition, similar measurements carried out on animals following 24 hours of recovery from

anesthesia revealed that this interval was insufficient for full functional recovery of BBB integrity in older rats, as the measurements of the density and extent of vascular leaks were still comparable among recovery and non-recovery rats (**Fig. 3A-B**).

Sevoflurane and Isoflurane Induce Dramatic Structural Changes in the Luminal Surfaces of BVECs That May Be Linked to BBB Compromise

The quantitative IHC data described above shows that BBB breakdown and the leak of plasma components into the brain tissue are already well-underway at the conclusion of the 3 hour treatment period. This suggests that the response of the BBB after exposure to inhalation anesthetics is rapid. To investigate the origin and nature of this rapid response, we next sought to determine if Sevoflurane and Isoflurane exert a direct effect on the BVECs that are essential for the structural and functional integrity of the BBB. To address this, we examined the effects of these anesthetics on the luminal surfaces of rat BVECs *in vivo* using scanning electron microscopy (SEM). Isolated rat brains were sliced to permit direct access to the interior of the brain blood vessels as well as to visualize the luminal surfaces of BVECs. **Fig. 4A** shows a SEM image of a transverse section through a leptomeningeal artery of a control animal which was tilted to provide a view of the BVECs that form the inner lining of the vessel. Closer examination of the luminal surfaces of BVECs revealed long rows of discrete cytoplasmic ridge-like protrusions, or tight junctional folds, at the margins of individual BVECs that delineate the location of BBB-associated tight junctions (**Fig. 4B**). These are best seen when viewed from directly overhead (**Fig. 4C**). In arterioles, these tight junctional folds most likely provide the extra membrane

necessary for expansion or stretching of BVECs without compromising the structural integrity of tight junctions during systolic dilation (**Fig. 4C**). In larger arterioles, BVECs are highly elongated and the BBB-associated cytoplasmic protrusions are oriented parallel to the long axis of the vessel, presumably to minimize turbulence during rapid blood flow (**Fig. 4C**). Also, the intervening luminal surface of BVECs displays numerous small microvilli (**Fig. 4C**).

Exposure of the animals to 3 hours of Sevoflurane or Isoflurane caused a dramatic flattening of the BVEC luminal surfaces in rats of all age groups (**Fig. 4D; Fig. 5**). Tight junctional folds at the margins of most BVECs were collapsed and flattened. This was often accompanied by a loss of the numerous small microvilli seen on BVECs of controls (e.g., compare **Fig. 4C** with **4D,** and **Fig. 5E** with **5F**). We also observed numerous holes at the margins of BVECs that appear to be true holes in the BVEC layer (e.g., **Fig. 4D**). However, whether or not these structures correspond to real gaps in the BBB and underlying basal lamina and thus focal sites of BBB leak is unknown.

Exposure to Sevoflurane and Isoflurane Can Be Toxic to BVECs

Analysis of the luminal surface morphology of BVECs also revealed some variations in the individual responses of BVECs to Sevoflurane and Isoflurane. Interestingly, the most severely affected BVECs were most frequently found in regions where blood vessels exhibited a sharp directional deviation or branching. Severely affected BVECs in these regions exhibited luminal surface membranes that were often

"pockmarked" with small holes, some of which were also located at cell margins in regions of BBB-associated tight junction folds (**Fig. 6A**). These were not specimen preparation artifacts since numerous adjacent BVECs in these same preparations often completely lacked these structural anomalies.

We also found that exposure to either Sevoflurane or Isoflurane led to the death of some BVECs (**Fig. 6**), although the underlying reason for the differential sensitivity of BVECs to the anesthetics used here remains to be established. For example, **Fig. 6A** shows two dying cells exhibiting unusually smooth luminal surface membranes, one with small holes scattered over the surface, and the other with these holes restricted to the cell margin in the region of tight junctional folds. The next stage in the death of BVECs is the stripping of the entire luminal surface membrane from the cell, thereby exposing an easily identified cell nucleus apparently still held in place by residual cytoplasmic components (**Fig. 6B-C**). Eventually, the nucleus and much of the residual cytoplasm are stripped off, presumably by the shearing action of continued blood flow (**Fig. 6D**). It is reasonable to predict that the death of BVECs creates gaps (and therefore compromises the integrity) of the BVEC layer and thus the BBB. However, whether sites of BVEC death actually correspond to focal regions of BBB leak in brain blood vessels remains to be demonstrated, and the relative contribution of BVEC loss to the extent of BBB leak still needs to be defined.

Vascular Integrity and Surface Morphology of BVECs Failed to Recover within 24 hours of Anesthetic Treatment

We next asked if the effects of these anesthetics on BBB integrity and the surface morphology of BVECs are reversed within 24 hours. This was tested by allowing animals to recover for 24 hours after the conclusion of the 3 hour exposure to Sevoflurane or Isoflurane. Quantitative IHC failed to show any significant reduction in the density of leaking vessels or in the extent of their leakage after a 24 hour recovery period, most notably in the Sevoflurane-treated animals (**Fig. 3**). This was corroborated by examination of the luminal surfaces of BVECs using SEM. BVECs in young and middle-aged animals appeared to be more comparable to controls after 24 hours of recovery than those in older animals (data not shown). We also monitored the emergence from anesthesia and orientation of the recovery rats. Interestingly, the emergence of rodents from anesthesia was clearly faster in Sevoflurane-treated animals compared to Isoflurane treated animals, with rats exposed to Isoflurane being more lethargic and subdued.

DISCUSSION

The present study shows that some commonly used inhalation anesthetics, such as Sevoflurane, rapidly cause increased BBB permeability in blood vessels in the rat cerebral cortex as demonstrated by the influx of IgG into the brain parenchyma, most notably in older animals. We also show a differential response of the BBB to specific inhalation anesthetics; with Sevoflurane having a much greater effect on increasing BBB permeability than Isoflurane. Given that the cerebral cortex is normally immunoprivileged, the presence of IgG in the brain parenchyma was used as a biomarker of BBB compromise. Small arteries and arterioles within the brain exhibited a greater extent of leak than small veins, venules, and capillaries, and were often surrounded by perivascular clouds of leaked IgG-immunopositive material, indicative of BBB breakdown. This apparent selectivity for arteries and arterioles is expected, since both are under considerably more hydrostatic pressure than their associated small veins, venules, and capillaries.

Anesthetics Compromise BBB Function through their Rapid and Direct Effects on BVECs

The underlying mechanisms through which anesthetics can trigger BBB permeability are unknown, but the immediate and dramatic morphological changes in the luminal surfaces of BVECs described here suggest that a direct effect of the anesthetics on these cells may be involved. In support of this, we show using SEM that exposure to Sevoflurane or Isoflurane induces an overall flattening of the luminal surfaces of BVECs. This was most conspicuous at the boundaries between adjacent BVECs, with

flattening and collapse of the tight junctional folds found in this region. Although Sevoflurane and Isoflurane are known to be potent vasodilators, whether or not this contributes to the observed flattening of tight junctional folds between adjacent BVECs is unknown [72].

The present study also shows that, in older animals, Sevoflurane was more effective than Isoflurane in generating these effects based on structural changes in BVECs, measurements of the relative density of leaking blood vessels, and the overall extent of vascular leakage in the brain parenchyma. In surgical settings, Sevoflurane is usually selected over Isoflurane, since in humans the average time to emerge, response to commands, orientation, and hospital stay are shorter [73, 74]. In our hands, Sevoflurane appeared to behave similarly in rats; Sevoflurane-treated animals were quicker to recover and orient themselves compared to Isoflurane-treated animals; the latter were more lethargic and subdued for a longer time period following the conclusion of anesthesia.

The age of the animal was found to be a key factor in determining the magnitude of the response of the BBB following exposure to a particular anesthetic. For example, despite the fact that Sevoflurane and Isoflurane exposure resulted in dramatic differences in the degree of BVEC luminal surface flattening among animals at different ages, the oldest animals in the Sevoflurane-treated group clearly showed the greatest degree of BBB permeability as well as the least recovery at 24 hours post-anesthesia. Indeed, we found that 24 hours of recovery was generally insufficient for

complete restoration of BBB functional integrity and normal BVEC luminal surface morphology in all age groups tested, but most notably in older animals. Extrapolating this to humans suggests that in elderly patients planning to undergo surgery and exposure to inhalation anesthetics, there may be a long-term benefit in purposely choosing a slower-acting anesthetic over a faster-acting one. The basis of this decision comes from the concept that the slower-acting anesthetic would presumably pose less risk for BBB compromise and, hopefully, minimize subsequent POD, which is supported by the data presented here. Further studies will be needed to identify specific anesthetics for use in surgery that are less disruptive to BBB function and thus better able to help patients avoid postoperative manifestations such as POD, POCD, and perhaps even subsequent dementia. For example, in this context, the data presented here would support the choice of Isoflurane over Sevoflurane for use in elderly patients.

Anesthetic-Mediated Death of BVECs Contributes to BBB Compromise

SEM revealed dying and dead BVECs in animals treated with Sevoflurane or Isoflurane, with an increased prevalence in Sevoflurane-treated animals (**Fig. 6**). Since these cells were relatively few and often surrounded by numerous other cells that appeared normal, it can be suggested that they were, for some unknown reason, more vulnerable to anesthetic treatment than surrounding cells. Not surprisingly, dying and dead BVECs were clearly more abundant in the 24 hour recovery group of animals, suggesting that it may take some time for affected BVECs to finally succumb to the effects of anesthetics (**Fig. 6**). Some features associated with the death

of BVECs have been reported in earlier studies of rats treated with a hypertonic arabinose solution [75] as well as in spontaneously hypertensive rats [76]. Regardless of the underlying reason for the observed death of BVECs, there is no doubt that their loss leaves a physical gap in the BBB that apparently does not get rectified within 24 hours. It is unknown if or how such gaps are repaired as well as the time frame for repair, but replacement of a lost BVEC with another derived from circulating endothelial progenitor cells originating in the bone marrow is one possibility [77-79]. Further work will be needed to test this repair mechanism as well as to investigate any potential therapeutic utility of stimulating such cell replacements.

Agreement of Our Data with the Results of Prior Studies

Our data agrees with a study by Tetrault et al., who demonstrated a dose-dependent breakdown of the BBB by Isoflurane in the cerebral cortex and thalamus in cats [80]. Likewise, Hu et al. showed BBB compromise in 18 month old Wistar rats that had undergone orthopedic surgery under Sevoflurane [81]. However, the experimental design of the present study differs from that of these earlier studies in two important ways. First, Tetrault et al. also treated the cats with a muscle relaxant and other anesthetics in addition to Isoflurane. The use of multiple compounds makes it difficult to definitively attribute the observed effects on the BBB solely to Isoflurane [80]. In the present study, in an effort to directly link the individual effects to Sevoflurane or Isoflurane, we avoided the use of additional agents with the exception of an obligatory brief use of CO_2 for euthanizing recovery and control rats. Second, Hu et al. carried out an orthopedic surgical procedure in their Sevoflurane-treated rats

[81]. It is known that surgical trauma, among other things, can induce expression of CCL2 by vascular endothelial cells, which can influence BBB permeability by facilitating transendothelial migration of macrophages into the brain parenchyma [82]. This introduces another variable that makes it difficult to distinguish the relative contributions of the inhalation anesthetics from the response to the surgical procedure on the observed outcomes. To avoid this, no surgical procedures were carried out in the present study. The results of all of these studies, however, differ from that published recently by Thal et al., as they failed to detect any effect of Isoflurane or Sevoflurane on inflicting brain edema, BBB compromise, or alteration in the expression of tight junction proteins associated with the BBB in young C57B16N mice [83]. Although it is certainly possible that the mouse responds differently than the rat and larger mammals to these anesthetics, the fact that this study was focused only on younger mice might have contributed to the different outcomes. Lastly, in the present study, we were also mindful of the increasing frequency of aging-associated chronic vascular changes and comorbidities that can afflict very old animals [84-86]. Such chronic states can have a significant impact on the experimental outcomes and can confuse interpretations of data [84-86]. For this reason, we decided against including extremely old rats in our study.

BBB Breakdown: A Common Theme Linking POD, POCD, and Dementia

About 50% of the elderly patients who undergo general anesthesia develop POD, and only half of these POD patients regain normal cognition on the second day [53]. In the context of the present study, this suggests that entry of plasma components into

the brain parenchyma through an anesthesia-induced increase in BBB permeability results in disruption of brain homeostasis. This acutely altered brain homeostasis could trigger neuronal dysfunction, leading to a manifestation of symptoms that collectively defines POD. During patient recovery, partial or complete restoration of BBB function, depending on the age and vascular health status of the individual, would be expected to correspond to partial or complete loss of POD symptoms. Furthermore, failure to completely recover BBB function, which may occur preferentially in elderly POD patients, could set into motion a long-term pathological progression that transgresses POD, leading to POCD and perhaps even dementia in the long-term as depicted in **Figure 7**. In the present study, we also demonstrate that some blood-borne IgGs have selective affinity for pyramidal neurons in the cerebral cortex. This binding of extravasated IgG to pyramidal neurons may also be disruptive to neuronal function and even trigger further pathological changes via the crosslinking and internalization of key surface membrane proteins. For example, we have previously reported that IgG binds selectively to amyloid-beta$_{1\text{-}42}$ (Abeta42)-burdened pyramidal neurons located in regions of pathology in the cerebral cortex of Alzheimer's disease patients [68]. We tested the possible mechanistic relationship between neuronal IgG binding and intraneuronal Abeta42 deposition in adult mouse brain slice cultures and demonstrated that IgG binding to pyramidal neurons enhances chronic endocytosis and selective intraneuronal deposition of Abeta42 in these cells [68]. The fact that BBB breakdown and selective binding of IgG to neurons are common events that occur in the brains of inhalation anesthetic-treated older rats and human Alzheimer's disease patients leads us to propose that BBB compromise may

be a common and requisite mechanistic link. Similar results and conclusions implicating BBB compromise and selective IgG binding to neurons in chronic epilepsy were reported in a study carried out on human temporal lobe epileptic tissues and in a rat model of epilepsy [87].

This study has some obvious limitations. The first is the small sample size of the group of older rats, due to their limited availability and long waiting periods for their delivery. This had a negative impact on statistical significance in spite of an easily discerned pattern of the effects of these inhalation anesthetics on BBB integrity. In addition, the treatment of the animals with anesthetics as carried out in the present study fails to match the induction of general anesthesia in humans, as we did not use any intravenous anesthetic agent, opioids, or muscle relaxants. Of course, in part, this was done purposefully in an effort to more clearly attribute the observed effects to a single agent, i.e., Sevoflurane or Isoflurane. Lastly, the selection of a single recovery point was subsequently found to be limiting since our data clearly revealed that 24 hours was insufficient for full recovery of BBB functional integrity, even in young and middle-aged rodents. Further studies using larger numbers of rats from all age groups that are allowed to recover for longer time periods will be needed.

Conclusions and Perspectives

The data presented here show that some inhalation anesthetics can increase BBB permeability, particularly in older subjects. In addition, we show that Sevoflurane has a greater effect on increasing BBB permeability in a rat model, and that older

Sevoflurane-treated animals failed to regain BBB integrity within 24 hours of exposure to anesthesia, as judged by the persistent presence of IgG in the brain parenchyma as a biomarker of vascular leak. These findings advocate for the identification and selection of inhalation anesthetics that are less disruptive to the BBB in the elderly, since individuals in this age group are most vulnerable to BBB breakdown and thus POD. From this study, it is clear that both anesthetics directly alter the luminal surface morphologies of BVECs, particularly in regions of BBB-associated tight junctional folds. Furthermore, the more severe effects of Sevoflurane on BVEC luminal surface morphology suggest that these changes are sufficient to exceed some threshold required for breach of BBB integrity. Based on these findings, we propose that BBB breakdown induced by some inhalation anesthetics perturbs brain homeostasis due to the influx of plasma components into the brain parenchyma. For example, IgG, a plasma component normally blocked from entry into the brain by the BBB, was found to extravasate into the brain parenchyma predominantly in Sevoflurane-treated animals. The observed selective binding of this IgG to neurons may further exacerbate neuronal dysfunction and thereby contribute to emergence of symptoms associated with POD. Furthermore, we suggest that failure to completely restore BBB function following surgery, which appears to be most prevalent in the elderly, could lead to POCD in the short-term and, if unresolved, may favor the later development of dementia in the long-term (**Fig. 7**). Therefore, maintenance of proper BBB function is crucial for preventing the occurrence and escalation of POD.

FIGURES

Figure 1: Age-Dependent Effects of Sevoflurane and Isoflurane on Blood-Brain Barrier Permeability

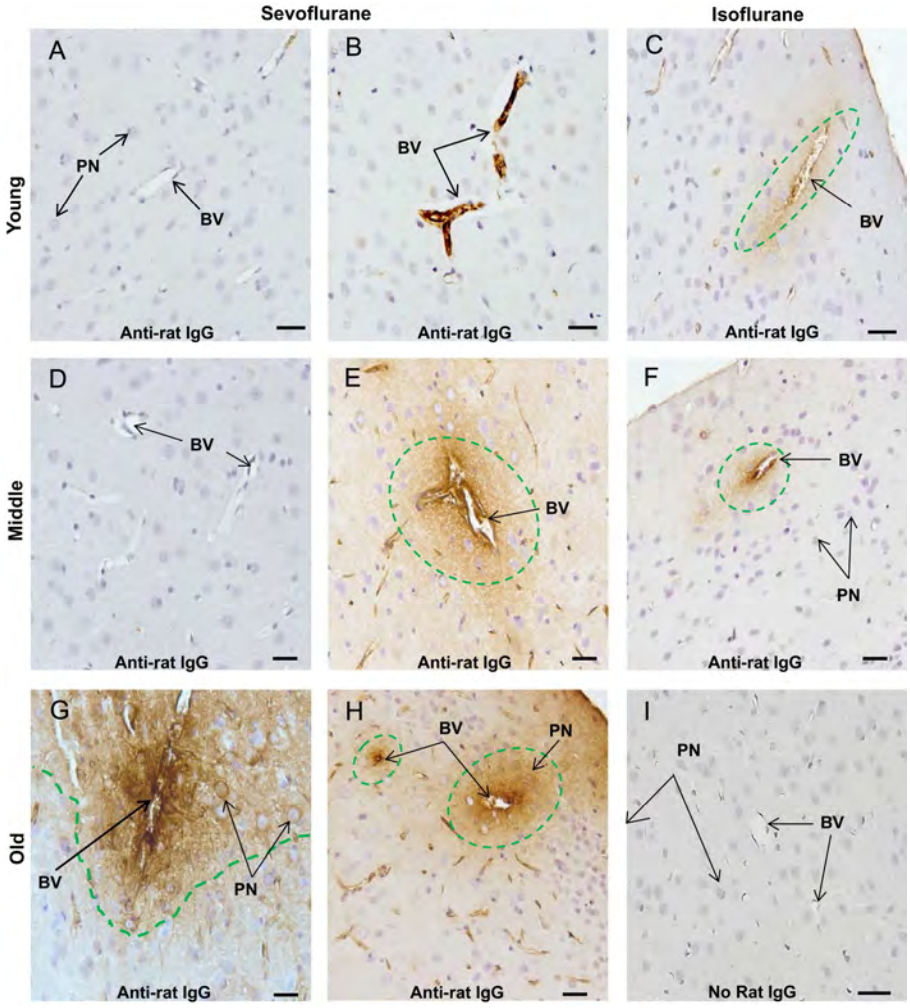

Histological sections of the cerebral cortex of young (**A-C**), middle-aged (**D-F**), and older (**G-I**) rats subjected to Sevoflurane and Isoflurane anesthesia for 3 hours were immunostained to reveal BBB leak from blood vessels and the influx of IgG into the brain tissue. The most prominent leaks were observed in the cerebral cortex of older rats exposed to Sevoflurane (**G-H**). (**I**) An IHC control section treated with blocking sera only to confirm the specificity of the anti-IgG antibody used to detect interstitial, extravasated IgG. PN - Pyramidal Neuron; BV - Blood Vessel. Scale bar = 100µm.

Figure 2: The Scoring System Used to Quantify the Extent of Anesthetic-Induced BBB Leak

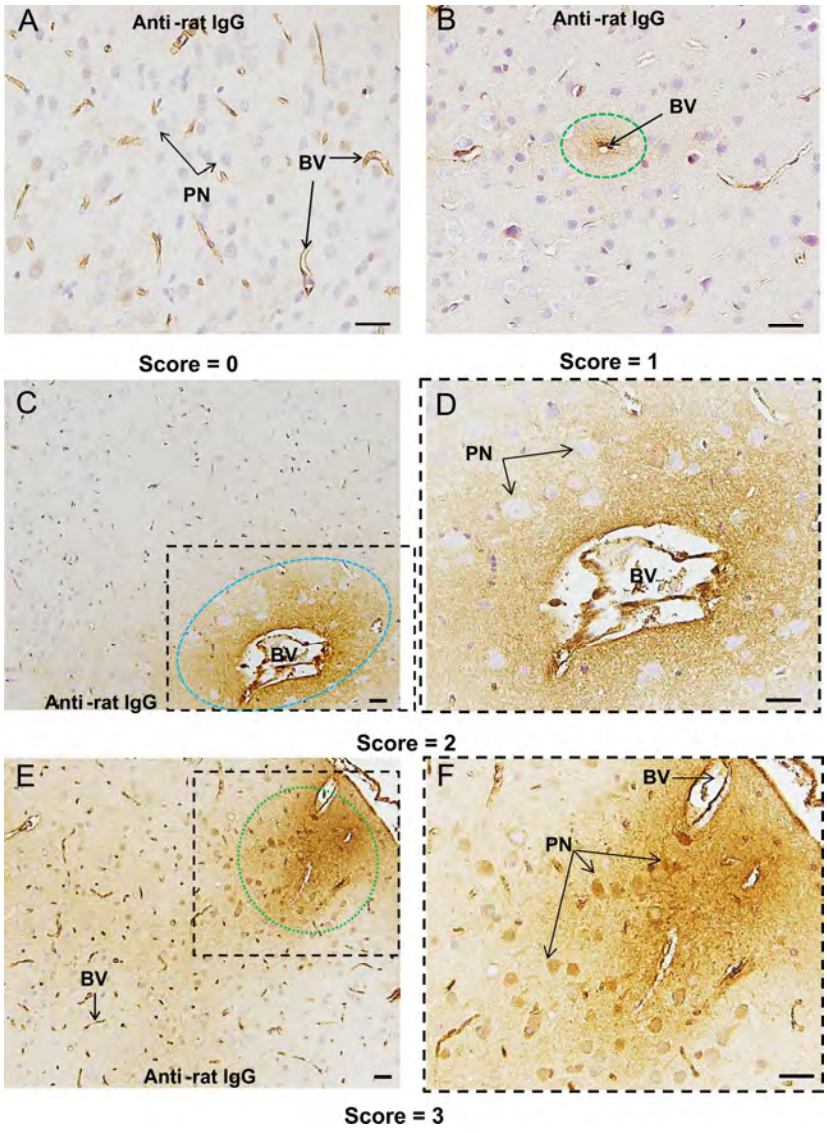

The extent of BBB leak from each blood vessel was assigned a score ranging from 0-3 based on the appearance of perivascular leak clouds. (**A**) A score of 0 corresponds to no leak. (**B-F**) Scores ranging from 1-3 reflect a progressive increase in the size of leak clouds, which is also taken to reflect the extent of the leak. (**E-F**) A score of three indicates a large IgG-positive perivascular leak cloud that also contains IgG-positive neurons within or near the leak cloud. (**D** and **F**) Enlarged regions of **C** and **E**, respectively. PN - Pyramidal Neurons; BV - Blood Vessels. Scale bar = 100µm.

Figure 3: Quantification of the Effects of Sevoflurane and Isoflurane Exposure and Age on the Density and Extent of BBB Leaks

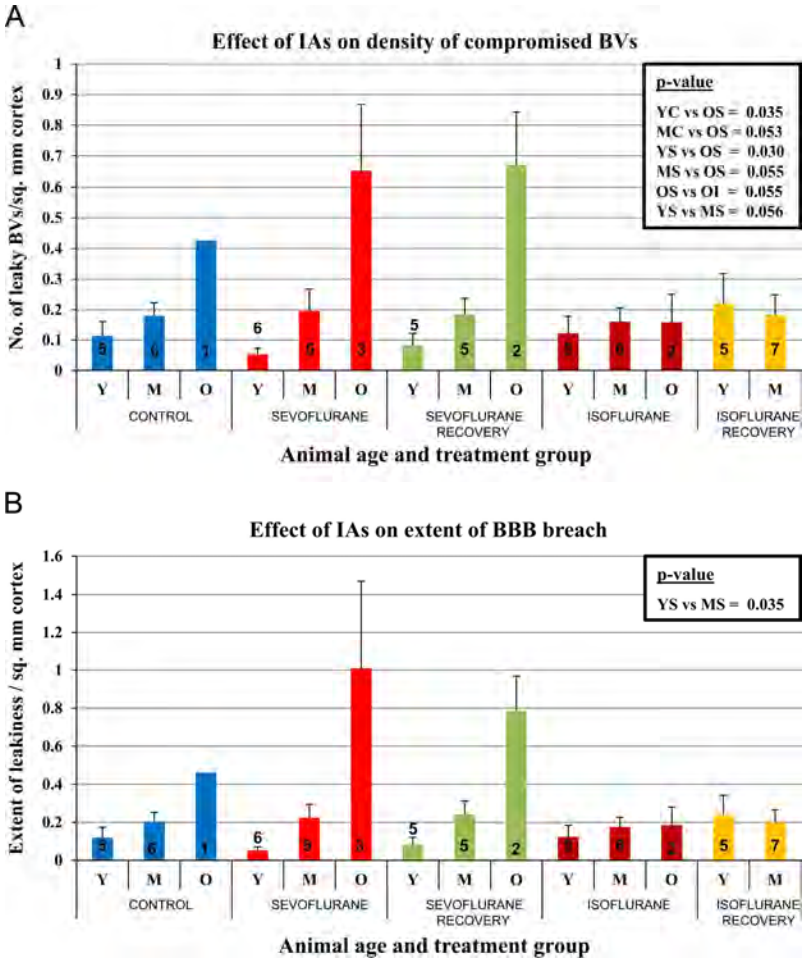

(**A**) The density of blood vessels with demonstrable BBB leaks was determined by counting the total number of leaking blood vessels per unit area of cerebral cortex. (**B**) The extent of BBB leak was quantified using the scoring system shown in Fig. 2. Control animals showed a gradual, age-dependent increase in BBB permeability, as evidenced by increases in both the density of leaky blood vessels in the cerebral cortex and the extent of leak from these vessels. Older animals subjected to Sevoflurane showed more dramatic increases in the density and extent of blood vessel leaks compared to controls and Isoflurane. A period of 24 hours was insufficient for recovery of BBB functional integrity from either Sevoflurane or Isoflurane. Y - Young; M - Middle; O - Old; S - Sevoflurane; I - Isoflurane; p (*) $\leq$ 0.05.

Figure 4: Sevoflurane Causes Dramatic Flattening of BVEC Luminal Surfaces

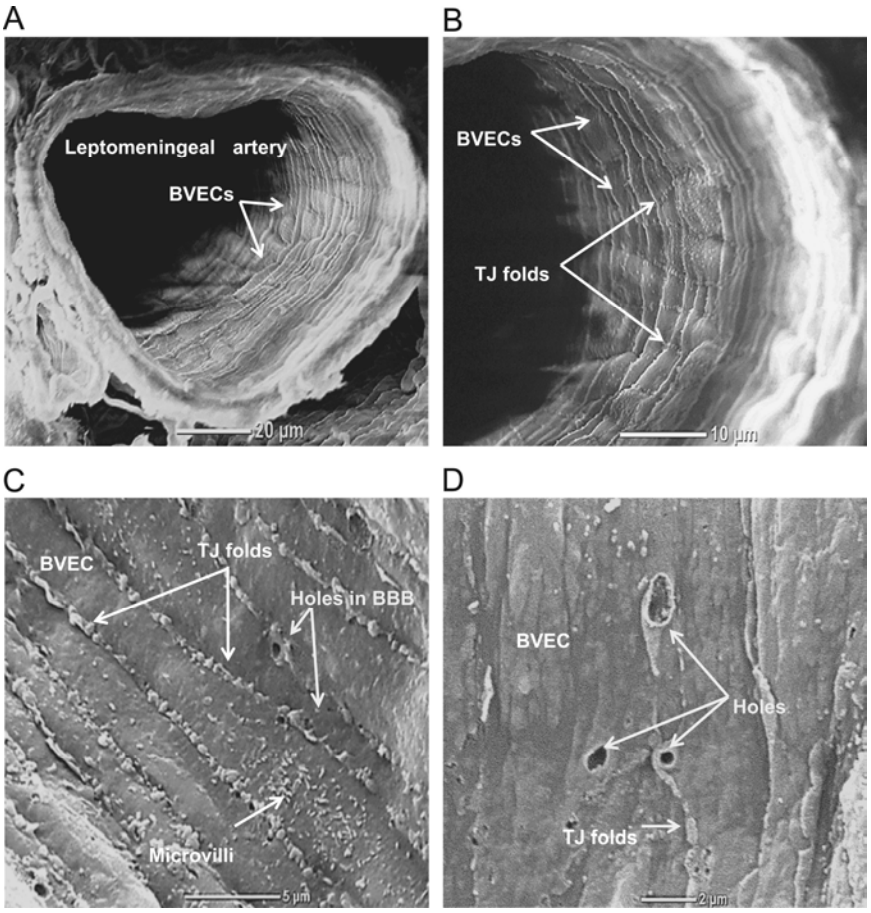

(A) Scanning electron microscopic image of a transverse section through a leptomeningeal artery of a control rat. (**B**) Enlarged portion of (**A**) showing the luminal surfaces of BVECs and long rows of discrete cytoplasmic protrusions that delineate the location of BBB-associated tight junctional folds at the cell margins of BVECs. (**C**) Higher magnification showing extensive, ridge-like protrusions of cytoplasm overlying BBB-associated tight junctional folds and oriented parallel to the long axis of the vessel. Between these junctional folds, the luminal surface displays numerous small microvilli. (**D**) Exposure of animals to Sevoflurane for 3 hours caused a dramatic overall flattening of the luminal surfaces of the BVECs, including the marginal tight junctional folds associated with BBB tight junctions and a loss of small microvilli. Holes were often observed at cell margins between adjacent BVECs. BVEC - Brain Vascular Endothelial Cell; TJ - Tight Junction.

Figure 5: Sevoflurane and Isoflurane Cause Comparable Flattening of the BVEC Luminal Surfaces

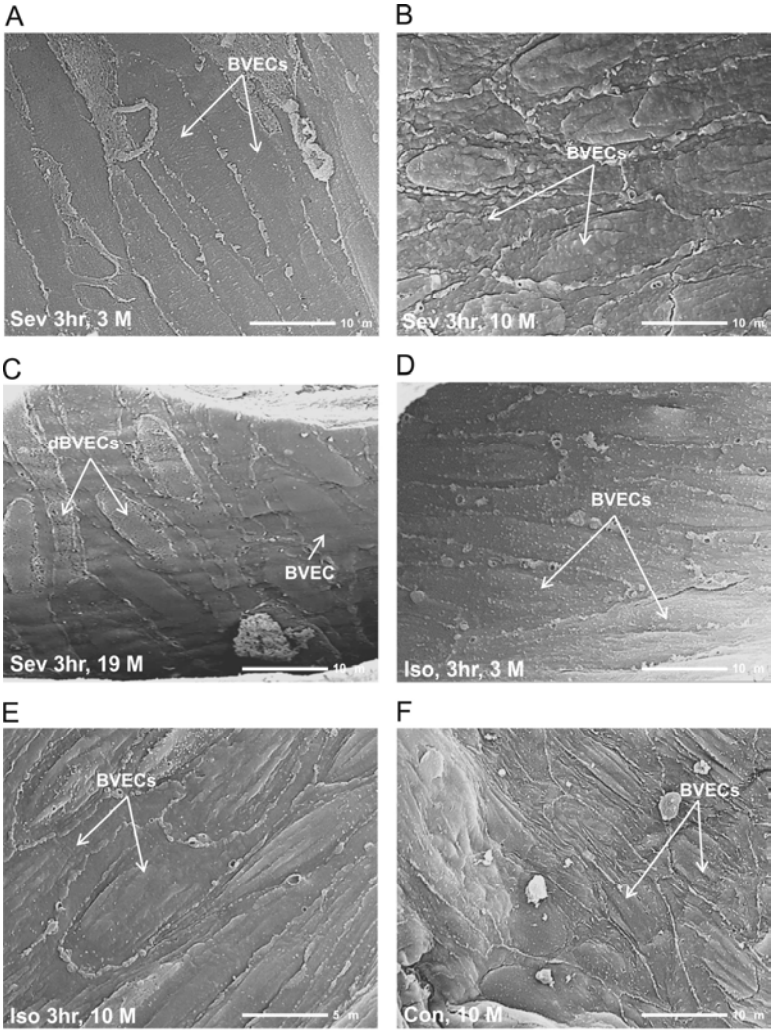

SEM images showing the luminal surfaces of BVECs lining the walls of brain blood vessels. Sevoflurane (**A-C**) caused changes in BVEC luminal surface topography that ranged from a pronounced surface flattening (**A**) to wrinkling (**B**). Scattered BVECs appeared to be dying as revealed by defects in their surface membranes, which were tightly opposed to underlying nuclei. Isoflurane (**D-E**) also caused comparable flattening of BVEC luminal surface membranes, whereas BVEC luminal surfaces in controls showed prominent marginal ridges/folds as well as small microvilli scattered over the cell surface (**F**). BVECs - Brain Vascular Endothelial Cells; dBVECs - Dying or Dead BVECs.

Figure 6: Sevoflurane and Isoflurane Can Induce the Death of BVECs, Resulting in Focal BBB Breakdown

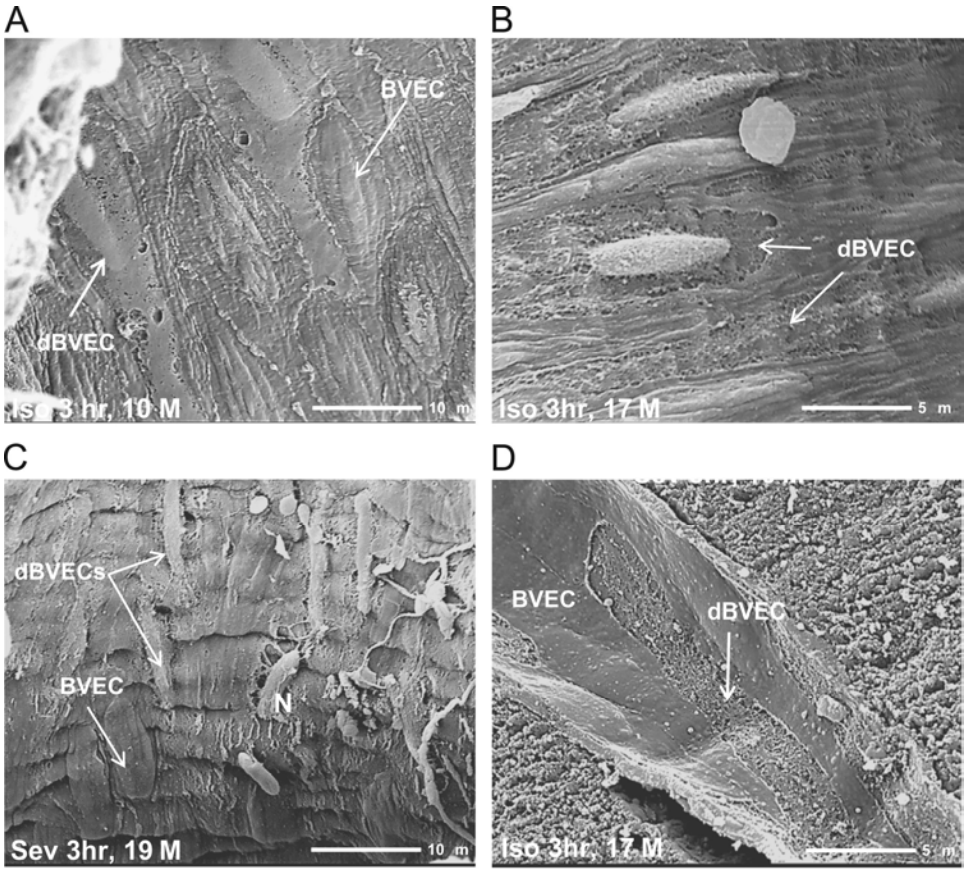

(**A**) The luminal surface membranes of some BVECs scattered throughout the walls of blood vessels were "pockmarked" with holes, especially at cell margins in the vicinity of BBB-associated tight junctional folds. This appears to be the first indication of impending cell death. (**B**) Next, the luminal surface membrane is completely stripped from the BVEC, exposing a nucleus presumably still held in place by residual cytoplasmic fibers. (**C**) BVECs at branch points of blood vessels are apparently most vulnerable to the effects of Sevoflurane and Isoflurane. (**D**) A large capillary showing the remnant of a dead BVEC with the nucleus stripped off by the shear forces of normal blood flow. BVECs - Brain Vascular Endothelial Cells; dBVECs - Dying or Dead BVECs.

Figure 7: Proposed Mechanism of Anesthetic-Induced Blood-Brain Barrier Breakdown and Its Mechanistic Relationship to Postoperative Delirium, Postoperative Cognitive Decline, and Dementia

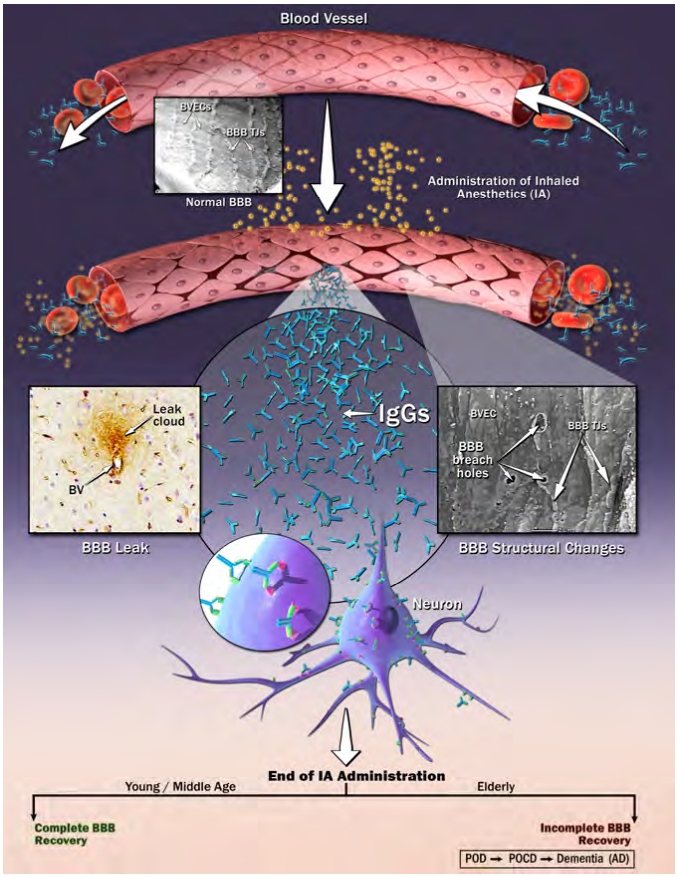

Here, we propose that the combination of BBB breakdown, plasma entry into the brain tissue, and the selective binding of brain-reactive IgGs to pyramidal neurons act together to contribute to disruption of normal neuronal activity and collectively elicit the symptoms that define POD. Further, we suggest that failure to completely restore BBB function following surgery, which appears to be most prevalent in the elderly, leads to POCD in the short-term and, if unresolved in the long-term, can favor the development of dementia. Thus, BBB breakdown may provide a common mechanistic link between POD, POCD, and dementia. BBB - Blood-Brain Barrier; BV - Blood Vessel; BVEC - Brain Vascular Endothelial Cell; IA - Inhaled Anesthetic; IgG - Immunoglobulin G; POD - Postoperative Delirium; POCD - Postoperative Cognitive Decline; TJ - Tight Junction.

CHAPTER IV:

The Heightened Vulnerability of the Pre-Adolescent & Elderly Populations to Anesthesia-Triggered Delirium is Linked to Increased Blood-Brain Barrier Permeability

ABSTRACT

Background

Postoperative delirium (POD) is a major problem in modern healthcare, and it is one of the most common postoperative complications faced by patients, particularly the very young and the very old. Pediatric and elderly POD are rampant and have been associated with the widespread use of anesthetics, especially Sevoflurane. Epidemiologic studies have established an association between exposure to Sevoflurane and long-term outcomes that include learning disabilities and behavioral and developmental disorders, especially in children 2 to 4 years of age. Here, we use both pre-adolescent and elderly rat models to ask whether this heightened sensitivity to Sevoflurane is linked to increased blood-brain barrier (BBB) permeability.

Methods

Two-week old (pre-adolescent), four-week old (adolescent), and twenty-six month old (elderly) rats were subjected to Sevoflurane or Isoflurane anesthesia for three hours. Animals were sacrificed and their brains were fixed by perfusion and

processed for immunohistochemistry (IHC) and scanning electron microscopy (SEM). IHC was used to detect the presence, location, and extent of BBB compromise, using blood-borne IgG as a marker of BBB leakage. SEM was used to directly visualize the effects of anesthesia on the luminal surfaces of brain vascular endothelial cells (BVECs) forming the BBB.

Results

Following Sevoflurane anesthesia, both pre-adolescent and elderly rats showed increased BBB permeability in the cerebral cortex as evidenced by the appearance of extravasated IgG and binding of brain-reactive autoantibodies to neurons, especially pyramidal neurons, compared to adolescent, adult, and untreated control rats. Increased BBB permeability associated with exposure to Sevoflurane in pre-adolescent rat brains was coincident with rapid brain and head growth and its associated neovascularization. SEM revealed Sevoflurane-induced structural alterations in cell surface topography, but especially at the interface between adjacent BVECs, the site corresponding to tight junctions of the newly formed BBB. Similar topographical changes were observed in the BVECs forming the BBB in the brains of elderly rats. These changes were not seen with Isoflurane.

Conclusions

Results suggest that the relatively high incidence of POD associated with Sevoflurane anesthesia in very young children and the elderly may be due to an anesthesia-induced increase in BBB permeability. We propose that this anesthesia-induced

increase in BBB permeability results in a large plasma influx into the brain parenchyma that disrupts brain homeostasis and neuronal activity, triggering POD and favoring long-term learning and behavioral sequelae. Pre-adolescents are most vulnerable to this effect because the brain of the very young is engaged in a period of exceptionally rapid growth and neurogenesis accompanied by extensive neovascularization and BBB formation. The elderly are vulnerable because the number of BVECs in brain blood vessels declines with age, and the remaining cells are forced to spread out and increase their surface area, which renders them more susceptible to potentially toxic effects of the anesthetic.

INTRODUCTION

Delirium is a highly prevalent neuropsychiatric or neurocognitive disorder that presents a major problem to modern healthcare. In general terms, delirium is a cerebral dysfunction that causes a major disturbance in a person's mental abilities that leaves them in a state of severe mental confusion. It is characterized by disturbances of consciousness, attention, cognition, perception, emotion, motor behavior, and the sleep-wake cycle. These symptoms can fluctuate in intensity throughout the day and can be interrupted by periods of variable lucidity [1, 56]. Patients suffering from delirium normally have a worse prognosis, prolonged hospital stay, increased hospital costs, increased risk for long-term cognitive impairment, and higher mortality rates [7, 88, 89]. In fact, it has been reported that ICU patients exhibiting delirium have a 2 to 4 fold increase in mortality rates [90]. Many factors can trigger delirium, which makes treating this disorder a daunting task. Furthermore, delirium has proven to be hard to recognize and diagnose, meaning it is often overlooked [90]. Unfortunately, delirium remains the most common psychiatric syndrome found in the hospital setting [1].

Postoperative Delirium (POD) is a prevalent form of delirium. Many factors can act singly or synergistically to drive POD, including exposure to certain drugs and anesthetics [1, 6, 81, 89-91]. As with general delirium, patients suffering from POD face increased length of stay in the hospital, more frequent medical complications, and increased mortality [88]. Furthermore, studies have shown that patients suffering from POD are much more likely to develop Postoperative Cognitive Decline (POCD)

and dementia [89]. Studies have estimated that POD presents itself in 10-40% of patients [88]. It has long been recognized that certain types of patients, most notably the very young (less than 4 years) and the elderly (older than 70 years), who underwent anesthesia for surgery, went on to exhibit POD [58, 90, 92-94].

POD is one of the most common postoperative complications faced by elderly patients undergoing surgery [6, 16]. It is estimated that POD occurs in up to 45% of elderly surgical patients [88]. POD is very prevalent in the elderly population for several reasons. One, elderly patients normally have other underlying comorbidities, such as dementia, diabetes, and vascular disease. Two, elderly patients may often be dehydrated, malnourished, and socially isolated, which all increases their risk for POD [88]. POD has become a serious problem in modern healthcare, and the problem will only become worse, as people that are 65 years of age and older comprise the most rapidly growing segment of the U.S. population [6]. In fact, it is projected that the world's older population (65+) will triple between 2009 and 2050, going from 516 million to 1.53 billion [6, 17]. This realization caused POD to emerge as an area of research interest, since the elderly commonly suffer from POD.

The effects of anesthesia on young, developing brains have long been a subject of research interest [94-96]. The brain is believed to be most susceptible to anesthetic insult during periods of intensive synaptogenesis, which occurs in humans roughly between the third trimester and three years of age [93, 97-100]. It is important to note that if a pregnant woman undergoes anesthesia, the volatile anesthetic can pass from

the mother to her child *in utero* at a critical time when the child's brain is rapidly developing [95, 96]. Delirium in the pediatric setting, known as pediatric delirium, is a significant problem that affects children undergoing anesthesia. There is a 25-40% prevalence rate of pediatric delirium in the pediatric intensive care unit [101, 102]. Children emerging from anesthesia are known to display the following symptoms: restlessness, agitation, excitation, inconsolable crying, delusions, struggling, and moaning [102, 103]. Studies done on very young animals report that exposure to anesthesia can result in neurodegeneration and increased neuronal apoptosis, impaired neurogenesis, increased neuroinflammation, deficits in behavioral development, and immediate and lasting cognitive impairment [92, 93, 95, 97, 98, 102, 104-107].

While numerous studies have indicated that many surgical patients given general anesthesia develop POD, the mechanism(s) by which anesthesia induces POD remains elusive. We have hypothesized that POD is caused by a temporary, anesthetic-induced breakdown of the blood-brain barrier (BBB). The BBB, which is formed in part by the vascular endothelium in the brain, is a highly selective barrier that prevents the entry of blood-borne cells and plasma components into the brain parenchyma and thus is crucial for maintaining brain homeostasis and the normal functioning of neurons in the CNS [8, 29, 67, 108-110]. In view of this, we have suggested that the anesthesia-induced increase in BBB permeability allows an influx of plasma components into the brain tissue that disrupts brain homeostasis and causes erratic neuronal misfiring. In the short-term, this culminates into the array of symptoms that hallmark POD. In the long-term, if not reversed or only partially

reversed, this could trigger chronic opening of the BBB and lead to subsequent postoperative cognitive decline (POCD) and Dementia.

In 2015, our lab published a preliminary paper looking at the effects of Sevoflurane and Isoflurane on the brain [45]. We tested the hypothesis that inhaled anesthetics (IAs) disrupt brain vascular endothelial cells (BVECs) and cause an increase in BBB permeability. Rats of three age groups (3-5 months; 10-12 months; 17-19 months) were anesthetized for three hours using either Sevoflurane or Isoflurane. Immunohistochemistry (IHC) revealed an increase in BBB permeability in older animals treated with Sevoflurane but not Isoflurane. Extravasated immunoglobulin G (IgG) showed affinity for pyramidal neurons. Scanning electron microscopy (SEM) of rat blood vessels exhibited substantial flattening of BVEC luminal surfaces in anesthesia-treated rats. The results suggested an aging-linked BBB compromise following exposure to Sevoflurane. Disruption of brain homeostasis following plasma influx into the brain parenchyma and binding of plasma components such as immunoglobulins to neurons may contribute to POD. Therefore, we proposed that exposure of the elderly to certain IAs can cause BBB compromise that disrupts brain homeostasis and neuronal function, and subsequently contributes to POD. If unresolved, this may progress to POCD and Dementia.

Based on the preliminary findings above, we decided to look further into this aging-linked BBB compromise and subsequent POD. Specifically, we wanted to look at the two age groups most affected by anesthesia and POD: the very young and the elderly.

Young children are undergoing rapid growth and brain development; we hypothesize that this rapid growth and development may render them more susceptible to chemical insult, such as exposure to anesthesia. Conversely, the elderly are susceptible to anesthetics for quite the opposite reason. It was reported long ago that during the aging process, the number of endothelial cells in brain blood vessels declines; therefore, the remaining endothelial cells are forced to elongate and spread out in order to fill the space between cells [85, 111-113]. We hypothesize that this decrease in endothelial cells and consequent elongation of remaining cells renders these cells susceptible to anesthetic exposure, as the cells now present a larger surface area for contact with anesthesia.

Here, we use both a pre-adolescent rat model and an elderly rat model to ask whether this heightened sensitivity to Sevoflurane is linked to increased blood-brain barrier (BBB) permeability and POD. Two-week old (pre-adolescent), four-week old (adolescent), and twenty-six month old (elderly) rats were subjected to Sevoflurane or Isoflurane for three hours. Animals were sacrificed and fixed by perfusion. Brains were processed for IHC and SEM. IHC was used to detect the presence, location, and extent of BBB compromise. SEM was used to directly visualize the effects of anesthesia on the luminal surfaces of brain vascular endothelial cells (BVECs) forming the BBB.

MATERIALS AND METHODS

Animals

Forty-five wild-type Sprague Dawley rats (Envigo) were maintained on food and water *ad libitum* in an AAALAC-accredited vivarium with a 12-hour light/dark cycle. Animal use was approved by the RowanSOM IACUC.

Animal Treatment

Fifteen two-week old (pre-adolescent), eighteen four-week old (adolescent), and twelve twenty-six month old (elderly) rats were subjected to Sevoflurane (1–3%) or Isoflurane (1–3%) for 3 hours. See **Table 1** for a breakdown of the animals used in this study. Anesthesia was first induced by exposing rats in an induction chamber to about 3% Sevoflurane or Isoflurane. Once surgical plane anesthesia was attained, they were removed from the induction chamber and put on a heat pad (T/Pump by Stryker, Kalamazoo, MI). Surgical plane anesthesia was maintained by supplying the anesthetic via a nose cone. The concentration of the anesthetic was gradually lowered but the animal was not allowed to either progress to deeper sleep or to regress to a wakeful state. The state of anesthesia was constantly monitored by testing for the pedal withdrawal reflex (toe pinch) and by pinching the tail. In addition, vital signs such as rate and depth of respiration were monitored and maintained (at 32±3 respirations per minute) by regulating the mixture of anesthetic and oxygen. Body temperature was maintained by a heated pad and by covering the body. A calibrated Midmark Matrx VMR table top anesthesia machine with a VIP 3000 well-fill style vaporizer was used to supply Sevoflurane (Sevothesia™; Henry Schein; Dublin, OH;

NDC: 11695-0501-2) and Isoflurane (Isothesia™; Henry Schein; Dublin, OH; NDC 11695-6776-2) with oxygen as the carrier gas. Separate vaporizers for Sevoflurane and Isoflurane were acquired and used as each rodent received only one type of anesthetic. The concentration of anesthetic required for maintaining surgical plane anesthesia varied between the age-groups and individuals. Rats were euthanized at the end of the third hour by exsanguination − the animal was perfused with phosphate-buffered saline (PBS) followed by freshly prepared 4% paraformaldehyde (PFA) in PBS. The control group included rats of all three age-groups that were not exposed to either anesthetic and were euthanized by CO2 asphyxiation. To achieve the best preservation of the brain tissue, all animals were fixed by perfusion using freshly prepared 4% PFA in PBS. Brains were quickly removed and, using a brain block, coronal sections were cut anteroposteriorly for bright-field microscopy, IHC, and SEM. Left hemispheres were sliced into 4mm thick sections for IHC; right hemispheres were sliced into 2mm thick sections for scanning electron microscopy. From the left hemispheres a total of four tissue blocks were generated − anterior, middle, posterior, and cerebellar. Anterior, middle, and posterior tissue blocks comprising different regions of cerebral cortex were the primary focus of this study.

Tissue Preparation, Immunohistochemistry, and Scanning Electron Microscopy

Brain tissues for IHC were fixed in 4% PFA and prepared for routine embedding in paraffin and sectioning as described previously [68]. Sections representing each brain region (anterior, middle, and posterior) were randomly selected for detection of extravasated IgG using IHC. IHC was performed using the protocol and reagents

described previously [68]. Extravasation of IgG has been widely used as a biomarker of BBB breach [45, 68-71, 114]. To detect IgG, biotinylated anti-rat IgG (Vector Laboratories, BA-9400, 1:20 in Dako antibody diluent) was used as the primary antibody [68, 69]. Cortical regions from each section were photographed using a Nikon Microphot-FXA microscope, and images were analyzed using NIS-Elements Imaging Software (Nikon Instruments Inc., USA). For SEM, brain tissue was fixed in 4% PFA, rinsed in PBS, and post-fixed with 1% osmium tetroxide. After washing in buffer, tissues were dehydrated in ethanol and then embedded in Carbowax Polyethylene Glycol (PEG, avg. mol. wt. = 6,000) (Electron Microscopy Sciences, USA). PEG was used as a removable embedding medium to physically support the architecture of the blood vessels while slicing through the delicate brain tissue to expose their luminal surfaces. After shaving the face of the samples to expose blood vessels, they were placed back in ethanol followed by amyl acetate. Samples were then dried in an E3100 critical point dryer (Quorum Technologies, USA) and rendered conductive by coating with a thin (~40Å) layer of gold using a Desk II sputter coater (Denton Vacuum, USA). Tissues were examined using an Apreo SEM (FEI, a subsidiary of Thermo Fisher Scientific).

EXPERIMENTAL RESULTS

Sevoflurane (and Isoflurane to a Lesser Degree) Increases BBB Permeability in Pre-adolescent and Elderly Rats

To assess the effects of the inhaled anesthetics on the functional integrity (permeability) of the BBB, pre-adolescent (2-weeks old), adolescent (4-weeks old), and elderly (26-months old) rats were subjected to surgical plane anesthesia using Sevoflurane or Isoflurane for 3 hours and then euthanized. Brains were fixed by perfusion, and IHC was utilized to detect and compare the leak of plasma components from blood vessels into the surrounding brain tissue of anesthetic-treated and untreated (control) rats. IgG, which is normally excluded from the brain tissue via the BBB, was used as a biomarker of plasma leak into the brain (**Fig. 1**). Results showed that leak of IgG into the brain interstitium was not detected in untreated (control) pre-adolescent or adolescent rats, but occasional leaks from blood vessels (mostly small arterioles) were observed in the cerebral cortex of elderly control rats, appearing as small IgG-positive leak clouds surrounding the leaking vessel (**Fig. 1A-C**). By contrast, IgG leaks from cortical blood vessels were much more prevalent and prominent in both pre-adolescent (**Fig. 1D, G, J**) and elderly (**Fig. 1F, I, L**) animals treated with Sevoflurane or Isoflurane than in adolescent animals receiving the same anesthesia (**Fig. 1E, H,** and **K**). In pre-adolescent and elderly animals exposed to Sevoflurane or Isoflurane, certain neuronal subtypes (especially pyramidal neurons) in the vicinity of the leak were selectively IgG-immunopositive (**Fig. 1G, I, J, L**). Overall, leaks in the brain vasculature and neuronal IgG binding were much more extensive in Sevoflurane-treated pre-adolescent and elderly animals (**Fig. 1G-I**) than

in Isoflurane-treated animals (**Fig. 1D-F**). Interestingly, brain blood vessels showing plasma leaks were only rarely observed in adolescent (4-week-old) animals exposed to Sevoflurane or Isoflurane.

Age-Dependent Changes in the Luminal Surface Topography of Brain Vascular Endothelial Cells Associated with Development and Maintenance of the BBB

During infancy and pre-adolescence, the brain undergoes a dramatic increase in size. This period of remarkable growth and development requires a corresponding continuous expansion of the brain vasculature (neovascularization). In each of these newly formed vessels, adjacent brain vascular endothelial cells (BVECs) that form the inner lining must establish new tight junctional contacts that contribute to the BBB so as to strictly regulate what enters into the brain tissue from the blood. Here, we used SEM to examine changes in the luminal surface topography of BVECs associated with development of the marginal tight junctions during the establishment and maintenance of the BBB. To achieve this, brains were fixed by perfusion and embedded in polyethylene glycol (PEG, avg. mol. wt. = 6,000). PEG was used as a removable embedding medium which physically supported the delicate architecture of the brain tissue and blood vessels while slicing through the tissue to expose the luminal surfaces of BVECs. As shown in **Figure 2**, this approach allowed direct examination of the luminal surfaces of adjacent BVECs, including tight junctional contacts at their cell margins that contribute to the BBB, in longitudinal, oblique, and cross-sectional profiles. We first compared the luminal surface topography of BVECs in pre-adolescent, adolescent, and elderly control animals not exposed to inhalation

anesthetics. Marked age-associated differences were noted at the margins of BVECs. For example, in pre-adolescent animals, BVECs were more closely packed than in comparable vessels of older animals and oriented parallel to the long axis of the vessel. Much of their cytoplasm along with nuclei bulged into the lumen (**Fig. 2A**). At the interface of adjacent elongated BVECs, prominent, continuous, sheet-like cytoplasmic extensions (here referred to as contact flaps) projected upwards into the lumen, running parallel to the direction of blood flow. These contact flaps resembled the membrane ruffles commonly seen at the leading edges of migrating cells in culture. Contact flaps occur at adjacent cell margins, where tight junctions are known to provide the initial seal for the BBB (**Fig. 2A**). In adolescent control animals not exposed to anesthetics, BVECs tended to be flatter with small microvilli scattered over their surfaces. Contact flaps associated with the BBB were much less prominent than in 2-week old pre-adolescent animals, showing remnants of the larger sheet-like processes interspersed among much shorter contact flaps (**Fig. 2B**). In elderly (26-month old) control animals, most BVECs were flattened and well-spread out, with much smaller contact flaps projecting upwards into the lumen and maintaining a fairly uniform height while running along adjacent cell margins (**Fig. 2C**).

Sevoflurane and Isoflurane Induce Changes in BVEC Luminal Surface Topography That May Be Linked to Increased BBB Permeability

Two-week old (pre-adolescent), four-week old (adolescent), and twenty-six month old (elderly) rats were subjected to Sevoflurane (1-3%) or Isoflurane (1-3%) for 3 hours. In pre-adolescent rats, exposure to Sevoflurane led to a pronounced flattening

of the luminal surfaces of BVECs, resulting in fewer microvilli and a collapse of contact flaps between adjacent cells (**Fig. 3A-B**). Similar changes in BVECs were seen in adolescent (4-week old) rats (**Fig. 3C-D**). In 26-month old rats, the luminal surfaces of BVECs were often so flattened that it was difficult to delineate the borders between adjacent cells (**Fig. 3E-F**). The effects of Isoflurane on BVECs were similar in that the luminal surfaces of these cells were considerably flattened with loss of microvilli, but differed from Sevoflurane in that contact flaps associated with the BBB remained distinctive in the three age groups examined (**Fig. 4A-C**).

DISCUSSION

The negative effects of anesthesia that selectively target pediatric and elderly patients have been known for a very long time [58, 94-96]. Particularly intriguing is the well-known heightened vulnerability of individuals in both age groups to postoperative delirium (POD) [58, 90, 94]. Mechanisms underlying the linkage between anesthesia and POD are poorly understood [92]. In a previous study using a rat model, we presented evidence that the inhalation anesthetic Sevoflurane, and to a lesser extent the inhaled anesthetic Isoflurane, induces transient increases in blood-brain barrier (BBB) permeability, leading to a leak of plasma components into the brain parenchyma [45]. Here, we have used pre-adolescent (2-weeks old), adolescent (4-weeks old), and elderly (26-months old) rats to ask whether or not the observed selective vulnerability of pre-adolescents and the elderly to POD is due to age-specific changes in BBB structural/functional status. Immunohistochemistry (IHC) and scanning electron microscopy (SEM) were used to monitor BBB structure/function.

This study has three major findings. First, using SEM, we show that brain vascular endothelial cells (BVECs) that line the lumen of blood vessels exhibit prominent age-related differences in cell shape and luminal surface topography. In pre-adolescent (2-weeks old) rats, BVECs are elongated parallel to the long axis of the vessel and are densely packed, with cell bodies bulging into the lumen and luminal surfaces dotted with numerous microvilli. At their margins, which is the region containing tight junctions associated with the BBB, the marginal cytoplasm forms large sheet-like

contact flaps that project upwards into the lumen. In adolescent (4-weeks old) and elderly (26-months old) rats, BVEC luminal surfaces undergo a pronounced overall flattening, where the sheet-like contact flaps transition between these two age groups into a shortened ridge of uniform height delineating the cell margins. Second, IHC using IgG as a biomarker of plasma extravasation shows that exposure of rats to Sevoflurane (and to a lesser degree Isoflurane) transiently increases BBB permeability more dramatically in pre-adolescent and elderly rats than in adolescent rats, suggesting a link between the extent of BBB permeability and expression of POD. The frequent observation that extravasated IgG shows selective binding affinity for the surfaces of certain types of neurons raises the possibility that this binding, and perhaps antibody crosslinking, disturbs the normal pattern of neuronal activity, which could conceivably contribute to expression of delirium. Lastly, we show that the transient increase in BBB permeability induced by anesthetics is accompanied by marked overall flattening or smoothing of BVEC luminal surface topography, including the collapse of their marginal contact flaps and loss of microvilli.

Our results suggest that anesthetics cause changes in the physical properties of BVEC luminal surface membranes that mediate their flattening, and that these changes are accompanied by increased BBB permeability. Whether or not these changes in BBB permeability are due to impaired function of tight junction proteins or changes in the physical properties of the surface membranes remains to be determined. Furthermore, the rapid brain growth, extensive neovascularization, and *de novo* establishment of the BBB continuously occurring in the newly forming blood vessels of pre-adolescent

brains makes this stage particularly vulnerable to conditions that challenge the structural/functional integrity of the BBB and can therefore lead to expression of POD. In elderly rats, the combination of increased BVEC spreading due to decreased cell density, flattening of luminal surface membranes, and collapse of contact flaps at cell margins upon exposure to these anesthetics would also favor transient BBB compromise and POD in this age group. We propose that this anesthesia-induced increase in BBB permeability results in a plasma influx into the brain parenchyma that disrupts brain homeostasis and neuronal activity, triggering POD. In the elderly, if left unresolved, it can lead to postoperative cognitive decline (POCD) and perhaps be a trigger for later dementia. A diagram summarizing the interplay of these events that may predispose both young children and the elderly to POD is presented in **Figure 5**.

Some patients who receive anesthesia for surgery and subsequently display POD, particularly the very young and very old, go on to exhibit lasting cognitive dysfunction [92, 115]. In the young, it has been reported that exposure to anesthesia and surgery are associated with later abnormal behavioral, learning, and neurodevelopmental outcomes [116]. It was also reported that exposing children to anesthesia and surgery is associated with an increase in diagnosis of learning disabilities or attention-deficit/hyperactivity disorder (ADHD) [116]. Cognitive performance and the ability to compensate for possible deficits decline with advancing age, which makes undergoing anesthesia and surgery a major risk for the elderly [117]. Many who undergo surgery come out delirious, and they may never

fully regain the mental capacity they had prior to anesthesia and surgery. It has been suggested that, in pre-adolescent individuals, exposure to anesthesia during critical phases of CNS development can trigger a number of structural changes in the developing brain, including loss of pyramidal neurons via cell death that may contribute to more permanent functional deficits. At the other end of the aging spectrum, many aging-associated changes that occur in blood vessels have been reported that may help explain frequent observations of increased BBB permeability. These changes include increased basement membrane thickness, local gliofibrillar proliferation, a decrease in the number of mitochondria in BVECs, and, most importantly, a decrease in the overall number of BVECs, the latter of which requires existing BVECs to spread out more extensively in an effort to adequately cover the luminal surfaces of blood vessels and compensate for cell loss [85, 111-113]. All of these changes naturally lead to an increased prevalence of BBB leakage during aging [118-121]. Also, several studies have reported that the number of BVECs per unit area in rats decreases continually from birth to 30 months old [111, 112, 122]. It is conceivable that the resulting requirement for a greater extent of BVEC spreading in brain blood vessels of the elderly makes these cells particularly sensitive to various stressors and chemical insults, including anesthesia. Our data agree with Lee et al. who showed that aged brains have greater BBB permeability than younger adult brains following a controlled cortical impact (CCI). Furthermore, they show that BBB disruption after CCI injury is intensified in the elderly and most likely contributes to a worse outcome after traumatic brain injury [123]. Jevtovic-Todorovic et al. have emphasized that exposure of the very young and very old to anesthesia could be

detrimental to the brain, pointing out that children who undergo anesthesia during their first two years of life experience a higher incidence of postoperative psychological disturbances than older children [93]. They also raise a question as to whether exposing children to anesthetics could be promoting excessive activation of neuroapoptosis and death of large populations of developing neurons, and that the longer a child is exposed to anesthesia, the more likely that child will exhibit some form of learning disability later in life [93].

This study has several strengths. One strength is that this study focuses on the effects of a single anesthetic (Sevoflurane or Isoflurane) on rats of various age groups, making it possible to attribute observed effects to a single anesthetic. Another strength is the use of SEM to examine directly the effects of anesthesia on large areas of the brain's endothelial lining and the interface of adjacent BVECs that contributes to the BBB. There are also a few weaknesses. The first is the small sample size of the group of elderly rats, due to the extreme cost associated with housing and providing for these animals for such extended periods of time. That being said, there was an easily discernable pattern of effects of these inhalation anesthetics on BBB integrity in the elderly animals. Additional studies using larger numbers of rats from all age-groups would be helpful in bolstering further conclusions. Second, although also seen as a strength as mentioned above, the treatment of animals with an individual anesthetic, as carried out in the present study, can also be viewed as a weakness, since it fails to match the induction of general anesthesia in humans, which typically also

includes other combinations of intravenous anesthetic agents, opioids, or muscle relaxants.

In conclusion, the data presented here suggest that Sevoflurane is more potent than Isoflurane in causing increased BBB permeability in the rat model, particularly in young pediatric (pre-adolescent) and elderly subjects. Both anesthetics directly alter the luminal surface topography of BVECs, particularly in regions of BBB-associated tight junctions. We propose that Sevoflurane compromises the BBB in pre-adolescent individuals because their brains are engaged in a period of rapid growth and neovascularization, which includes the initial formation and establishment of the BBB. By contrast, in the elderly, we propose that Sevoflurane favors increased BBB permeability because of the aging-associated changes in their blood vessels, including a decrease in the number of BVECs that line the luminal surfaces of these vessels. This forces the remaining BVECs to further spread out while retaining firm connections to adjacent cells, a feature that may make them particularly sensitive to insults, including anesthesia. In both cases, increased BBB permeability allows an influx of plasma components into the brain parenchyma, which disrupts brain homeostasis and proper neuronal functioning. For example, binding of IgG to the surfaces of neurons may further exacerbate neuronal dysfunction and misfiring, thereby contributing to the emergence of symptoms associated with POD. We suggest that subsequent failure to completely restore BBB function following surgery could lead to postoperative cognitive decline (POCD) in the short-term and, if unresolved, may favor the development of dementia in the long-term. Therefore, maintenance of

proper BBB function is crucial for preventing the occurrence and escalation of POD, POCD, and later cognitive changes. These findings also suggest the potential benefits of identifying and using inhalation anesthetics that are less disruptive to the BBB, especially for the particularly vulnerable young pediatric and elderly populations.

FIGURES

Table 1: List of Animals Used in this Study

Identification Number	Age	DOB	DOE	Anesthesia Used
Pediatric Rat 1	~4 weeks	10/8/2016	11/7/2016	Iso
Pediatric Rat 2	~4 weeks	10/8/2016	11/7/2016	Iso
Pediatric Rat 3	~4 weeks	10/8/2016	11/7/2016	Control
Pediatric Rat 4	~4 weeks	10/8/2016	11/7/2016	Control
Pediatric Rat 5	~4 weeks	10/8/2016	11/8/2016	Sevo
Pediatric Rat 6	~4 weeks	10/8/2016	11/8/2016	Sevo
Pediatric Rat 7	~4 weeks	10/8/2016	11/8/2016	Control
Pediatric Rat 8	~4 weeks	10/24/2016	11/21/2016	Sevo
Pediatric Rat 9	~4 weeks	10/24/2016	11/21/2016	Sevo
Pediatric Rat 10	~4 weeks	11/13/2016	12/14/2016	Sevo
Pediatric Rat 11	~4 weeks	11/13/2016	12/14/2016	Sevo
Pediatric Rat 12	~4 weeks	11/13/2016	12/14/2016	Iso
Pediatric Rat 13	~4 weeks	11/13/2016	12/15/2016	Iso
Pediatric Rat 14	~4 weeks	11/13/2016	12/15/2016	Iso
Pediatric Rat 15	~4 weeks	11/13/2016	12/14/2016	Sevo
Pediatric Rat 16	~4 weeks	11/15/2016	12/15/2016	Iso
Pediatric Rat 17	~4 weeks	11/15/2016	12/15/2016	Iso
Pediatric Rat 18	~4 weeks	11/15/2016	12/15/2016	Control
Pediatric Rat 19	~2 weeks	12/7/2016	12/22/2016	Sevo
Pediatric Rat 20	~2 weeks	12/7/2016	12/22/2016	Sevo
Pediatric Rat 21	~2 weeks	1/1/2017	1/17/2017	Iso
Pediatric Rat 22	~2 weeks	1/1/2017	1/17/2017	Iso
Pediatric Rat 23	~2 weeks	1/1/2017	1/17/2017	Iso
Pediatric Rat 24	~2 weeks	1/1/2017	1/17/2017	Control
Pediatric Rat 25	~2 weeks	1/1/2017	1/17/2017	Control
Pediatric Rat 26	~2 weeks	1/1/2017	1/17/2017	Control
Pediatric Rat 27	~2 weeks	1/1/2017	1/17/2017	Control
Pediatric Rat 28	~2 weeks	1/1/2017	1/17/2017	Control
Pediatric Rat 29	~2 weeks	1/1/2017	1/17/2017	Iso
Pediatric Rat 30	~2 weeks	1/1/2017	1/17/2017	Iso
Pediatric Rat 31	~2 weeks	1/1/2017	1/18/2017	Sevo
Pediatric Rat 32	~2 weeks	1/1/2017	1/18/2017	Sevo
Pediatric Rat 33	~2 weeks	1/1/2017	1/18/2017	Sevo
Old Age 1	~26 months	11/1/2014	12/22/2016	Control
Old Age 2	~26 months	11/1/2014	12/22/2016	Control
Old Age 3	~26 months	11/1/2014	12/27/2016	Sevo
Old Age 4	~26 months	11/1/2014	12/27/2016	Sevo
Old Age 5	~26 months	11/1/2014	12/27/2016	Iso
Old Age 6	~26 months	11/1/2014	12/27/2016	Sevo
Old Age 7	~26 months	11/1/2014	12/27/2016	Sevo
Old Age 8	~26 months	11/1/2014	12/27/2016	Iso
Old Age 9	~26 months	11/1/2014	12/27/2016	Iso
Old Age 10	~26 months	11/1/2014	12/28/2016	Sevo
Old Age 11	~26 months	11/1/2014	12/28/2016	Iso
Old Age 12	~26 months	11/1/2014	12/28/2016	Iso

This is a comprehensive list of the animals used in this study. Control - Unanesthetized Animals; DOB - Date of Birth; DOE - Date of Expiration; Iso - Isoflurane; LPS - Lipopolysaccharides; Sevo - Sevoflurane.

Figure 1: Sevoflurane Selectively Increases BBB Permeability in the Cerebral Cortex of Pre-Adolescent and Elderly Rats

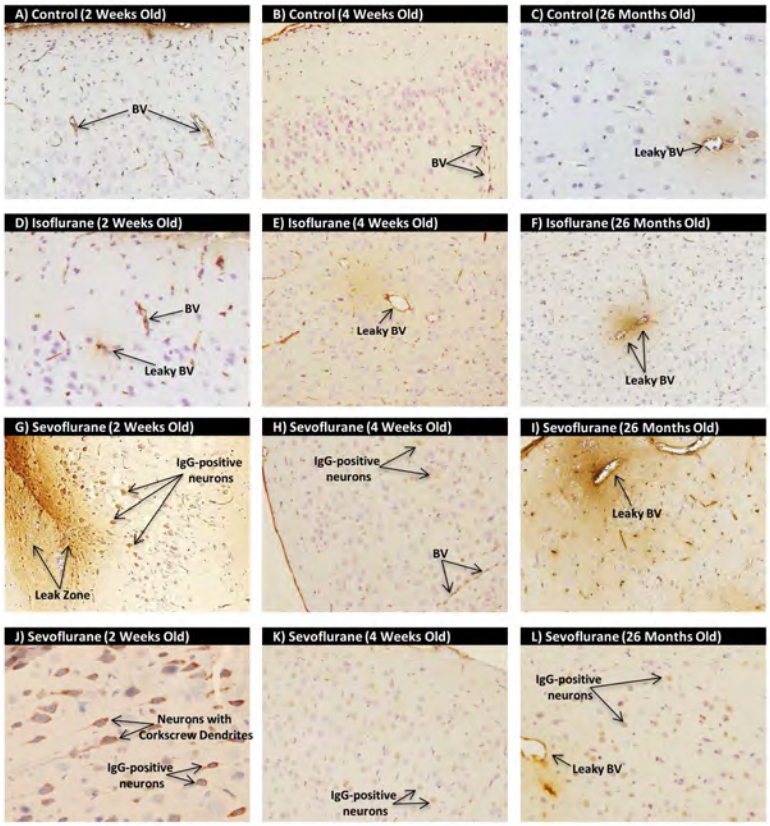

Histological sections of the cerebral cortex of pre-adolescent (2-week old), adolescent (4-week old), and elderly (26-month old) rat brains immunostained to detect IgG. (**A-C**) In brains from 2-week and 4-week old rats, IgG is restricted to the lumen of blood vessels (BV), whereas some vessels in 26-month old rats show small amounts of perivascular IgG in the brain parenchyma indicative of increased BBB permeability. (**D-F**) Rats in each of the age groups exposed to Isoflurane showed evidence of small increases in BBB permeability to IgG. (**G-I**) In rats exposed to Sevoflurane, both the youngest (2-week old) and oldest (26-month old) animals show dramatic increases in BBB permeability as evidenced by prominent perivascular IgG-positive leak clouds. In some sections of Sevoflurane-treated animals at 2-weeks and 26-months of age, IgG appeared to bind selectively to pyramidal neurons in the vicinity of the leak cloud, while this was only rarely observed in 4-week old animals exposed to Sevoflurane. BV - Blood Vessel; IgG - Immunoglobulin G.

Figure 2: Age-Dependent Changes in BVEC Luminal Surface Topography Associated with Development and Maturation of the BBB

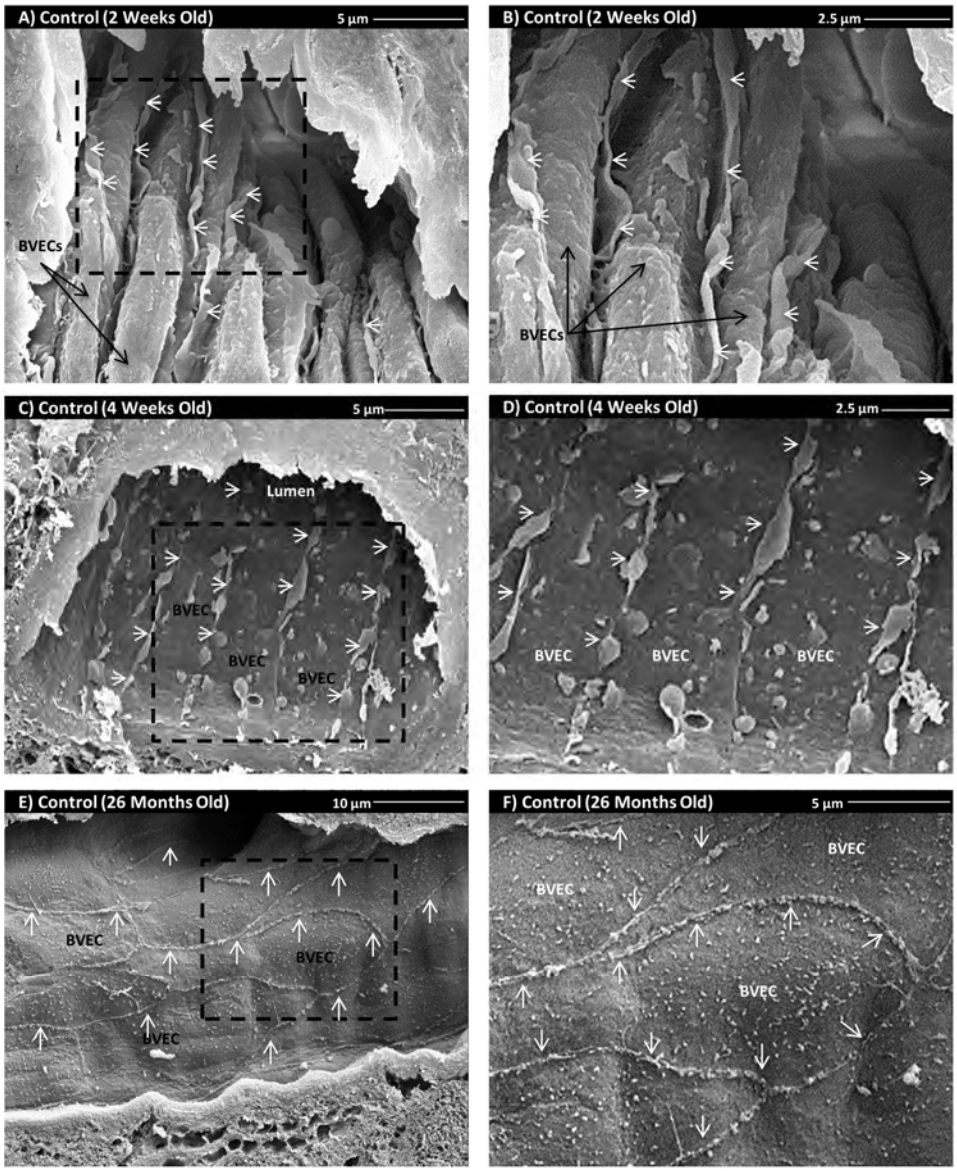

Figure 2: Age-Dependent Changes in the Luminal Surface Topography of Brain Vascular Endothelial Cells (BVECs) Associated with Development and Maturation of the BBB.

SEM was used to examine age-related changes in the luminal surface topography associated with development and maturation of BBB-associated tight junctions located at the margins of adjacent BVECs. (**A-B**) In brain blood vessels of 2-week old rats, BVECs are oriented parallel to the long axis of the vessel with much of their perinuclear cytoplasm bulging upward from the floor and projecting into the lumen. Regions of contact between adjacent cells that include the BBB are highlighted by the presence of prominent, sheet-like cytoplasmic extensions (contact flaps) originating from each cell that project upward into the lumen (arrows) and run along the entire length of adjacent BVECs. (**C-D**) By 4-weeks of age, individual BVECs have undergone marked flattening, leaving large areas of the luminal surface covered by parallel rows of contact flaps of variable height (arrows). In elderly rats (26-month old), BVEC luminal surfaces are considerably flattened and display a considerable number of small microvilli. The margins of adjacent cells display much smaller contact flaps (arrows) of roughly uniform height projecting upwards from the luminal surface, and the seams between favorably oriented plasma membranes of adjacent cells are notable (solid arrowheads). BVEC - Brain Vascular Endothelial Cell.

Figure 3: Sevoflurane Causes a Pronounced Flattening of the Luminal Surface Topography of BVECs and Collapse of BBB-Associated Contact Flaps at Cell Margins

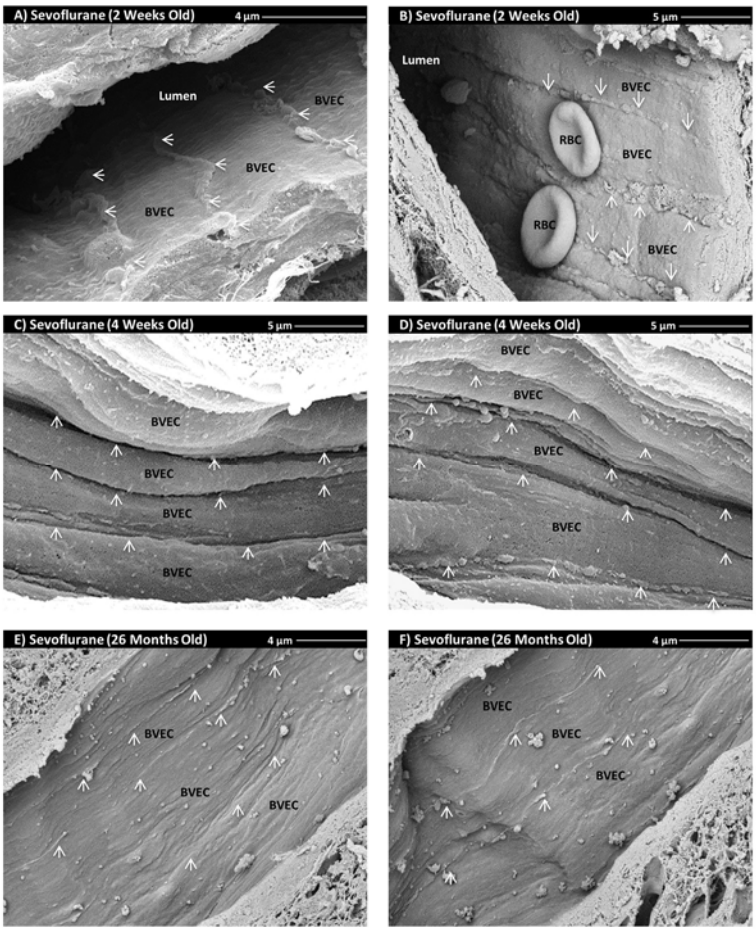

SEM was used to assess the luminal surfaces of blood vessels in pre-adolescent (2-week old), adolescent (4-week old), and elderly (26-month old) rats after exposure to Sevoflurane. (**A-B)** In two-week old rats, exposure to Sevoflurane was associated with a marked smoothing of the luminal surfaces of BVECs. Contact flaps in the region of BBB-associated tight junctions were no longer vertical and were collapsed onto the marginal surfaces of BVECs. (**C-D**) Sevoflurane-treated four-week old rats showed similar changes in the luminal surfaces of BVECs. (**E-F**) In elderly (26-month old) rats exposed to Sevoflurane, adjacent BVECs showed considerable luminal surface flattening, with marginal BBB-associated contact flaps often difficult to discern. BVEC - Brain Vascular Endothelial Cell; RBC - Red Blood Cell.

Figure 4: Isoflurane Also Causes a Pronounced Flattening of the Luminal Surface Topography of BVECs but Has Less of an Effect on the Morphology of BBB-Associated Contact Flaps

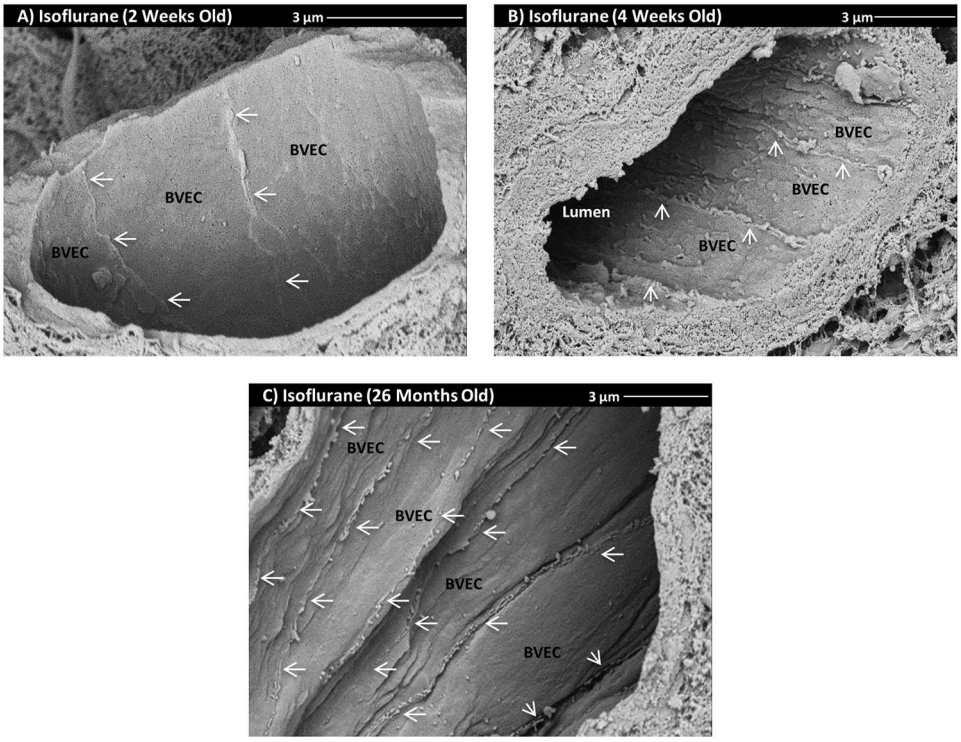

(**A-C**) SEM was used to assess the effects of exposure to Isoflurane on the luminal surface topography of BVECs in 2-week old, 4-week old, and 26-month old rats. Luminal surfaces of BVECs were considerably flattened in all age groups, with BVECs of 2-week old and 26-month old rats nearly devoid of microvilli. Some microvilli persisted in 4-week old rats (**B**). (**C**) BBB-associated contact flaps remained more prominent in Isoflurane-treated rats than in Sevoflurane-treated rats. BVEC - Brain Vascular Endothelial Cell.

Figure 5: Proposed Mechanism for the Heighted Incidence of Delirium in the Very Young and Very Old Following Exposure to Inhaled Anesthetics such as Sevoflurane and Isoflurane

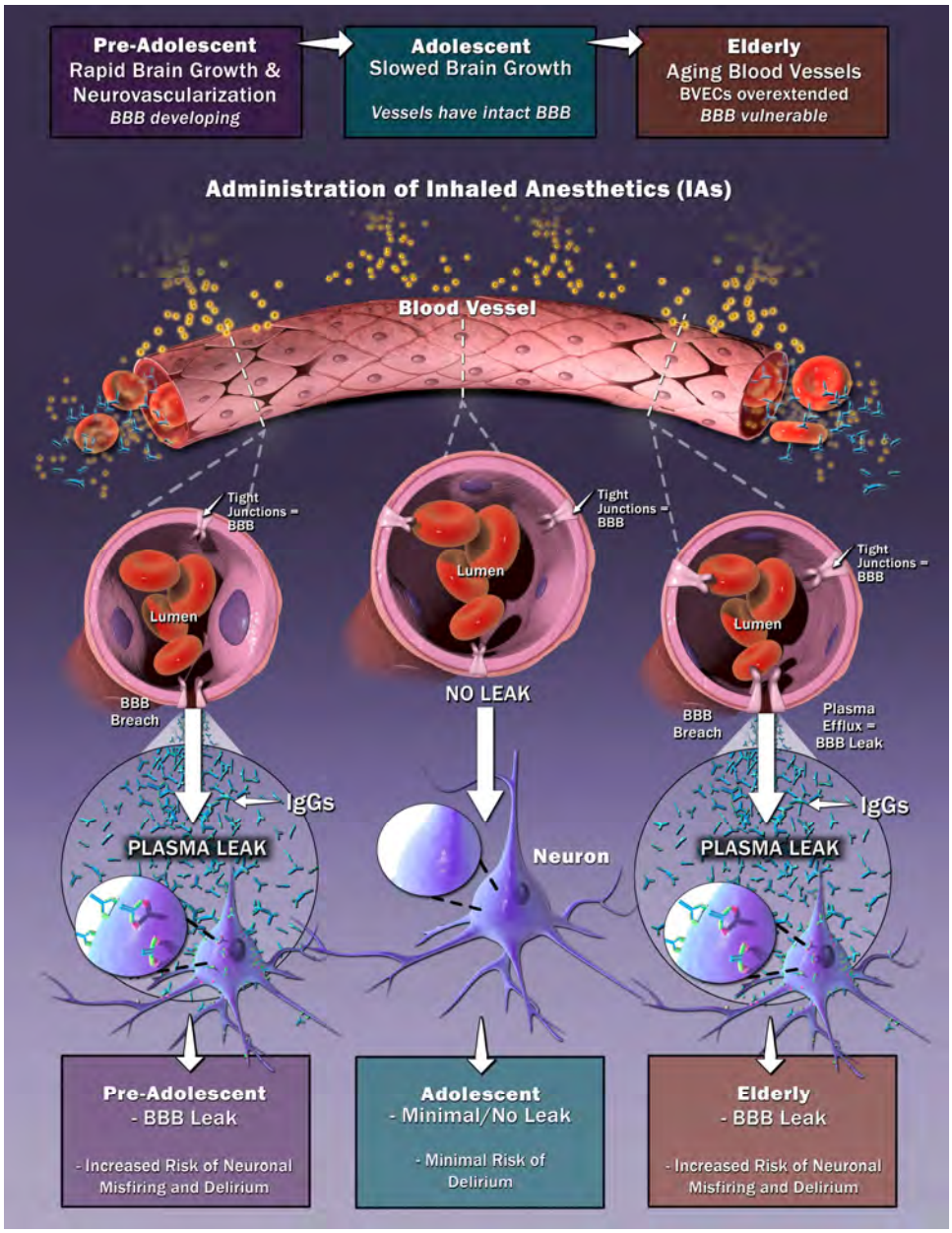

Figure 5: Proposed Mechanism for the Heighted Incidence of Delirium in the Very Young and Very Old Following Exposure to Inhaled Anesthetics such as Sevoflurane and Isoflurane.

Results of this study carried out on rats suggest that the heightened sensitivity of pre-adolescent children and the elderly to inhaled anesthetics, particularly Sevoflurane, may be due to an anesthesia-induced increase in BBB permeability. We propose that **pre-adolescents** are particularly vulnerable to Sevoflurane-induced delirium because the brain is engaged in a period of rapid growth which includes considerable neovascularization. The growth of blood vessels requires a continuous process of initial formation and establishment of BBB-associated tight junctions between adjacent BVECs, a process that likely renders the forming BBB of these vessels more vulnerable to the disruptive effects of inhaled anesthetics, such as Sevoflurane and Isoflurane, as shown in 2-week old rats. In **adolescents**, the growth in the size of the brain is greatly slowed, thus reducing the rate of neovascularization and increasing the proportion of blood vessels in the brain with an established BBB. As shown repeatedly in previous immunohistochemical studies on the human brain, the **elderly** are more prone to increased BBB permeability due to aging-associated changes in blood vessels, a feature which makes them particularly sensitive to insults, including anesthesia. We propose that increased plasma influx through a permeable BBB disrupts brain homeostasis and normal patterns of neuronal activity, triggering POD in the short-term. In pre-adolescents, this may be linked to later, long-term cognitive changes and deficits. In the elderly, this may lead to subsequent postoperative cognitive decline (POCD) and perhaps later dementia. BBB - Blood-Brain Barrier; BVEC - Brain Vascular Endothelial Cell; IA - Inhaled Anesthetic; IgG - Immunoglobulin G; TJ - Tight Junction.

CHAPTER V:

Effects of Anesthetics and Select Agents on the Barrier Function of Human Brain Vascular Endothelial Cells *In Vitro*

ABSTRACT

Background

Delirium is a highly prevalent neurocognitive disorder that presents a major problem to modern healthcare. Patients suffering from delirium normally have a worse prognosis, prolonged hospital stay, increased hospital cost, long-term cognitive impairment, and higher mortality rates. A subtype of delirium known as Postoperative Delirium (POD) is one of the most common postoperative complications faced by elderly patients undergoing surgery. A large percentage of patients that are 65 years and older exhibit POD after being subjected to general anesthesia. Many subsequently develop Postoperative Cognitive Decline (POCD) and Dementia. Unraveling the mechanism by which anesthesia induces POD in patients is one goal of this study.

Objective

We test the hypothesis that inhaled anesthetics (IAs) and other select agents directly affect brain vascular endothelial cells (BVECs) and increase blood-brain barrier (BBB) permeability.

Methods

Immunocytochemistry (ICC) was performed on hCMEC/D3 cells (a human brain vascular endothelial cell line) to visualize tight junction protein expression and distribution. Tight junction protein expression was also verified by Western Blot of confluent hCMEC/D3 cells. Live cell imaging was utilized to monitor the short-term response of hCMEC/D3 cells to anesthesia and other select agents. Both Trans-Endothelial Electrical Resistance (TEER) measurements and permeability assays were utilized in order to determine the effects of anesthesia and other select agents on BBB permeability. Endothelial cells exposed to Pertussis toxin were examined and used as positive controls of BBB disruption. Finally, endothelial cells were also exposed to histamine and acetaminophen, as both drugs are known to disrupt the BBB.

Results

Immunocytochemistry verified that hCMEC/D3 cells express tight junction proteins at cell-cell contacts, supporting the use of this cell line as an *in vitro* BBB model. Western Blot also verified that the hCMEC/D3 cell line expresses tight junction proteins. TEER measurements revealed that Sevoflurane, Isoflurane, and Propofol cause a reduction in TEER values, which is equivalent to an increase in BBB permeability. Permeability assays confirmed an increase in BBB permeability after exposure to Sevoflurane, Isoflurane, and Propofol. Pertussis toxin, Histamine, and Acetaminophen induced cell contraction in hCMEC/D3 cells.

Conclusion

Sevoflurane, Isoflurane, and Propofol directly affect the surface membranes of BVECs, leading to an increase in BBB permeability, while Pertussis toxin, Histamine, and Acetaminophen induce BVEC contraction, which is an action that exerts tractional forces on the tight junctions responsible for maintaining the barrier properties of the BBB. We propose that, in each instance, this increase in BBB permeability allows an influx of plasma components into the brain tissue that results in a loss of brain homeostasis, disrupts neuronal function, and leads to the manifestation of POD in the short term and potentially POCD and Dementia in the long term.

INTRODUCTION

Delirium is a highly prevalent neuropsychiatric or neurocognitive disorder that presents a major problem to modern healthcare. Patients suffering from delirium normally have a worse prognosis, prolonged hospital stay, increased hospital cost, long-term cognitive impairment, and higher mortality rates. Many factors can predispose one to develop delirium, which makes treating this disorder a daunting task. Unfortunately, delirium is the most common psychiatric syndrome found in the hospital setting. In fact, a form of delirium known as postoperative delirium (POD) is one of the most common postoperative complications faced by elderly patients undergoing surgery.

POD is a major problem in modern healthcare, and it will only become worse because the world's older population (65+) is projected to triple between 2009 and 2050. This realization caused POD to emerge as an area of research interest. Many precipitating factors can cause one to develop POD, including exposure to anesthetics. Studies have indicated that many patients who were given general anesthesia have developed delirium; however, no studies have explained the mechanism by which anesthesia induces POD in patients. Unraveling the mechanism is one goal of this study.

Our lab has hypothesized that POD is caused by a temporary, anesthesia- or drug-induced breakdown of the blood-brain barrier (BBB). The BBB, which is formed by the vascular endothelium in the brain, is a highly selective barrier that separates the circulating blood from the brain and prevents a large number of substances from

entering the brain. We believe that BBB breakdown after exposure to anesthetics allows an influx of plasma components into the brain tissue that disrupts brain homeostasis and causes neuronal misfiring. In the short-term, this culminates into the array of symptoms that hallmark POD. In the long-term, if not reversed or only partially reversed, this could trigger subsequent Postoperative Cognitive Decline (POCD) and Dementia.

Preliminary *in vivo* studies conducted in our lab revealed that exposure to the inhalation anesthetics (IAs) Sevoflurane and Isoflurane causes immediate structural changes in brain vascular endothelial cells (BVECs), including an overall flattening of surface membranes and loss of the tight junction ridge. These structural changes can lead to the formation of holes in the vascular endothelial lining. Enhanced IgG-positive immunostaining of brain tissue revealed that exposure to Sevoflurane leads to an increase in BBB permeability [45].

After examining the effects of IAs on rat BVECs *in vivo* [45], it was decided to then examine the effects of IAs on BVECS *in vitro* using the hCMEC/D3 cell line, which is a well-established human cerebral microvascular endothelial cell line. It is widely used as an *in vitro* model of the BBB because it expresses a variety of brain endothelial markers, tight junction (TJ) proteins, adherens junction (AJ) proteins, and transporters [48, 124-128].

First, hCMEC/D3 cells were raised to 100% confluence in glass-bottom petri dishes,

and then Immunocytochemistry (ICC) was performed on the cells in order to detect the tight junction proteins expressed at cell borders. Next, IAs were administered to these cells. Live cell imaging prior to, during, and after the treatment was used to observe and study the effects of IAs on the structure and behavior of human BVECs (**Fig. 1**).

Once these initial screening runs were complete, the cells were seeded and raised on Transwell Inserts in twelve-well plates. The Transwell Inserts divide each well into two chambers: an upper apical (luminal) chamber and a lower basolateral (abluminal) chamber (**Fig. 2A**). Raising hCMEC/D3 cells to 100% confluence on the inserts allows the cells to establish a permeability barrier between the chambers that is similar to the BBB *in vivo*. Once the cells reached 100% confluence and established their barrier function, they were exposed to IAs and later to other select agents (i.e., Pertussis toxin, Histamine, and Acetaminophen). Trans-Endothelial Electrical Resistance (TEER) was used to evaluate BBB integrity prior to and after IA exposure. TEER values were evaluated to determine if there was a change in BBB permeability. An increase in TEER values is associated with a decrease in BBB permeability, whereas a decrease in TEER values is associated with an increase in BBB permeability. TEER was measured before and after IA exposure (**Fig. 2B**). Next, permeability experiments were performed. The rate of transfer of fluorescent dyes or fluorescent dye-dextran conjugates from the upper chamber to the lower chamber was measured.

Other experiments were also conducted using this *in vitro* model of the BBB. The ultimate goal was to elucidate the mechanism of anesthesia-induced delirium in surgical patients, as well as to identify any means by which this disorder could be lessened or prevented altogether.

MATERIALS AND METHODS

Cell Culture

A vial of hCMEC/D3 cells was removed from liquid nitrogen storage and quickly transported to a 37°C hot water bath. The vial was immersed in a 37°C water bath and allowed to thaw for 1-2 minutes. Once thawed, the cryovial was transferred to a laminar flow hood and disinfected with 70% ethanol. Excess 70% ethanol was aspirated from the thread area of the screw cap, then the vial was opened and the cells were transferred to a pre-prepared culture vessel containing pre-warmed Endothelial Cell Basal Medium-2 (EBM-2) (Lonza) containing FBS and growth supplements as described previously [124]. The culture vessel was then placed in an incubator. After 24 hours, when cells are attached to the bottom of the culture vessel, we replaced the medium with fresh medium. Cells were maintained in this dish for 3-4 days until they reached 80-90% confluency, and then they were passaged/subcultured.

Subculturing/Passaging the Cells

When the cells reached approximately 80-90% confluence, they were passaged/subcultured. First, the cell culture medium was carefully aspirated out of the cell culture vessel and discarded. Then, the cell monolayer was rinsed with PBS three times. Next, Trypsin-EDTA solution (2ml per 25cm^2 of vessel surface) was added to the cells. The cells were incubated in the Trypsin-EDTA solution at 37°C for 1-3 minutes to allow the cells to detach from the vessel surface. Detachment of the cells from the vessel surface was observed in an inverted microscope (Nikon). Gently tap the sides or bottom of the vessel to loosen any cells still sticking to the vessel surface.

Once the cells finished detaching from the vessel surface, they were detrypsinized by adding complete growth medium (4ml per 25cm^2 of vessel surface) to the cell suspension. Next, the cells were spun down at 1500rpm for 3 minutes and then resuspended in fresh complete growth medium. The resuspended cells were then used to seed Petri dishes or flasks. The flask was then placed back into the incubator. The following day, the seeded dishes and flasks were examined to ensure the cells had reattached and were actively growing. The cell medium was changed on day 3. The cells were passaged twice before use. They can be used until passage 35 without loss of BBB properties.

Immunocytochemistry (ICC)

hCMEC/D3 cells were seeded onto glass-bottom petri dishes (MatTek Corporation, USA) and raised to 100% confluence. They were maintained at 100% confluence for 3 days in order to maximize tight junction protein expression. ICC was then performed in order to visualize the tight junction proteins expressed by the hCMEC/D3 cells. ICC was performed as follows: aspirate the cell culture medium from the glass-bottom petri dish and then rinse the cells with PBS three times. The cells are then fixed in 4% Paraformaldehyde (PFA) for 15 minutes at room temperature. Next, the cells are washed with PBS two times, followed by a third wash in PBS-T. Then, the cells were permeabilized with 0.2 % Triton X-100 for 10 minutes at room temperature. The cells were then washed with PBS-T three times and blocked with 3% Bovine Serum Albumin (BSA) for 30 minutes at room temperature. Cells were treated with primary antibody (1°-Ab) for 1 hour at room temperature (or

overnight at 4°C). The following 1°-Ab's were used: Mouse Anti-Claudin-5 (1:100) (Invitrogen 35-2500), Mouse Anti-Occludin (1:100) (Invitrogen 33-1500), and Rabbit Anti-ZO-1 (1:200) (Cell Signaling 8193). The cells were washed with PBS-T four times and then treated with a fluorescent-labeled secondary antibody (2°-Ab) for 1 hour at room temperature; the cells were covered to avoid photo bleaching. The following 2°-Ab's were used: goat anti-mouse Alexa Fluor 488 (1:1000-1:1500), and goat anti-rabbit Cy3 (1:1000-1:2000). Next, while covered, the cells were washed with PBS-T 4 times and then stained with Hoechst (Hoechst 33342) for 15 minutes. Finally, the cells were washed with PBS-T three times (while covered) and then imaged on an Axio Observer Z1 inverted microscope (Zeiss, Germany).

Total Protein Extraction

hCMEC/D3 cells were seeded into a tissue culture flask (CELLTREAT 229341, Pepperell, MA, USA) and raised to 100% confluence. They were maintained at 100% confluence for 3 days in order to maximize tight junction protein expression. TriPure Isolation Reagent (MilliporeSigma 11667165001, Burlington, MA, USA) was used to do a total protein extraction using the manufacturer's protocol. Once finished, the samples were stored at -80°C.

Western Blot Procedure

Western blot was performed to verify the expression of tight junction proteins in hCMEC/D3 cells. Western blotting was carried out using the Mini-PROTEAN 3 System (Bio-Rad, Hercules, CA, USA). First, 12% SDS-polyacrylamide separating

gels were cast and overlaid with 4% stacking gels. The total protein extraction obtained from hCMEC/D3 cells was then added to the gel alongside PageRuler Plus Prestained Protein Ladder (ThermoFisher, Waltham, MA, USA). The gels were run at 100V for the stacking region and then 120V for the separating region. The proteins in the gels were then transferred to Hybond Enhanced Chemiluminescence (ECL) nitrocellulose membranes (GE Healthcare, Chicago, IL, USA) at 100V for 40 minutes. After the transfer was complete, the membranes were blocked in 5.0% non-fat dried milk dissolved in PBS-Tween (PBS-T). Then, the membranes were incubated in primary antibodies overnight at 4°C with agitation. The following primary antibodies were used: Mouse Anti-Claudin-5 (1:100) (Invitrogen 35-2500), Mouse Anti-Occludin (1:100) (Invitrogen 33-1500), Rabbit Anti-ZO-1 (1:200) (Cell Signaling 8193), and β-actin (1:40,000). The following morning, blots were thoroughly rinsed in PBS-T then placed in the appropriately diluted peroxidase-conjugated secondary antibody and incubated for one hour at 4°C. The following secondary antibodies were used: Rabbit Anti-Mouse IgG-Peroxidase conjugated (Sigma A9044) and Goat Anti-Rabbit IgG-HRP conjugated (ThermoFisher A16104). Once the incubation was complete, the membranes were thoroughly rinsed in PBS-T and then quickly rinsed in dH2O to remove phosphate buffer. Blots were then developed using the SuperSignal West Femto Maximum Sensitivity Substrate (ThermoFisher 34094) and autoradiography film (Lab Scientific XAR ALF 1824, Danvers, MA, USA).

Live Cell Imaging During Anesthesia

Live cell imaging was done using an Axio Observer Z1 inverted microscope (Zeiss, Germany) with a stage top incubator (Tokai Hit, Japan). hCMEC/d3 cells were raised to 100% confluence in glass-bottom petri dishes (MatTek Corporation, USA). The cells were maintained at 100% confluence for 3 days in order to maximize tight junction protein expression and then transferred to the stage top incubator. A calibrated Midmark Matrx VMR table top anesthesia machine with a VIP 3000 well-fill style vaporizer was used to supply Sevoflurane (Sevothesia™; Butler Schein™ Dublin, OH; NDC: 11695-0501-2) and Isoflurane (Isothesia™; Butler Schein™; Dublin, OH; NDC 11695-6776-2) with oxygen as the carrier gas. Separate vaporizers for Sevoflurane and Isoflurane were acquired and used. The stage top incubator has gas ports that the vaporizers were connected to, allowing anesthesia to be pumped directly into the stage top incubator. Cells were exposed to either 3% Sevoflurane or 3% Isoflurane for 3 hours. Live cell imaging prior to, during, and after IA treatment was used to directly observe and study the effects of IAs on the structure and behavior of BVECs.

Trans-Endothelial Electrical Resistance (TEER) Experiments

hCMEC/D3 cells were seeded on 3.0µm Transwell Inserts (MilliporeSigma CLS3462, Burlington, MA, USA) in twelve-well plates. The cells were raised to 100% confluence, and then maintained at 100% confluence for 3 days in order to maximize tight junction protein expression. Raising hCMEC/D3 cells to 100% confluence on the inserts allowed the cells to establish a permeability barrier between the chambers that is similar to the BBB *in vivo*. After the cells reached 100%

confluence and established their barrier function, they were exposed to anesthesia. Trans-Endothelial Electrical Resistance (TEER) was used to evaluate BBB integrity prior to and after exposure to anesthesia. Two hours prior to anesthetic treatment, the cell medium was changed. After two hours, TEER was measured using an EVOM2 Epithelial Volt/Ohm (TEER) Meter (World Precision Instruments, Sarasota, FL, USA). The Transwell Inserts were then transferred to a stage top incubator (Tokai Hit, Japan) and subjected to Sevoflurane (4%) or Isoflurane (4%) for one or three hours, Sevoflurane + DMSO (1%) for one hour, or Propofol for one hour. Immediately after exposure to anesthesia, TEER was again measured. The TEER values of each anesthetic were compared and used to determine which anesthetic is least harmful to the BBB.

Permeability Experiments

hCMEC/D3 cells were seeded on 3.0µm Transwell Inserts (MilliporeSigma CLS3462, Burlington, MA, USA) in twelve-well plates. The cells were raised to 100% confluence, and then maintained at 100% confluence for 3 days in order to maximize tight junction protein expression. After the cells reached 100% confluence and established their barrier function, they were exposed to anesthesia. Two hours prior to anesthetic treatment, the cell medium was changed. After two hours, the cells were exposed to Sevoflurane (4%) or Isoflurane (4%) for one or three hours, Sevoflurane + DMSO (1%) for one hour, or Propofol for one hour. Immediately after exposure to anesthesia, permeability experiments were performed. Fluorescein (MilliporeSigma F6377) and RITC-Dextran (MilliporeSigma R8881) were added to

the apical (upper) chamber of the Transwell Inserts. Then, the rate of dye transfer from the apical chamber into the basolateral (lower) chamber was measured. The dye transfer rate of control cells was compared with the dye transfer rate of cells exposed to Sevoflurane, Isoflurane, and Propofol, and this was used to determine the potency/harmfulness of these anesthetics, with the goal of determining which anesthetic is least harmful to the BBB.

Immunocytochemistry following Exposure to Isoflurane, Sevoflurane, or Sevoflurane + DMSO

hCMEC/D3 cells were seeded onto glass-bottom petri dishes (MatTek Corporation, USA) and raised to 100% confluence. They were maintained at 100% confluence for 3 days in order to maximize tight junction protein expression. The confluent hCMEC/D3 cell monolayers were then exposed to Isoflurane, Sevoflurane, or Sevoflurane + DMSO. ICC was then performed (as described above) in order to visualize the distribution and expression of the tight junction-associated cytoplasmic scaffolding protein ZO-1 within these cells.

Time Lapse Imaging of hCMEC/D3 Cells Being Exposed to Sevoflurane and DMSO

hCMEC/D3 cells were seeded onto glass-bottom petri dishes (MatTek Corporation, USA) and raised to 100% confluence. They were maintained at 100% confluence for 3 days in order to maximize tight junction protein expression. The cell culture medium covering these cells was removed and replaced with EBM-2 Complete

Medium containing 1% DMSO. The cells were then placed in a stage top incubator (Tokai Hit, Japan) on an Axio Observer Z1 inverted microscope (Zeiss, Germany) and exposed to 4% Sevoflurane for one hour. A Time Lapse recording was started before and ended after exposure to Sevoflurane and DMSO using the Zeiss Axio Observer Z1 inverted microscope.

Floating Cell Experiments

hCMEC/D3 cells were raised to 100% confluence in glass-bottom petri dishes (MatTek Corporation, USA). The cells were maintained at 100% confluence for 3 days in order to maximize tight junction protein expression. These cells were then prepared for exposure to anesthesia. Prior to anesthesia, a separate dish of cells was split, and the split cells were added to the dish containing the confluent monolayer. The goal was to determine if floating cells would aid the transfer of anesthesia from the air to the cell monolayer. These cells were then exposed to Sevoflurane (4%) for one hour. Live Cell Imaging during the experiment was used to assess the effects of Sevoflurane on the cell monolayer.

Pertussis Toxin Experiments

Pertussis toxin is reported to be a potent disruptor of the BBB [129, 130]; it should act as a positive control by disrupting the hCMEC/D3 cell monolayer. hCMEC/d3 cells were raised to 100% confluence in glass-bottom petri dishes (MatTek Corporation, USA). The cells were maintained at 100% confluence for 3 days in order to maximize tight junction protein expression. These dishes were transferred to

a stage top incubator (Tokai Hit) and then exposed to a 10μg/ml dosage of Pertussis toxin for 15 minutes. Live cell imaging was used to observe the effects in real time.

Verification that hCMEC/D3 Cells Express the Histamine H1 Receptor

Histamine is a known disruptor of the BBB, so it was decided to obtain Histamine and expose the hCMEC/D3 cells to it. However, before exposing the cells to Histamine, they were first screened for the presence of Histamine receptors using an antibody for the Histamine H1 Receptor (ProSci 79-814). Confluent hCMEC/D3 cell monolayers were probed with this histamine receptor antibody in cells with and without membrane permeabilization.

Histamine and Acetaminophen Experiments

hCMEC/d3 cells were raised to 100% confluence in glass-bottom petri dishes (MatTek Corporation, USA). The cells were maintained at 100% confluence for 3 days in order to maximize tight junction protein expression. These dishes were transferred to a stage top incubator (Tokai Hit) and then exposed to various dosages of Histamine or Acetaminophen. Live cell imaging was used to observe the effects in real time.

Statistics

Using Student's t-test, statistical significance was calculated and a $p \leq 0.05$ was considered statistically significant. Variation within each treatment group was represented by standard error.

EXPERIMENTAL RESULTS

Immunocytochemistry and Western Blot Verify that hCMEC/D3 Cells Express Tight Junction Proteins

Immunocytochemistry was performed on the hCMEC/D3 cells in order to visualize tight junction protein expression and distribution. The tight junction proteins Claudin-5, Occludin, and ZO-1 were detected at cell-cell contacts (**Fig. 3**). This indicates that the hCMEC/D3 cell line retains a tight junction organization similar to the normal human brain endothelium, and it supports the use of the hCMEC/D3 cell line as an *in vitro* model of the BBB.

Tight junction protein expression was also verified by Western Blot of confluent hCMEC/D3 cells. Western Blots verified that hCMEC/D3 cells express ZO-1 (**Fig. 4**). Western Blots for Claudin-5 and Occludin were inconclusive.

TEER Decreases and Permeability Increases after hCMEC/D3 Cells Are Exposed to Anesthesia

TEER measurements were performed on Control cells, Isoflurane-treated cells (1hr or 3hr), Sevoflurane-treated cells (1hr or 3hr), Sevoflurane + DMSO-treated cells (1hr), and Propofol-treated cells (1hr). Comparison of the Control and Sevoflurane-treated cells reveals that a one-hour Sevoflurane exposure causes a significant reduction in TEER, which is equivalent to an increase in BBB permeability. However, a three-hour Sevoflurane exposure did not cause a significant decrease in TEER values, and neither did treatment with Sevoflurane + 1% DMSO. Meanwhile, Propofol-treated

cells cause an even larger reduction in TEER. TEER measurements were also obtained from SK-N-MC cells. SK-N-MC is a non-endothelial human neuroblastoma cell line. Comparison of TEER measurements obtained from hCMEC/D3 cells with SK-N-MC cells reveals that Sevoflurane (1hr) and Propofol exposure cause TEER to drop, and therefore permeability to rise, towards levels more indicative of non-endothelial cells that have no barrier function (**Fig. 5**).

Comparison of the dye transfer rate between Control, Isoflurane-treated (1hr or 3hr), and Sevoflurane-treated (1hr or 3hr) hCMEC/D3 cells reveals that Fluorescein (376Da) passes through these monolayers at a similar rate. Fluorescein passes through Sevoflurane + DMSO-treated monolayers and Propofol-treated monolayers at higher rates than the other monolayers (**Fig. 6A**). Passage of RITC-Dextran (10kDa) is largely inhibited by control cells, Isoflurane-treated cells (1hr or 3hr), and Sevoflurane-treated cells (1hr). However, exposure to Sevoflurane (3hr), Sevoflurane + DMSO, and Propofol increases the permeability of the hCMEC/D3 cell monolayer and allows more RITC-Dextran to pass through (**Fig. 6B**).

No Change in the Distribution or Expression of the Tight Junction-Associated Scaffolding Protein ZO-1 in hCMEC/D3 Cells Exposed to Isoflurane, Sevoflurane, or Sevoflurane + DMSO

Immunocytochemistry revealed the distribution and expression of the tight junction-associated cytoplasmic scaffolding protein ZO-1 within confluent hCMEC/D3 cell monolayers that were exposed to Isoflurane (**Fig. 7A-B**), Sevoflurane (**Fig. 7C-D**), or

Sevoflurane + DMSO (**Fig. 7E-F**). No change was seen in the distribution or intensity of expression of ZO-1.

Addition of DMSO or Floating Cells to the Cell Culture Medium Did Not Aid the Transfer of Anesthesia from the Air to the Cell Monolayer

hCMEC/D3 cells were given cell culture medium containing 1% DMSO and then exposed to 4% Sevoflurane for one hour. A Time Lapse recording was started before and ended after exposure to Sevoflurane and DMSO. **Figure 8A** shows cells prior to exposure to Sevoflurane and DMSO. **Figure 8B** shows cells after a one-hour exposure to Sevoflurane and DMSO. Addition of DMSO to the cell culture medium did not appear to aid Sevoflurane in transferring from the air to the endothelial cell monolayer, as no cell contraction was seen during or after exposure.

hCMEC/D3 cells were also given cell culture medium containing resuspended cells and then exposed to 4% Sevoflurane for one hour. A Time Lapse recording was taken prior to, during, and after exposure to Sevoflurane. Addition of resuspended (or floating) cells to the cell culture medium did not appear to aid the transfer of Sevoflurane from the air to the endothelial cell monolayer (**Fig. 9**).

Cell Contractility Was Detected after Exposure to Pertussis Toxin

Live Cell Imaging was used to directly visualize the effects of Pertussis toxin on hCMEC/D3 cells. Endothelial Cell contractility was seen in some cells (**Fig. 10**).

hCMEC/D3 Cells Express the Histamine H1 Receptor

Confluent hCMEC/D3 cell monolayers were stained with an antibody for the Histamine H1 Receptor after the membranes were not permeabilized (**Fig. 11B-D**) or permeabilized (**Fig. 11E-F**). As can be seen, these cells do express the Histamine H1 receptor, with the receptor distribution being punctate in cells with surface membranes intact, as expected.

Histamine and Acetaminophen Induce Contraction in hCMEC/D3 Cells

Exposure to 45ng/ml Histamine & 180ng/ml Histamine caused no contraction in either subconfluent or confluent cells (**Fig. 12; Fig. 13**). Exposure to 2.5µg/ml Histamine induced some cell contraction in both subconfluent and confluent cells (**Fig. 12; Fig. 13**). Meanwhile, exposure of confluent cells to 60µg/ml Acetaminophen caused no cell contraction (**Fig. 14**), whereas exposure of subconfluent cells to 0.5mg/ml Acetaminophen resulted in mild contraction (**Fig. 15**).

DISCUSSION

Immunocytochemistry verified that hCMEC/D3 cells express the tight junction proteins Claudin-5, Occludin, and ZO-1 at cell-cell contacts. Expression of ZO-1 was also verified by Western Blot. Overall, these results indicate that the hCMEC/D3 cell line retains a tight junction organization similar to that of the normal human brain endothelium, and it supports the use of the hCMEC/D3 cell line as an *in vitro* model of the BBB.

TEER measurements were performed on Control, Isoflurane-treated, Sevoflurane-treated, and Propofol-treated hCMEC/D3 cells, and comparison of these groups revealed that a one-hour exposure to Sevoflurane or Isoflurane causes a reduction in TEER, which is equivalent to an increase in BBB permeability. Interestingly, exposure to three hours of Sevoflurane or Isoflurane did not cause a significant reduction in TEER, nor did exposure to Sevoflurane + DMSO. However, exposure to Propofol, which is a potent injectable/intravenous anesthetic, did cause a large reduction in TEER. We believe that this occurred because the inhaled anesthetics are insoluble, meaning they are unable to pass across the cell culture medium and interact with the endothelial cell monolayer. On the other hand, the intravenous anesthetics are soluble agents, meaning they can mix with the cell culture medium and come in direct contact with the endothelial cell monolayer. This allows them to exert a larger effect on the cell monolayer than the inhaled anesthetics. TEER measurements were also obtained from SK-N-MC cells. As expected, these cells had the lowest TEER values of any we recorded. This is because SK-N-MC is a non-endothelial human

neuroblastoma cell line. Since these cells are not endothelial cells, they would not be expected to have a barrier function, and therefore they would also be expected to have high permeability and low TEER values. Comparison of TEER measurements obtained from hCMEC/D3 cells and SK-N-MC cells revealed that Sevoflurane, Isoflurane, and Propofol cause TEER to drop (and therefore permeability to rise) towards levels more indicative of non-endothelial cells that have no barrier function. Taken together, these results support the notion that exposure to anesthetics causes changes in vascular endothelial cells that result in increased barrier permeability and leak of plasma components into the brain.

Permeability experiments were performed using Fluorescein (a small molecule) and RITC-Dextran (a much larger molecule). After comparing the dye transfer rate among Control, Isoflurane-treated (1hr or 3hr), and Sevoflurane-treated (1hr or 3hr) hCMEC/D3 cells, Fluorescein was found to pass through these monolayers at a similar rate. This was expected, as Fluorescein is a small 376Da molecule, so small that even a functional barrier is not expected to greatly inhibit its passage. However, Fluorescein passes through Sevoflurane + DMSO-treated monolayers and Propofol-treated monolayers at higher rates than the other monolayers, again suggesting that these agents lead to an increase in barrier permeability. Control (unanesthetized) cells largely blocked the passage of RITC-Dextran across the cell monolayer. This was also expected, as RITC-Dextran is a large 10kDa molecule, and a functional endothelial monolayer would inhibit the passage of a molecule of this size. Isoflurane-treated cells (1hr or 3hr) and Sevoflurane-treated cells (1hr) also inhibited

the passage of RITC-Dextran. However, exposure to Sevoflurane (3hr), Sevoflurane + DMSO, and Propofol increased the permeability of the hCMEC/D3 cell monolayer and allowed more RITC-Dextran to pass through, again suggesting that these agents increase barrier permeability. These results, in particular the finding that exposure to Sevoflurane for 3 hours increases permeability, are contradictory to what was found above during TEER measurements. During TEER measurements, exposure to Sevoflurane for 3 hours was found to have a higher TEER value (and therefore lower permeability) than exposure to Sevoflurane for one hour. We believe that this is due to the variability and human error present during TEER measurements. The device used in our lab to measure TEER is a "chopstick" style probe that the user holds in place in the Transwell insert and uses to get a TEER measurement. However, the TEER measurement can vary depending on the following factors: the depth that the probe is inserted into the Transwell insert, the angle at which the probe is inserted, whether or not the probe touches the bottom or sides of the Transwell insert, and the temperature of the probe and the cell culture medium. We believe that this variability in obtaining TEER values is why the results differ between TEER studies and permeability studies.

hCMEC/D3 cells were exposed to Isoflurane, Sevoflurane, or Sevoflurane + DMSO and then immunostained in order to see the effects of the various chemical agents on the expression and distribution of the tight junction-associated scaffolding protein ZO-1. Immunocytochemistry revealed comparable immunostaining of ZO-1 intensities, indicating that ZO-1 distribution in the cells was not disrupted by

exposure to Isoflurane, Sevoflurane, or Sevoflurane + DMSO. This would suggest that the tight junctions are still fully functional during anesthetic insult, and that anesthesia must be disrupting the BBB and increasing BBB permeability in some other way. Based on the SEM data presented in Chapter 3 and Chapter 4, we believe that anesthesia's main mechanism of action is related to the effects of anesthetics on the surface plasma membranes of the endothelial cells. The SEM data strongly supports this, as they show dramatic endothelial cell surface flattening and lack of microvilli on cell surfaces after exposure to anesthesia, indicating that exposure somehow changes the physical properties of the plasma membrane.

A Time Lapse recording was made of hCMEC/D3 cells that were exposed to Sevoflurane + DMSO for one hour. Addition of DMSO to the cell culture medium did not aid Sevoflurane in transferring from the air to the endothelial cell monolayer, as no cell contraction was seen during or after exposure. This was unexpected, as we expected DMSO to aid the transfer of inhalation anesthetics across the cell culture medium to the endothelial cell surface, which would be evidenced by increased cell contraction. However, one reason that may explain why cell contraction is not seen in these cells is that DMSO incorporates itself into the lipid bilayer and allows the cell membranes to "relax" while under strain. In other words, the inhaled anesthetics may very well be transferring across the cell culture medium and interacting with the cell monolayer; cell contraction may just not be seen due to the use of DMSO. Other studies report that DMSO increases cell permeability, meaning it is likely that Sevoflurane and DMSO are both acting upon the cells, and Live Cell Imaging is just

not the proper method for examining the effects of these agents on the endothelial cells.

To address the possibility that cell membranes must come in direct contact with inhalation anesthetics, a fully confluent monolayer of hCMEC/D3 cells was split and added to the cell culture medium of another fully confluent monolayer of endothelial cells just prior to exposure to Sevoflurane (4%) for one hour. Live Cell Imaging during the experiment was used to assess the effects of Sevoflurane on the cell monolayer. The blood is full of various cells, and we wondered if these cells aided the transfer of inhalation anesthetics to the endothelial surface. Therefore, we decided to mimic the blood seen in one's blood vessels *in vivo* by adding free-floating cells to the cell culture medium to determine if they would aid the transfer of inhalation anesthetics from the atmosphere across the cell culture medium to the monolayer surface. However, addition of new cells to the cell culture medium did not appear to cause any visible changes to the cells in the monolayer. A potential limitation here is that the suspended cells are static, i.e., they are not moving at high speed in the petri dish as they are in the arteries that circulate blood. This may be essential for the rapid transfer of inhalation anesthetics from the blood to the tissue. Further work will be required to resolve this, perhaps using fluid-flow systems or artificial blood vessels in sealed chambers.

Pertussis toxin is a well-known and potent disruptor of the BBB; therefore, we decided to use it as a positive control by attempting to disrupt the hCMEC/D3 cell

monolayer with it. We treated the endothelial cell monolayer with Pertussis toxin, and the endothelial cells can be seen contracting with cell rounding after exposure. Therefore, Pertussis toxin does have some disruptive effect on the barrier function of BVECs by inducing cell contractility. Although we have not tested this directly, we assume that increased contractility will exert additional tractional forces on cell-cell junctions, including the tight junctions responsible for maintaining the barrier properties of the BBB.

These have been several reports in the literature that make the interesting observation that the elderly, especially those with Alzheimer's disease, have altered levels of histamine in the blood. In view of the fact that histamine can induce contraction of endothelial cells, leading to a loss of fluid from blood vessels during inflammation, we sought to test the effects of histamine on hCMEC/D3 cells. To accomplish this, it was first necessary to confirm that hCMEC/D3 cells express the histamine receptor; this was done using IHC and an antibody for the Histamine H1 receptor. IHC results show that these cells do express the Histamine H1 receptor. Lower doses (45ng/ml Histamine & 180ng/ml Histamine) resulted in no detectable contraction in either subconfluent or confluent cells. However, a higher dose of Histamine (2.5µg/ml) did induce contraction in both subconfluent and confluent cells. In addition, we tested the effects of Acetaminophen exposure on confluent cells. A lower dose (60µg/ml) of Acetaminophen caused no contraction, but a higher dose (0.5mg/ml Acetaminophen) did cause contraction. In both cases, treatment with higher doses is relevant since the blood vascular system is first exposed to higher doses of various drugs before they are

diluted by distribution to the various tissues.

Exposure to Isoflurane and Sevoflurane induces BBB breakdown by causing structural changes in BVECs, including a profound flattening of surface membranes and the loss of the BBB-associated tight junction ridge. These structural changes lead to the formation of holes at BVEC perimeters in the region of the tight junctions. We propose that these holes are primarily responsible for the increase in BBB permeability that was evidenced when measuring TEER and performing permeability assays. We believe these holes allow plasma components to leak into the brain tissue, which disrupts brain homeostasis and neuronal function and leads to the manifestation of POD in the short term and potentially POCD and Dementia in the long term.

FIGURES

Figure 1: Live Cell Imaging Apparatus

A) A Stage Top Incubator that allows one to observe the effects of anesthetics and drugs on cells in real time. **B)** The Control Unit for the Stage Top Incubator. This controls the CO_2 concentration and temperature within the stage top incubator as well as the temperature of the microscope objective lens. **C)** Special lids that are placed on petri dishes within the stage top incubator and used to deliver drugs to these dishes.

Figure 2: Transwell Inserts Create a Two-Chamber System

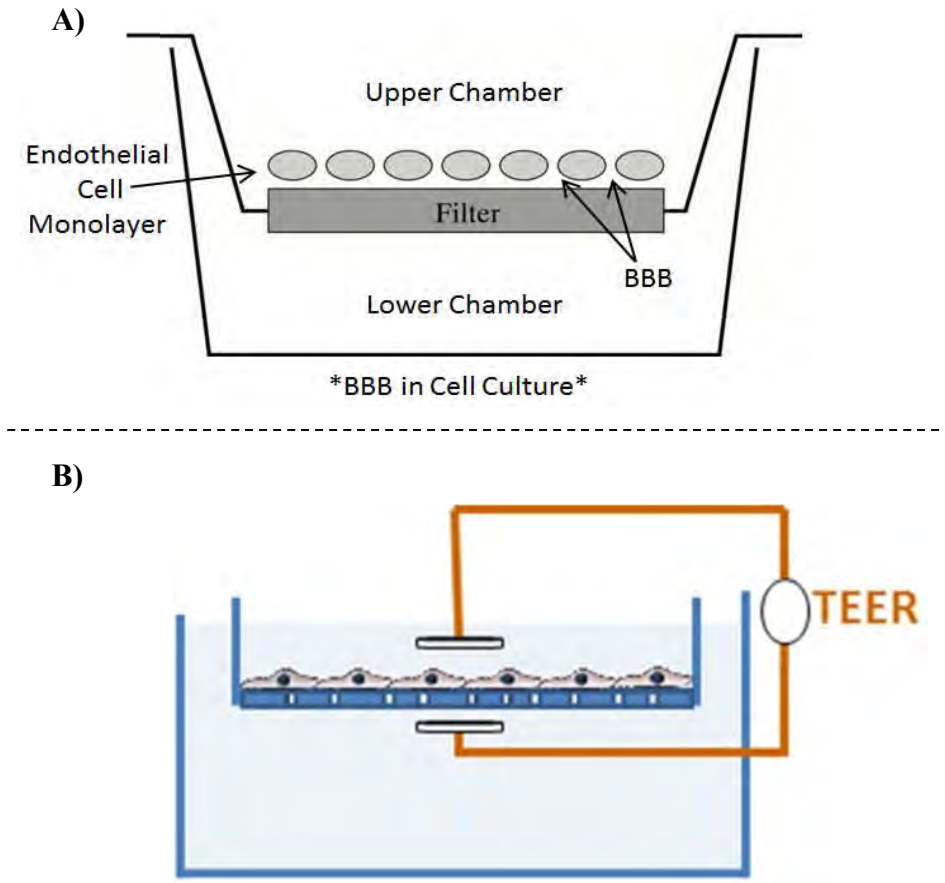

A) A schematic diagram of a Transwell Insert, which creates a two-chamber cell culture system. The Transwell Insert divides the well into an upper chamber and a lower chamber. When endothelial cells are raised to 100% confluence on these inserts, they establish a permeability barrier between the two chambers. This barrier is similar to the BBB *in vivo,* as the upper chamber represents the apical (luminal) surface within a blood vessel and the lower chamber represents the basolateral (abluminal) surface on the outside of a blood vessel. **B)** Transwell Inserts with a fully confluent endothelial cell monolayer were used to conduct Trans-Endothelial Electrical Resistance (TEER) and permeability experiments. When measuring TEER, an electrode is placed in both the upper and lower chambers, and then the electrical resistance across the membrane with the endothelial cell monolayer is measured. This was taken from [33].

Figure 3: Characterization of hCMEC/D3 Cells through Tight Junction Protein Expression

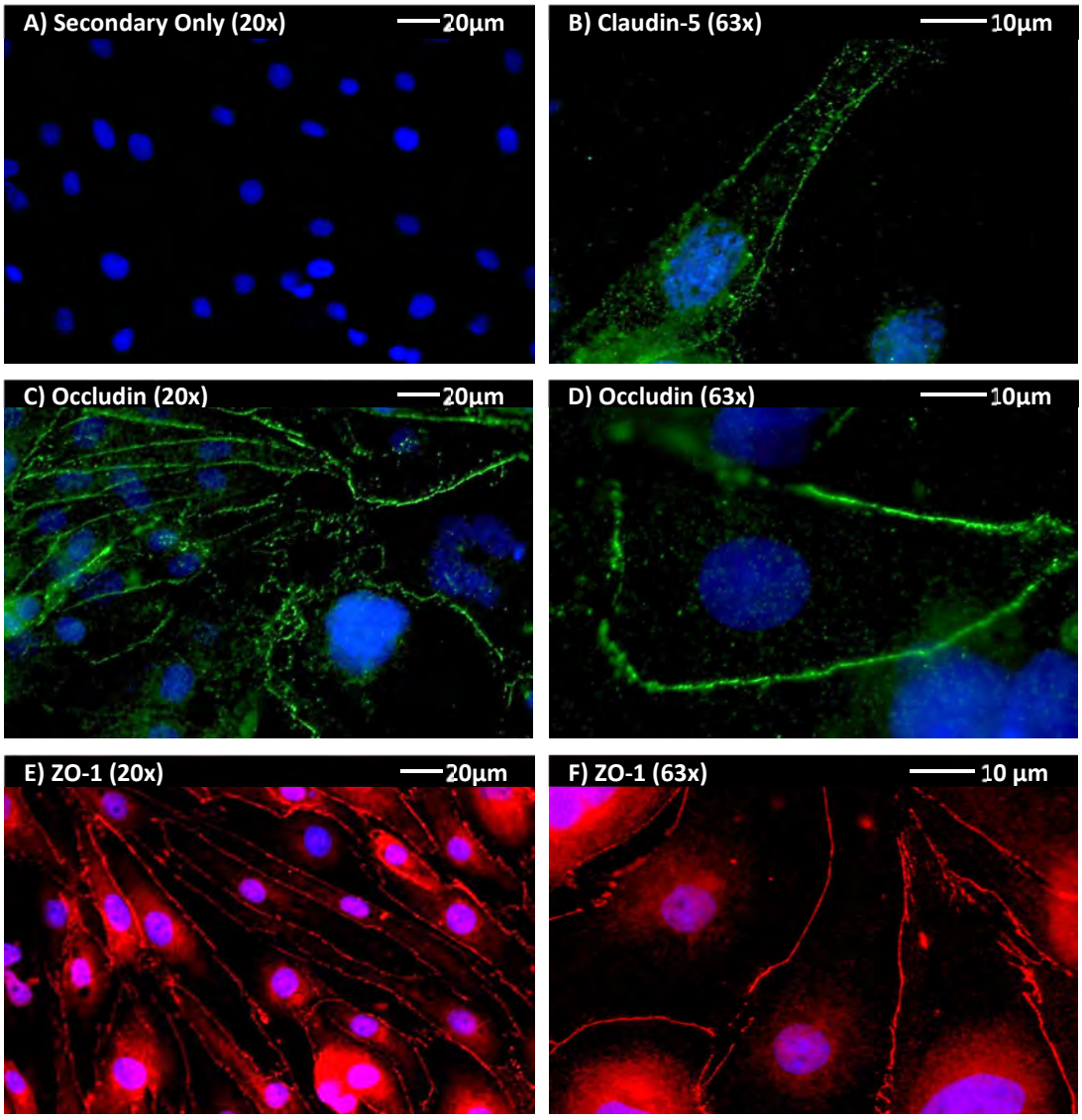

Confluent hCMEC/D3 cell monolayers were stained with antibodies for the integral transmembrane tight junction proteins Claudin-5 (**B**) and Occludin (**C-D**) and for the tight junction-associated cytoplasmic scaffolding protein ZO-1 (**E-F**), as indicated. Nuclei in blue were stained with Hoechst.

Figure 4: Western Blot Verifies Tight Junction Protein Expression

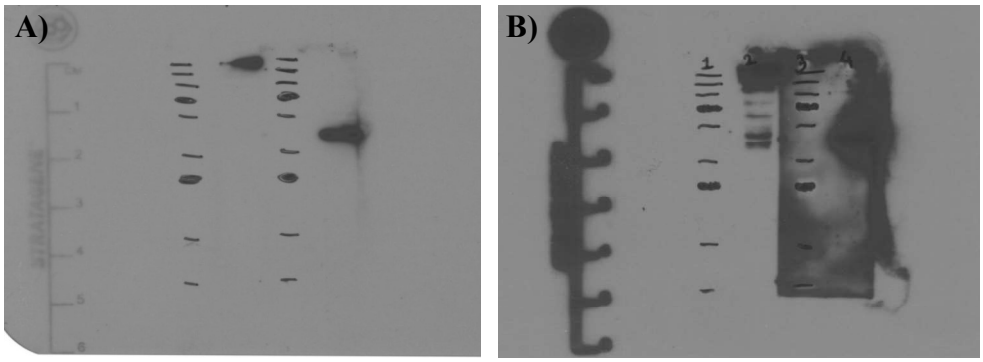

Tight junction protein expression was verified by Western Blot of confluent hCMEC/D3 cells. The membranes above were exposed for **A)** 1 minute or **B)** 3 minutes, and they developed a nice band for β-actin (positive control) at 42kDa and a nice band for ZO-1 at 225kDa. Therefore, the Westerns verified that hCMEC/D3 cells express ZO-1.

Figure 5: TEER Values Decrease after Exposure to Anesthesia

A)

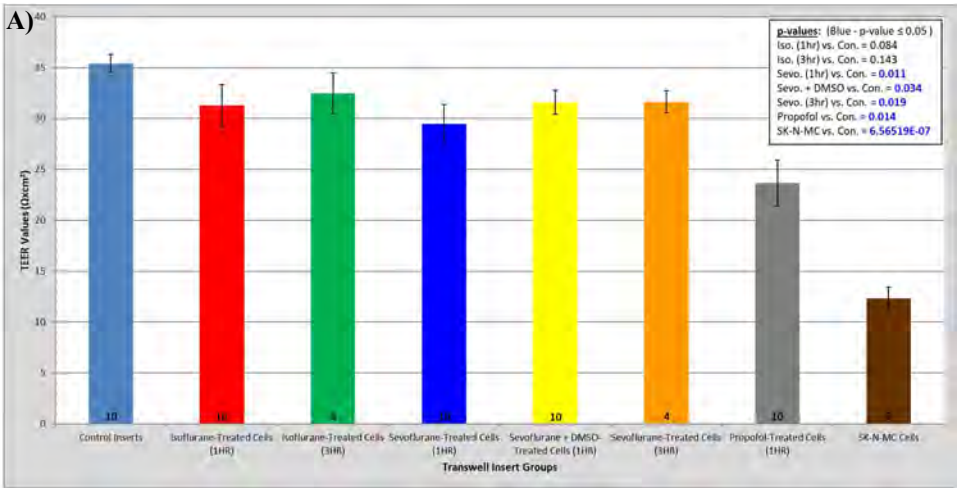

B)

	Average:	St. Dev:	St. Error:	Replicate #:
Control Inserts	35.392	2.803730848	0.886617542	10
Isoflurane-Treated Cells (1HR)	31.248	6.603885725	2.08833203	10
Isoflurane-Treated Cells (3HR)	32.48	3.986109214	1.993054607	4
Sevoflurane-Treated Cells (1HR)	29.456	5.974499886	1.889302752	10
Sevoflurane + DMSO-Treated Cells (1HR)	31.584	3.76308148	1.18999085	10
Sevoflurane-Treated Cells (3HR)	31.64	2.120125782	1.060062891	4
Propofol-Treated Cells	23.632	13.45502863	2.254853647	10
SK-N-MC Cells	12.32	1.58391919	1.12	2

TEER measurements were performed on Control cells, Isoflurane-treated cells (1hr or 3hr), Sevoflurane-treated cells (1hr or 3hr), Sevoflurane + 1% DMSO-treated cells (1hr), and Propofol-treated cells (1hr). **A)** Comparison of the Control and Sevoflurane-treated cells reveals that a one-hour Sevoflurane exposure causes a significant reduction in TEER. However, a three-hour Sevoflurane exposure did not cause a significant decrease in TEER values, and neither did treatment with Sevoflurane + 1% DMSO. Meanwhile, exposure to Propofol causes an even larger reduction in TEER. TEER measurements were also obtained from SK-N-MC cells. SK-N-MC is a non-endothelial human neuroblastoma cell line. Comparison of TEER measurements obtained from hCMEC/D3 cells with SK-N-MC cells reveals that Sevoflurane (1hr) and Propofol exposure cause TEER to drop, and therefore permeability to rise, towards levels more indicative of non-endothelial cells that have no barrier function. **B)** A table of the data used to create the graph presented in **(A)**.

Figure 6: Permeability Increases after Exposure to Anesthesia

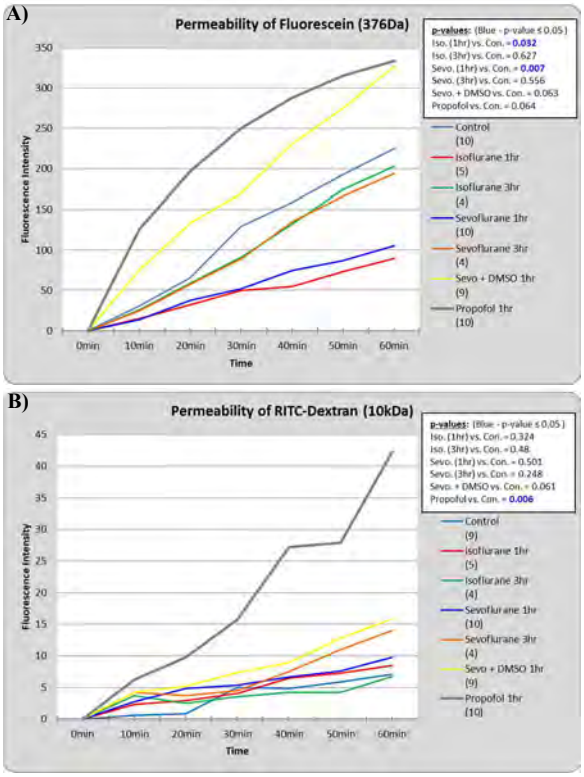

Permeability assays were performed on Transwell Inserts containing both control and anesthesia-treated hCMEC/D3 cells. Fluorescein and RITC-Dextran were added to the upper chamber of the Transwell Inserts, and then the dye transfer rate was determined over the course of 60 minutes. **(A)** Comparison of the dye transfer rate among Control, Isoflurane-treated (1hr), Isoflurane-treated (3hr), Sevoflurane-treated (1hr), and Sevoflurane-treated (3hr) hCMEC/D3 cells reveals that Fluorescein (376Da) passes through these monolayers at a similar rate. Fluorescein passes through Sevoflurane + DMSO-treated monolayers and Propofol-treated monolayers at higher rates than the other monolayers. **(B)** Passage of RITC-Dextran (10kDa) is largely inhibited by control cells, Isoflurane-treated cells (1hr and 3hr), and Sevoflurane-treated cells (1hr). However, exposure to Sevoflurane (3hr), Sevoflurane + DMSO, and Propofol increases the permeability of the hCMEC/D3 cell monolayer and allows more RITC-Dextran to pass through. The replicate number for each run is given in parentheses after the run title (see **A** and **B**). Sevo - Sevoflurane.

Figure 7: Tight Junction Protein Expression of hCMEC/D3 Cells after Exposure to Isoflurane, Sevoflurane, and Sevoflurane + DMSO

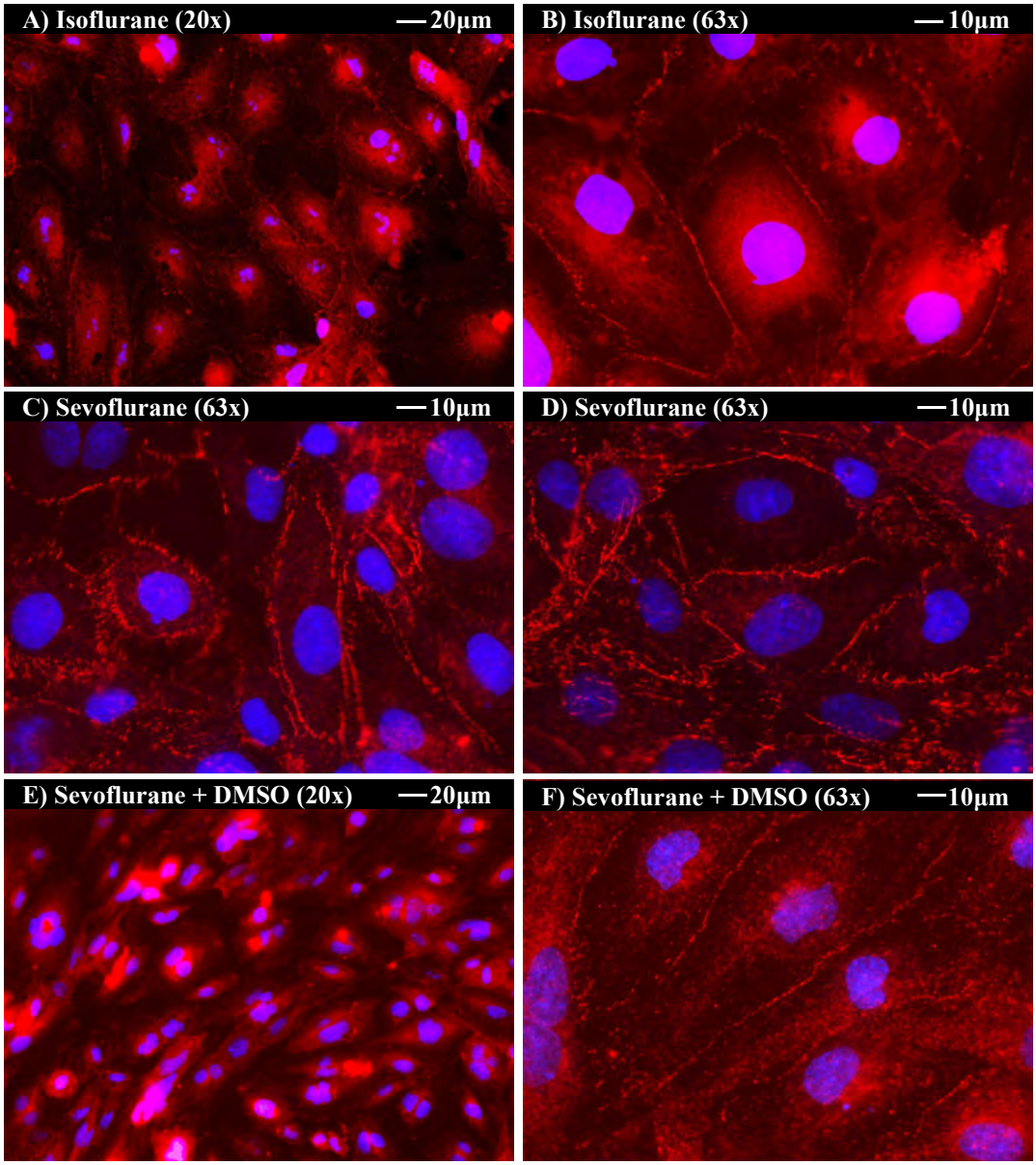

Figure 7: Tight Junction Protein Expression of hCMEC/D3 Cells after Exposure to Isoflurane, Sevoflurane, and Sevoflurane + DMSO.

Confluent hCMEC/D3 cell monolayers were exposed to Isoflurane (**A-B**), Sevoflurane (**C-D**), and Sevoflurane + DMSO (**E-F**). The cell monolayers were then stained with the antibody for the tight junction-associated cytoplasmic scaffolding protein ZO-1 (red staining). Nuclei in blue were stained with Hoechst. Immunocytochemistry revealed comparable immunostaining of ZO-1 intensities, indicating that ZO-1 distribution in the cells was not disrupted by exposure to Isoflurane (**A-B**), Sevoflurane (**C-D**), or Sevoflurane + DMSO (**E-F**). The endothelial cells exposed to Isoflurane (**A-B**) have straight, uniform marginal tight junctions, which suggests that they are not under tension due to cell contraction. However, the Sevoflurane-treated cells (**C-D**) have serrated or saw-toothed edges, which indicates that the cells and their associated tight junctions are under tension, most likely due to cell contraction. This does not appear to be the case for the cells exposed to Sevoflurane + DMSO (**E-F**). This is most likely because DMSO incorporates itself into the lipid bilayer and allows the cell membranes to "relax" when under strain.

Figure 8: Time Lapse of hCMEC/D3 Cells Being Exposed to Both Sevoflurane and DMSO for One Hour

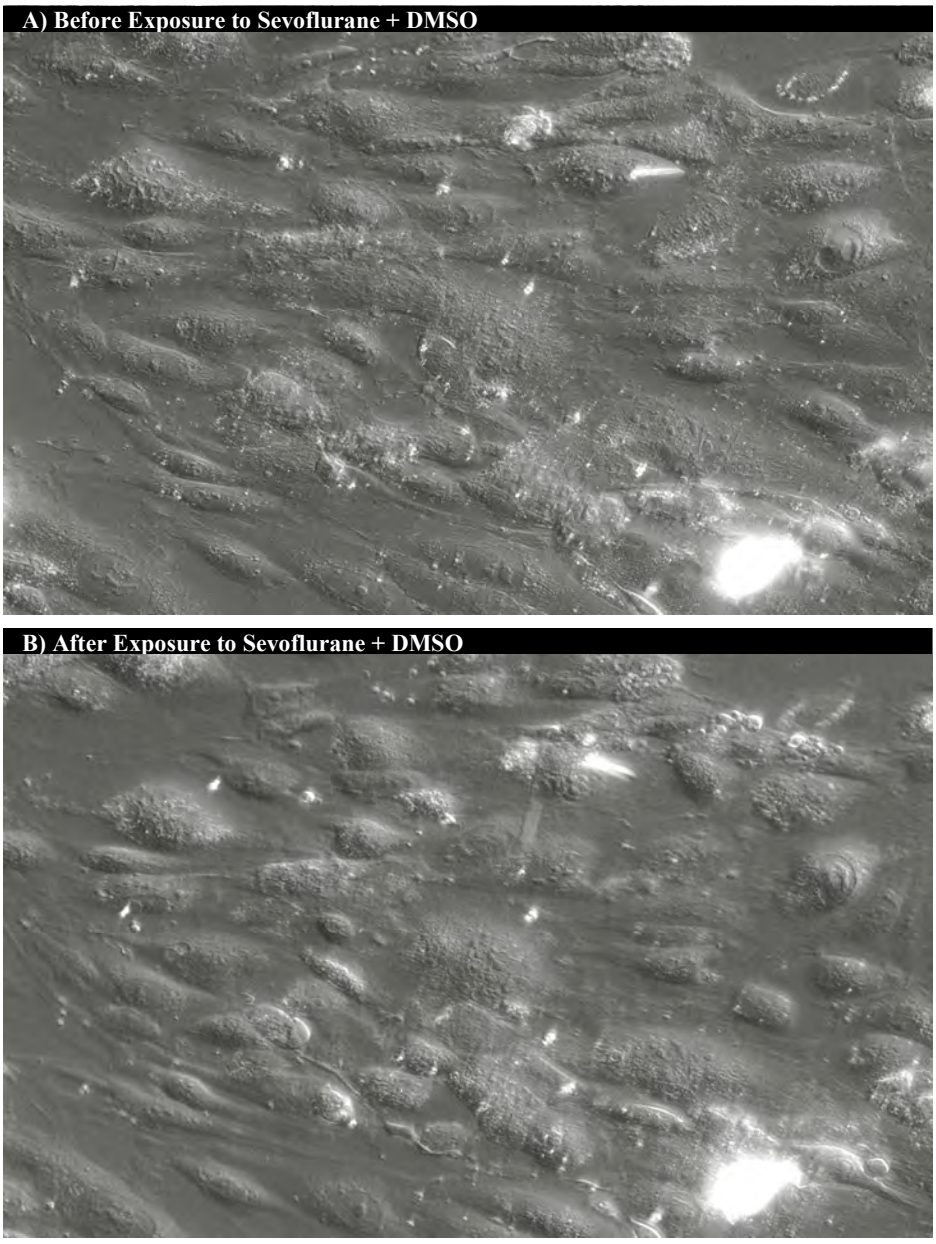

hCMEC/D3 cells were given cell culture medium containing 1% DMSO and then exposed to 4% Sevoflurane for one hour. **A)** Cells prior to exposure to Sevoflurane and DMSO. **B)** Cells after a one-hour exposure to Sevoflurane and DMSO. Addition of DMSO to the cell culture medium did not aid Sevoflurane in transferring from the air to the endothelial cell monolayer, as no cell contraction was seen during or after exposure.

Figure 9: Floating Cells Did Not Aid the Transfer of Anesthesia from the Air to the Cell Monolayer

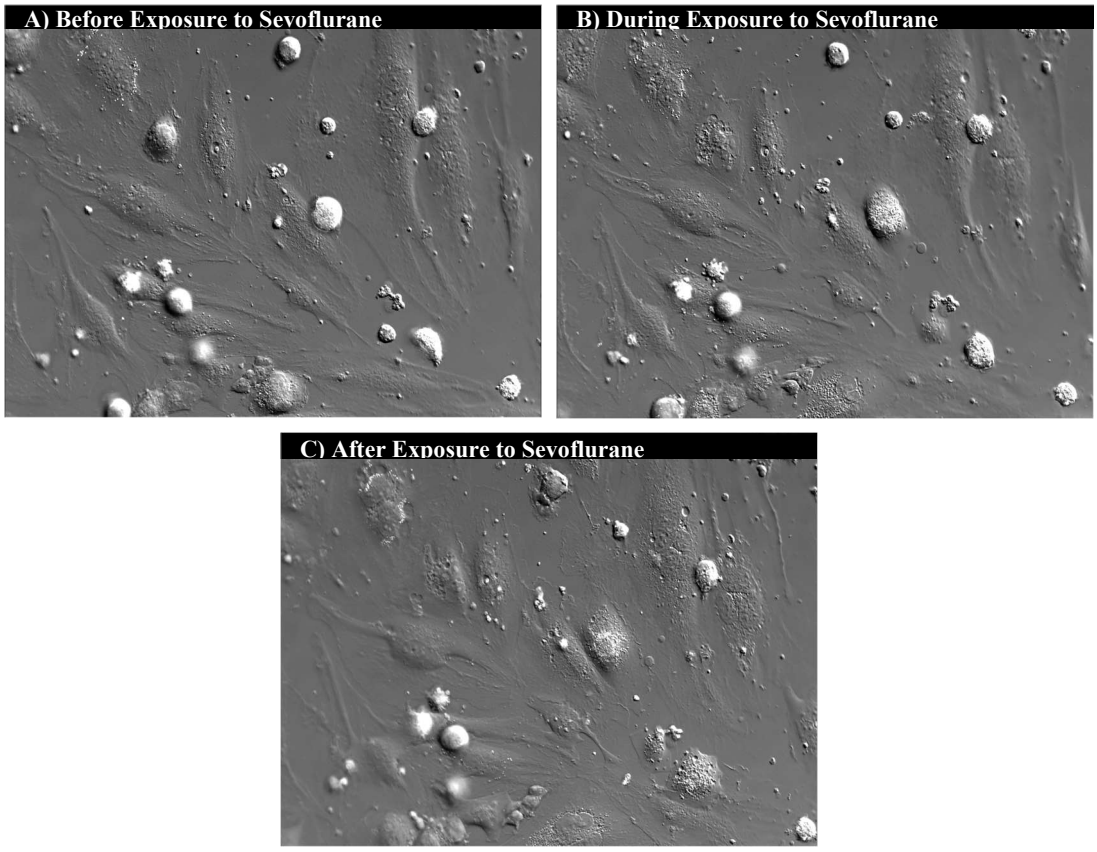

hCMEC/D3 cells were raised to 100% confluence in glass-bottom petri dishes and then prepared for exposure to anesthesia. Prior to anesthesia, a separate confluent monolayer of endothelial cells was split, and the split cells were then added to the dish containing the confluent monolayer. These cells were then exposed to Sevoflurane (4%) for one hour. Live Cell Imaging prior to (**A**), during (**B**), and after (**C**) the experiment was used to assess the effects of Sevoflurane on the cell monolayer. Unfortunately, the addition of new cells to the cell medium did not appear to aid in the transfer of anesthesia from the air to the endothelial cell monolayer.

Figure 10: Cell Contractility Was Detected after Exposure to Pertussis Toxin

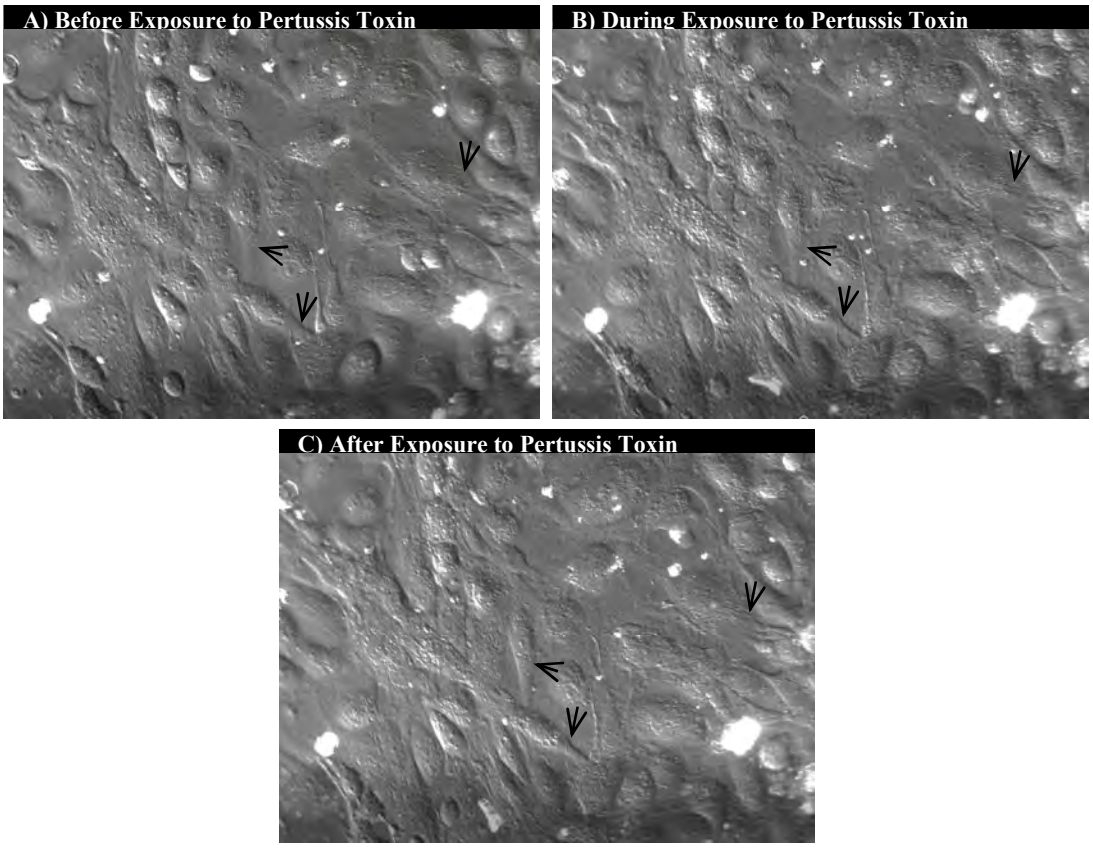

hCMEC/d3 cells were raised to 100% confluence in glass-bottom petri dishes. The cells were maintained at 100% confluence for 3 days in order to maximize tight junction protein expression. These dishes were transferred to the stage top incubator and then exposed to a 10µg/ml dosage of Pertussis toxin for 15 minutes. Live cell imaging was used to observe the effects in real time. Live Cell Imaging prior to (**A**), during (**B**), and after (**C**) the experiment was used to assess the effects of Pertussis Toxin on the cell monolayer. Endothelial Cell contractility was seen amid select cells.

Figure 11: Immunocytochemistry Was Used to Verify that hCMEC/D3 Cells Express the Histamine H1 Receptor

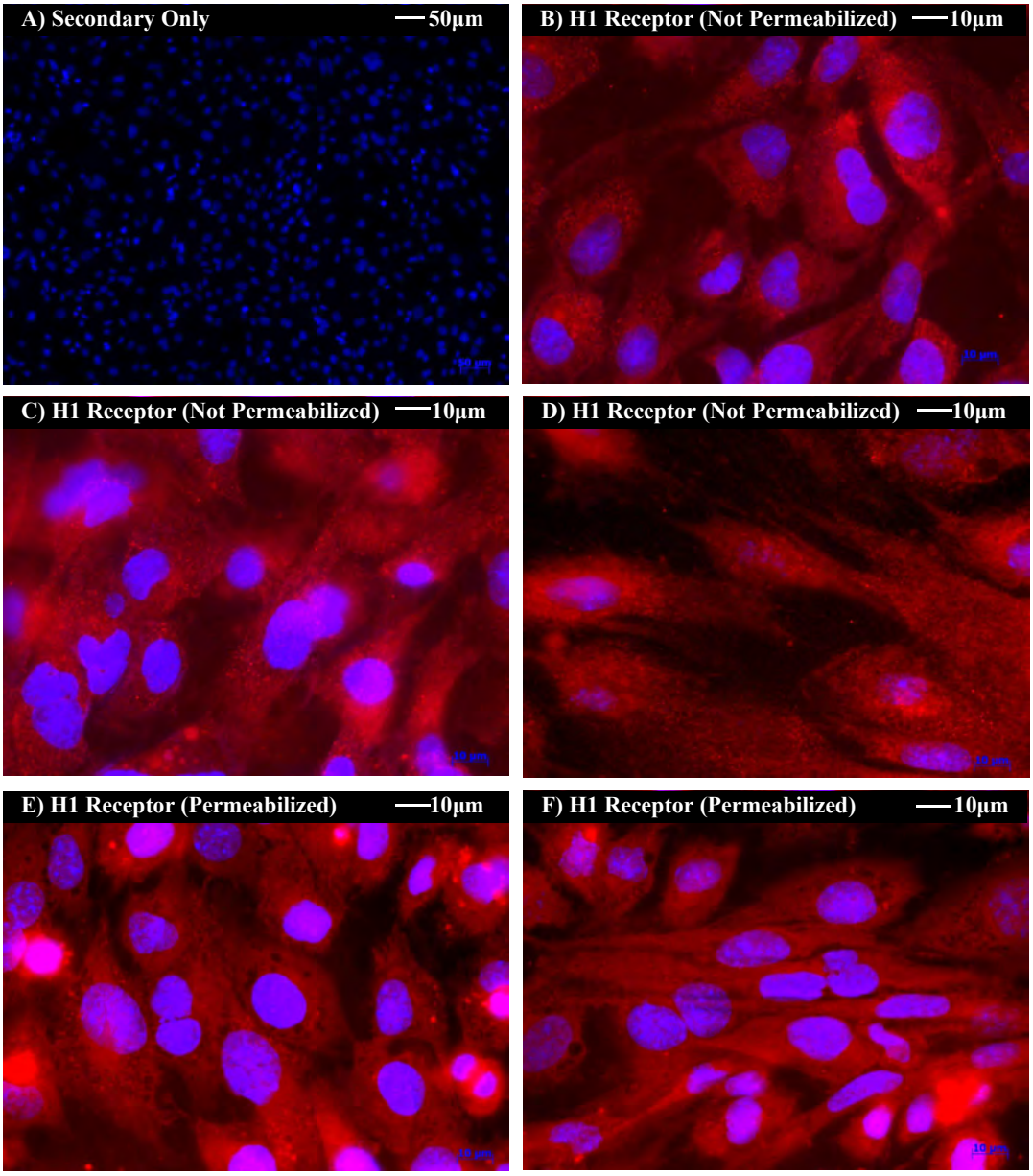

Figure 11: Immunocytochemistry Was Used to Verify that hCMEC/D3 Cells Express the Histamine H1 Receptor.

Confluent hCMEC/D3 cell monolayers were stained with an antibody for the Histamine H1 Receptor after the membranes were not permeabilized (**B-D**) or permeabilized (**E-F**). Nuclei in blue were stained with Hoechst. The nonpermeabilized cells display cell surface-bound histamine receptors (**B-D**). In particular, notice the punctate bright spots on the cell surface. In the permeabilized cells (**E-F**), both internal and external histamine receptors are superimposed, giving a more uniform (less punctate) appearance. These images confirm the presence of the Histamine H1 Receptor on the surfaces of hCMEC/D3 cells.

Figure 12: Histamine Induces Contraction in Confluent hCMEC/D3 Cells

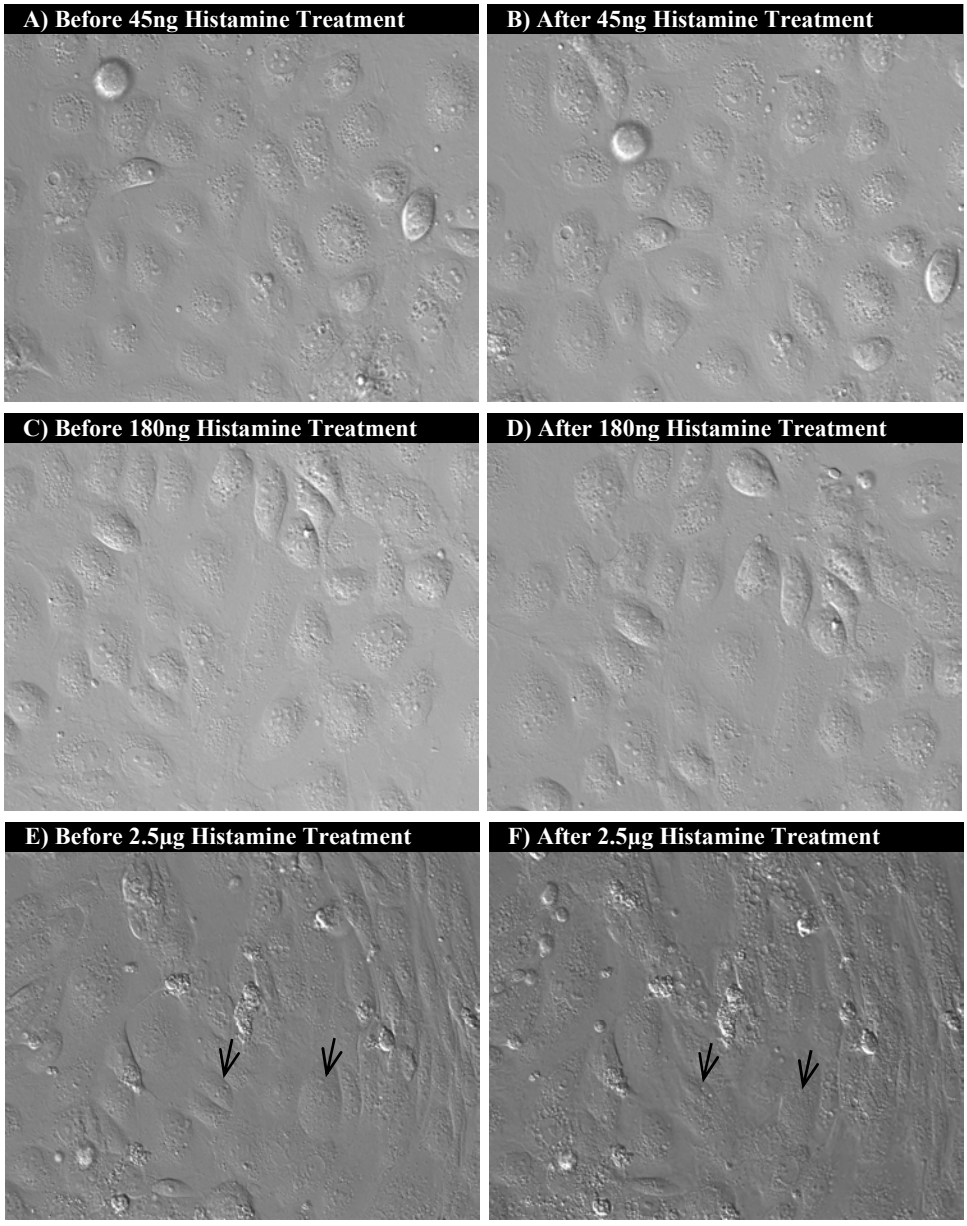

Exposure to 45ng/ml Histamine (**A-B**) & 180ng/ml Histamine (**C-D**) did not cause contraction in confluent cells, while exposure to 2.5µg/ml Histamine (**E-F**) induced cell contraction in confluent cells.

Figure 13: Histamine Induces Contraction in Subconfluent hCMEC/D3 Cells

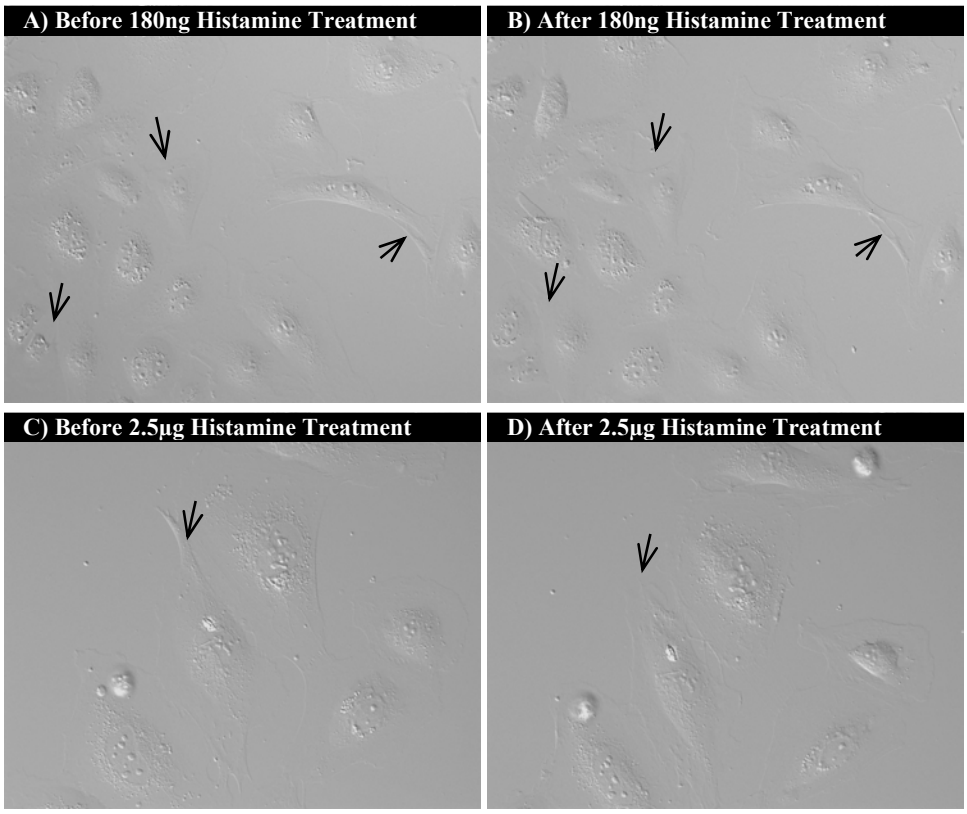

Exposure to 180ng/ml Histamine (**A-B**) caused no contraction in subconfluent cells, while exposure to 2.5µg/ml Histamine (**C-D**) induced cell contraction in subconfluent cells.

Figure 14: Acetaminophen Did Not Induce Contraction in Confluent hCMEC/D3 Cells

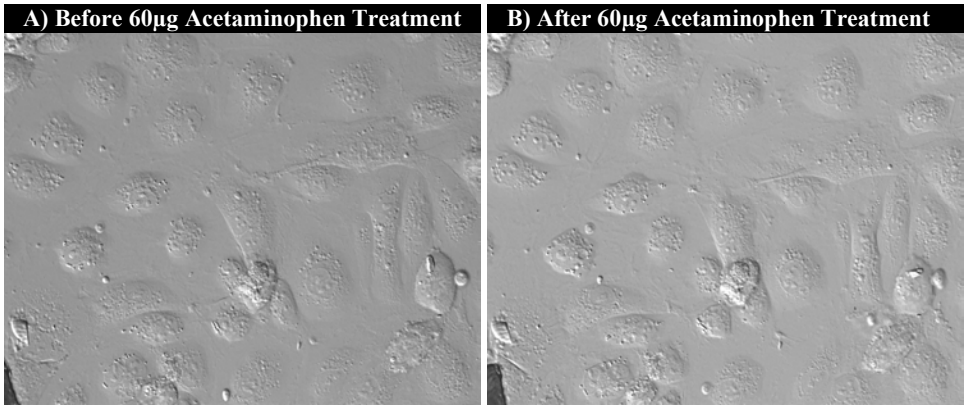

Exposure to 60µg/ml Acetaminophen (**A-B**) did not induce contraction in confluent cells.

Figure 15: Acetaminophen Induces Contraction in Subconfluent hCMEC/D3 Cells

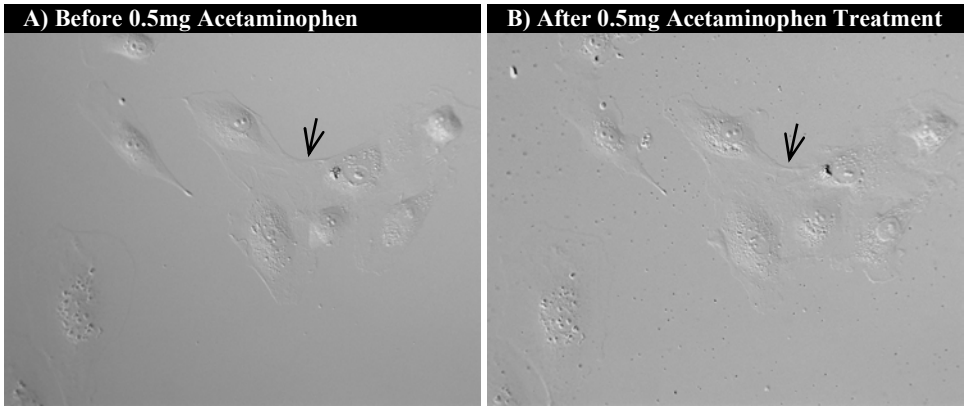

Exposure to 0.5mg/ml Acetaminophen (**A-B**) did induce mild cell contraction in subconfluent cells.

CHAPTER VI:

Administration of Lipoxin after LPS Insult Reduces Inflammation and Blood-Brain Barrier Permeability in Rats

ABSTRACT

Background

The blood-brain barrier (BBB), formed by the vascular endothelium in the brain, is a highly selective barrier that is responsible for maintaining brain homeostasis and therefore proper neuronal function. Disruption of the BBB, which causes an increase in BBB permeability, has been associated with a number of diseases. In particular, inflammation-induced BBB disruption has been associated with Alzheimer's disease (AD), Multiple Sclerosis (MS), Diabetes Mellitus (DM), and Stroke. Specialized pro-resolving lipid mediators (SPMs) such as Lipoxin are endogenous cell signaling molecules that are responsible for resolving inflammation. Here, we used a rat model to examine whether administration of Lipoxin could reduce inflammation and BBB permeability after a lipopolysaccharide (LPS) insult.

Methods

Rats were injected with LPS, and then three hours later they were given an injection of either Lipoxin or a placebo (normal saline). Some rats were sacrificed after 24 hours. Other rats were maintained for 72 or even 96 hours. These rats received an

additional injection of Lipoxin or placebo each day up until the day of sacrifice. Animals were sacrificed by perfusion-fixation. Brains were processed for Immunohistochemistry (IHC) and Scanning Electron Microscopy (SEM). IHC was used to detect the presence, location, and extent of BBB compromise. SEM was used to directly visualize the effects of anesthesia on the luminal surfaces of brain vascular endothelial cells (BVECs) that form the BBB.

Results

IHC revealed that treatment with 15mg/kg LPS induced both focal and global leaks in the BBB of rat brain blood vessels. However, treatment with Lipoxin resulted in a marked reduction in both the incidence and extent of LPS-induced BBB compromise and associated plasma leak. SEM allowed us to directly visualize the BBB and the luminal surfaces of BVECs. Through SEM, we saw that treatment with LPS induced changes in BVEC luminal surface topography and compromised BVEC viability. However, through SEM, we saw that treatment with Lipoxin following LPS administration reduced the level of BBB compromise and blocked the loss of BVECs from the endothelial luminal surface.

Conclusions

Results show that inflammation induces an increase in BBB permeability that results in a large plasma influx into the brain parenchyma that disrupts brain homeostasis and neuronal activity. We propose that this triggers POD in the short term and POCD and even dementia in the long term if things are left untreated. Results show that

administration of Lipoxin can restore proper BBB function and prevent plasma leak into the brain tissue by reducing inflammation.

INTRODUCTION

The Blood-Brain Barrier

The Blood-Brain Barrier (BBB), which is formed by the vascular endothelium in the brain, is a highly selective barrier that separates the circulating blood from the brain and prevents a large number of blood-borne substances from entering the brain. It also regulates the nutrient uptake and waste efflux between the brain and the circulating blood. The BBB is crucial for maintaining brain homeostasis and the normal functioning of neurons in the CNS [8, 29, 67, 108-110, 131]. Many diseases have been shown to be associated with altered permeability of the BBB, including meningitis, encephalitis, sepsis, and local and systemic infections. It has long been known that inflammation disrupts the BBB as well. Several diseases, including Alzheimer's disease (AD), Multiple Sclerosis (MS), Diabetes Mellitus (DM), and Stroke have been shown to be associated with both inflammation and BBB disruption [132].

Inflammation

The word inflammation is derived from the Latin word *inflammare*, which means "to burn" or "to set on fire" [133, 134]. Inflammation has long been recognized as a central process by which the body responds to and defends against harmful stimuli, such as invading pathogens, damaged cells, or toxic compounds. During this process, the body attempts to remove the harmful stimuli and initiate healing [135]. There are two forms of inflammation: acute and chronic. Chronic inflammation can last for

several weeks or months or even years. This form of inflammation is the body's response to chronic conditions such as allergies, asthma, rheumatoid arthritis, and autoimmune diseases. Chronic inflammation has also been shown to play an underlying role in cardiovascular disease, diabetes, Alzheimer's disease, and even aging [135].

Acute inflammation, on the other hand, refers to a rapid response of the immune system to a stimulus, and this form of inflammation has a short duration, lasting anywhere from a few days to a few weeks. In acute inflammation, there are a number of events that occur within the body to minimize injury or infection, with the overall goal of restoring the body to homeostasis [136]. Acute inflammation is characterized by redness, swelling, heat, and pain [135]. These cardinal signs of inflammation were described by the first-century Roman physician Aurelius Cornelius Celsus many years ago [134]. Briefly, the acute inflammatory process is initiated when tissues are injured. There are immune cells present in the tissue that, when activated after tissue damage, release chemicals that cause vasodilation (dilation of blood vessels in the affected area). Vasodilation causes the blood vessels to leak fluid into the surrounding tissue, which causes swelling. Furthermore, there is subsequent increased permeability of blood vessels in the affected area, which allows white blood cells such as neutrophils to migrate from inside the blood vessels into the affected tissue surrounding the blood vessel. Once in the damaged tissue, the white blood cells begin the repair process. Once repair is complete, the resolution of acute inflammation begins [133, 135, 137].

Resolution of Inflammation & Specialized Pro-resolving Lipid Mediators

Resolution of acute inflammation was once regarded as a passive process; however, it is now recognized to be an actively regulated process that is essential to maintaining host health. Over the past two decades, much time and effort has been put into researching this active resolution process, as stimulating the resolution of inflammation may prove to be more effective than targeting inhibition or antagonism of inflammation [138]. It is important that the acute inflammatory process is properly resolved; if it is not resolved, it can lead to chronic inflammation and tissue damage. Chronic inflammation is responsible for a number of serious diseases, including atherosclerosis, cancer, cardiovascular diseases, diabetes, and rheumatoid arthritis [135, 139]. Important steps in the acute inflammation resolution process include reducing or stopping neutrophil infiltration into inflamed areas, apoptosis of spent neutrophils, counter-regulating chemokines and cytokines, reprogramming macrophages from classically to alternatively activated, and the initiation of healing [135, 140].

Specialized pro-resolving lipid mediators (SPMs) are a class of endogenous cell signaling molecules that play a major role in the resolution of inflammation. SPMs are able to control the magnitude and extent of inflammatory events by activating local resolution programs [141]. The discovery of SPMs around two decades ago launched a whole new field of study known as resolution pharmacology that is dedicated to investigating the mechanisms that are involved in the active resolution of

inflammation [142]. SPMs serve as mediators of inflammation by regulating pro-inflammatory cells such as polymorphonuclear neutrophils (PMNs), monocytes, and macrophages [140]. Once inflammation has developed to an appropriate point, the body begins producing SPMs in order to prevent PMN infiltration, promote apoptosis, initiate the clearance of apoptotic cells by macrophages, and reprogram macrophages from a pro-inflammatory to a pro-resolving phenotype [139, 140].

By studying exudates, four families of SPMs were discovered: lipoxins (LX), resolvins (RV), protectins (PD), and maresins (MaR). These SPMs are actively synthesized during the resolution phase of acute inflammation; they are potent agonists that control the duration and magnitude of inflammation [138]. Lipoxins, which were the first SPMs to be identified, are synthesized from the omega-6 fatty acid arachidonic acid. The two main forms of lipoxin are LXA_4 and LXB_4. Lipoxins can interact with receptors on leukocytes to regulate their function. In particular, Lipoxin promotes monocyte migration and inhibits neutrophil infiltration into tissue sites [140, 143]. Resolvins, also known as resolution-phase interaction products, can be synthesized from the omega-3 fatty acids docosahexaenoic acid (DHA) and eicosapentaenoic acid (EPA), giving you the D series resolvins (RvD) and E series resolvins (RvE), respectively. Resolvins are potent anti-inflammatory compounds; they are able to block the production of pro-inflammatory mediators and regulate leukocyte trafficking. In particular, resolvins have been shown to stop the infiltration of PMNs [138]. Protectins and Maresins are also synthesized from DHA, but by different pathways than the D series Resolvins. Protectins reduce neural

inflammation, stimulate resolution, and reduce pain. Maresins, also known as macrophage mediators in resolving inflammation, are pro-resolving mediators produced by macrophages. Studies have shown that maresins limit the recruitment of PMNs and inhibit neutrophil infiltration, enhance macrophage phagocytosis and efferocytosis, reduce the production of pro-inflammatory factors, inhibit NF-κB activation, stimulate tissue regeneration, and reduce pain [139, 144].

Testing the Potential Beneficial Effects of Lipoxin on LPS-mediated BBB Compromise in Rats

In the late 1950s and early 1960s, studies revealed that gram-negative endotoxin is associated with BBB disruption. Lipopolysaccharide (LPS) is a gram-negative endotoxin in its more purified form, and it is known to disrupt the BBB and alter many other aspects of BBB function, including adsorptive transcytosis, immune cell trafficking, and various transport functions [132]. Banks et al showed that BBB disruption was present in animals 24 hours after a single injection of LPS. They also showed that LPS acts directly on brain vascular endothelial cells (BVECs) to cause this BBB disruption; BVECs line brain blood vessels, and the tight junctions holding BVECs together is what forms the functional BBB [132].

Based on these findings, we decided to induce inflammation and BBB disruption by administering LPS to rats for various lengths of time (24hours, 72 hours, and 96 hours). We hypothesized that administering Lipoxin to these rats would reduce inflammation and therefore BBB disruption. Rats were injected with LPS, and then

three hours later they were given an injection of either Lipoxin or a placebo (normal saline). Some rats were sacrificed after 24 hours. Other rats were maintained for 72 or even 96 hours. These rats received an additional injection of Lipoxin or placebo each day up until the day of sacrifice. Animals were sacrificed by perfusion-fixation. Brains were processed for IHC and SEM. IHC was used to detect the presence, location, and extent of BBB compromise. SEM was used to directly visualize the effects of anesthesia on the luminal surfaces of brain vascular endothelial cells (BVECs) forming the BBB.

MATERIALS AND METHODS

Animals:

Thirty-three wild-type Sprague Dawley rats (Envigo) were maintained on food and water *ad libitum* in an AAALAC-accredited vivarium with a 12-hour light/dark cycle. Animal use was approved by the RowanSOM IACUC.

Animal Treatment:

Rats aged 7-28 months were weighed and given an intravenous (IV) injection via the tail vein of 5-15mg/kg LPS from *Salmonella enteritidis* (MilliporeSigma, Burlington, MA, USA) dissolved in sterile normal saline. After three hours, the rats were then injected via the tail vein with either 5µg/kg Lipoxin or placebo. Some rats were sacrificed after 24 hours. Other rats were maintained for 72 hours or 96 hours. These rats received an additional injection of Lipoxin or placebo each day up until the day of sacrifice. See **Table 1** for a breakdown of the animals used in this study. To achieve the best preservation of the brain tissue, all animals were fixed by perfusion using freshly prepared 4% paraformaldehyde (PFA) in PBS. Brains were quickly removed and, using a brain block, coronal sections were cut anteroposteriorly for bright-field microscopy, immunohistochemistry (IHC), and scanning electron microscopy (SEM). Left hemispheres were sliced into 4mm thick sections for IHC; right hemispheres were sliced into 2mm thick sections for SEM. From the left hemispheres a total of four tissue blocks were generated − anterior, middle, posterior, and cerebellar. Anterior, middle, and posterior tissue blocks comprising different regions of cerebral cortex were the primary focus of this study.

Tissue Preparation, Immunohistochemistry, and Scanning Electron Microscopy: Brain tissues for IHC were fixed in 4% PFA and prepared for routine embedding in paraffin and sectioning as described previously [68]. Sections representing each brain region (anterior, middle, and posterior) were randomly selected for detection of extravasated IgG using IHC. IHC was performed using the protocol and reagents described previously [68]. Extravasation of IgG has been widely used as a biomarker of BBB breach [45, 68-71, 114]. To detect IgG, biotinylated anti-rat IgG (Vector Laboratories, BA-9400, 1:20 in Dako antibody diluent) was used as the primary antibody [68, 69]. Cortical regions from each section were photographed using a Nikon Microphot-FXA microscope, and images were analyzed using NIS-Elements Imaging Software (Nikon Instruments Inc., USA). For SEM, brain tissue was fixed in 4% PFA, rinsed in PBS, and post-fixed with 1% osmium tetroxide. After washing in buffer, tissues were dehydrated in ethanol and then embedded in Carbowax Polyethylene Glycol (PEG, avg. mol. wt. = 6,000) (Electron Microscopy Sciences, USA). PEG was used as a removable embedding medium to physically support the architecture of the blood vessels while slicing through the brain tissue to expose their luminal surfaces. After shaving the face of the samples to expose blood vessels, they were placed back in ethanol to dissolve the PEG and then transferred to amyl acetate. Samples were then dried with liquid carbon dioxide in an E3100 critical point dryer (Quorum Technologies, USA) and rendered conductive by coating with a thin (~40Å) layer of gold using a Desk II sputter coater (Denton Vacuum, USA). Tissues were examined using an Apreo SEM (FEI, a subsidiary of Thermo Fisher Scientific).

EXPERIMENTAL RESULTS

Treatment with 15mg/kg LPS Induced both Focal and Global Leaks in the BBB of Brain Microvessels

Sections through the cerebral cortex of rats treated with LPS showed leaks in the BBB (**Fig. 1**). These leaks result in an influx of plasma into the brain parenchyma (**Fig. 1A-F, H-I**). Leaks were most prominent in association with small arterioles, most likely because they, unlike their companion venules, are under pressure (**Fig. 1C-F**). IgG is a plasma component normally restricted from the brain tissue by a properly functioning BBB; therefore, we immunostained rat brain tissues using anti-IgG and used the presence of IgG in the brain intercellular space as an indicator or biomarker of a locally leaky BBB. We found that the leaked IgG often (but not always) has affinity for the surfaces of neurons, with an obvious preference for pyramidal neurons (**Fig. 1A, C, E-F**). Clearly, binding of brain-reactive autoantibodies to neurons is disruptive to neuronal function. If chronic, we have proposed that this could lead to more long-term consequences, including delirium, cognitive decline, and dementia in the elderly. BBB leaks were most conspicuous at 24 hours after exposure (**Fig. 1A-C**), which was the earliest time point examined, and they seemed to gradually disappear thereafter. Glial cells, astrocytes, and microglia were only very rarely IgG-immunopositive, unlike pyramidal neurons. At both 72 hours (**Fig. 1D-F**) and 96 hours (**Fig. 1G-I**) after LPS exposure, BBB leaks appeared to become less severe, suggesting that many blood vessels were able to recover their normal BBB function and thereby reduce the extent of BBB leak. This reduction is evidenced by the reduced amount of IgG detected in the brain intercellular space,

which may provide an opportunity for the leaked IgG to clear via interstitial fluid flow to the CSF. Reduction of the dose of LPS from 15mg/kg to 10mg/kg also resulted in leaks of a similar extent to those in animals treated with 15mg/kg LPS, with the difference between the two being primarily that the lower dose results in fewer vessels being affected (compare **Fig. 1** with **Fig. 2**). In animals treated with 5mg/kg LPS, both the number and extent of blood vessels showing BBB compromise were markedly reduced (data not shown).

Treatment with Lipoxin Resulted in a Marked Reduction in both the Incidence and Extent of LPS-Induced BBB Compromise and Associated Plasma Leak

Sections through the cerebral cortex of rats treated with LPS followed by Lipoxin within 3 hours of LPS treatment were examined (**Fig. 3**). Here, we again immunostained for IgG and used its presence in the brain tissue as an indicator of the leak of plasma from blood vessels into the brain parenchyma. At 24 hours after LPS insult and Lipoxin treatment, the number of BBB-compromised vessels was reduced as was the extent of their leak as detected in the cerebrocortical tissue sections, suggesting that Lipoxin has a beneficial effect, at least to some extent, of either blocking exacerbation of LPS-mediated BBB breakdown or, alternatively, allowing for more rapid recovery from LPS-mediated BBB breaches (**Fig. 3A-C; Fig. 4A-D**). At 72 hours and 96 hours after LPS insult and Lipoxin treatment, blood vessels showing substantial BBB leaks were only rarely observed, suggesting that Lipoxin may promote faster functional recovery of the BBB in affected blood vessels (**Fig. 3D-I; Fig. 5A-C**). The nature of how this recovery is mediated by Lipoxin cannot be

resolved by this IHC approach. Therefore, we employed scanning electron microscopy (SEM) to determine if direct visualization of the luminal surface endothelium of these vessels could shed some light on the effects of Lipoxin on brain vascular endothelial cells (BVECs).

Scanning Electron Microscopy Can Be Used to Directly Visualize the BBB and the Luminal Surface Topography of BVECs

SEM has the advantage of allowing examination of the luminal surfaces of BVECs over relatively large expanses of the blood vessel luminal surface. Here, a combination of embedding brain tissue in solid polyethylene glycol (PEG) and SEM was used to examine the luminal surface topography of BVECs and the marginal tight junctions associated with the BBB. To achieve this, brains were fixed by perfusion and embedded in PEG (avg. mol. wt. = 6,000), a removable (water-soluble) embedding medium which physically supports the delicate architecture of the brain tissue and blood vessels while slicing through the tissue to expose the luminal surfaces of blood vessels and their BVEC linings. As shown in **Figure 6**, this approach allows direct examination of the luminal surfaces of adjacent BVECs, including the tight junctional contacts at BVEC cell margins that contribute to the BBB, in longitudinal, oblique, and cross-sectional profiles. In untreated control brains, SEM revealed that BVECs have flattened luminal surfaces and are oriented parallel to the long axis of the vessel. Nuclei were often found to bulge upwards slightly and project into the lumen (**Fig. 6A**). All along the interface between adjacent elongated BVECs, prominent sheet-like cytoplasmic extensions (here referred to as

contact flaps), which contain extensive tight junctions that block paracellular plasma leak into the brain, project upwards into the lumen and run parallel to the direction of blood flow to minimize blood flow turbulence. These contact flaps resemble the membrane ruffles commonly seen at the leading edges of migrating cells in culture. They occur at adjacent cell margins, where the tight junctions are known to provide the initial seal for the BBB (**Fig. 6B-D**). In these healthy animals, BVECs tend to be roughly the same size in that each cell seems to cover a similar surface area of the blood vessel luminal epithelium.

Treatment with LPS Induced Changes in BVEC Luminal Surface Topography and Compromised BVEC Viability

In view of the fact that LPS was found to trigger BBB functional compromise, as was evident in the IHC results described above, we next asked if SEM could be used to detect, by direct visualization, morphological changes in the luminal surface topography of BVECs, especially in the specific region occupied by BBB-associated tight junctions located at the marginal interface of adjacent cells. At 24 hours after LPS insult and without Lipoxin treatment, LPS was found to cause a marked flattening of the luminal surfaces of BVECs, often with the marginal contact flaps flattened against the luminal surface (**Fig. 7A-B**). Microvilli were far less abundant, pointing to the fact that exposure of these cells to LPS induces these changes to the cell surface topography, an indication that BVEC plasma membranes are affected by LPS treatment. At 72 hours after LPS insult and without Lipoxin treatment, dead BVECs were detected in the luminal lining of blood vessels (**Fig. 7C, E-F; Fig. 8A-**

B). These dead cells are easily distinguished from adjacent living cells by virtue of the fact that their luminal surface membranes show obvious signs of breakdown. These signs include discontinuity of the plasma membranes as shown by the pock-marked surfaces and the disengagement of segments of the marginal surface membranes from adjacent cells. Cell remnants persist that contain a tangled web of cytoskeletal fibers with entrapped organelles (**Fig. 8B**). Some nuclei can still be seen in these dead cells, trapped in a web of cytoskeletal filaments. Other nuclei are often stripped off by the shear forces of the rapid blood flow (**Fig. 7F**). Most often, these dead cells are encountered individually in the blood vessel wall, and thus are surrounded by living cells with completely intact surface plasma membranes. What makes these isolated cells succumb to the effects of LPS, and why all cells are not similarly affected by LPS treatment, are unknown. Frequently, these regions of the blood vessels containing dead BVECs are seeding sites for forming blood clots or attachment points for individual platelets (**Fig. 7D-F; Fig. 8C**). At 96 hours after LPS insult, dead BVECs were most numerous as were clots, especially in regions of increased turbulence and shear force, such as sites of blood vessel bifurcation (**Fig. 7E-F; Fig. 8D-F**). The long-term consequences of the restricted blood flow in these tributaries is unknown, but the expectation is that the observed local diminished blood flow will result in hypoperfusion of the areas fed by these vessels, which could affect brain function in these locally deprived regions.

Treatment with Lipoxin following LPS Administration Reduced the Extent of BBB Compromise and, Most Importantly, Blocked the Loss of BVECs from the

Endothelial Lining of Brain Blood Vessels

IHC results described above clearly show that Lipoxin reduces both the incidence and extent of LPS-mediated BBB leak. We next asked whether treatment with Lipoxin had any observable beneficial effects on the luminal surface morphology of BVECs, including the BBB-associated tight junctions within the contact flaps at the interface of adjacent cells. At 24 hours after LPS insult and Lipoxin treatment, BVEC luminal surfaces still showed a similar degree of flattening as was observed in the LPS-only group, with fewer microvilli and marginal contact flaps flattened against the luminal surface compared to untreated controls (**Fig. 9A-B; Fig. 10A-B**). At 72 hours and 96 hours, the most conspicuous difference between the luminal surfaces of BVECs in LPS-only and LPS + Lipoxin-treated animals was the nearly complete lack of dead BVECs in the LPS + Lipoxin-treated group. This change alone may be sufficient to explain the observed widespread improvement and more rapid recovery of BBB function as evidenced in IHC preparations (**Fig. 9C-F; Fig. 10C-D**). This is based on the likely conclusion that regions of the blood vessel wall lined by dead BVECs can no longer present an effective barrier to prevent leak of plasma components into the brain interstitium, and therefore represent sites of BBB leak. Assuming this to be true, by blocking the death and loss of BVECs lining brain blood vessels, Lipoxin exerts a beneficial effect on the maintenance of BBB functional integrity, which can counteract the negative effects of LPS on barrier function.

DISCUSSION

Those who are hospitalized and undergo major surgery are known to have a much greater chance of suffering from delirium and cognitive decline post-surgery. The mechanism by which surgery leads to impairment of a person's memory has remained a mystery until recently [45]. We now know that post-surgical inflammation plays a key role in this process. Regulating the acute inflammatory process has been shown to be effective in diseases such as sepsis, obesity, and diabetes [145], leading to speculation that inflammation of the BBB may be a mechanism contributing to POD, as inflammatory conditions such as sepsis and wound infection are major causes of delirium [44]. Around two decades ago, a new class of endogenous cell signaling molecules known as specialized pro-resolving lipid mediators (SPMs) were discovered. These SPMs play a major role in the resolution of inflammation. Here, we used a rat model to examine whether administration of the SPM Lipoxin could reduce inflammation and BBB permeability after a lipopolysaccharide (LPS) insult. Immunohistochemistry (IHC) and scanning electron microscopy (SEM) were used to monitor BBB structure and function.

This study has five major findings. First, using IHC, we show that treatment with 15mg/kg LPS induces both focal and global leaks in the BBB of rat brain blood vessels. IgG is a plasma component normally restricted from the brain tissue; therefore, we immunostained rat brain tissues for IgG and used the presence of IgG in the brain tissue as an indicator or biomarker of a leaky BBB. We found that the leaked IgG often has an affinity for the surfaces of neurons, particularly pyramidal

neurons. BBB leaks were most conspicuous at 24 hours after exposure, while at both 72 hours and 96 hours after LPS exposure, BBB leaks appeared to become less severe, suggesting that many blood vessels were able to recover their normal BBB function. Second, using IHC, we show that treatment with Lipoxin results in a marked reduction in both the incidence and extent of LPS-induced BBB compromise and associated plasma leak. We again immunostained for IgG and used its presence in the brain tissue as an indicator of BBB leak. We found that 24 hours after LPS insult and Lipoxin treatment, the number of BBB-compromised vessels was reduced as was the extent of their leak evident in the tissue sections, suggesting that Lipoxin allows for more rapid recovery from LPS-mediated BBB breaches. At 72 hours and 96 hours after LPS insult and Lipoxin treatment, blood vessels showing BBB leaks were only rarely observed, suggesting that Lipoxin promotes faster BBB recovery in these blood vessels. Third, SEM allowed us to directly visualize the BBB and the luminal surfaces of BVECs. BVECs in untreated control brains showed flattened luminal surfaces and were oriented parallel to the long axis of the vessel, and BVEC nuclei often bulged upwards slightly and projected into the lumen. Prominent sheet-like cytoplasmic extensions that we refer to as contact flaps can be found all along the interface between adjacent elongated BVECs. These contact flaps project upwards into the lumen and run parallel to the direction of blood flow. They occur at adjacent cell margins, where the tight junctions are known to provide the initial seal for the BBB. Fourth, through SEM, we show that administration of LPS induces changes in BVEC luminal surface topography and compromises BVEC viability. LPS was found to cause a marked flattening of the luminal surfaces of BVECs in rats 24 hours after

LPS insult. Microvilli were also far less abundant than in control brains. At 72 hours after LPS insult, dead BVECs were detected in the luminal lining, with their nuclei often being stripped off by the shear forces of the rapid blood flow. At 96 hours after LPS insult, dead BVECs were most numerous as were clots, especially in regions of increased turbulence and shear force. Fifth, through SEM, we show that treatment with Lipoxin following LPS administration reduces the level of BBB compromise and blocks the loss of BVECs from the endothelial luminal surface. At 24 hours, BVEC luminal surfaces showed a similar degree of flattening as was observed in the LPS-only group, with fewer microvilli and marginal contact flaps flattened against the luminal surface compared to untreated controls. At 72 hours and 96 hours, the most conspicuous difference between the luminal surfaces of BVECs in LPS-only and LPS + Lipoxin-treated was the nearly complete lack of dead BVECs in the LPS + Lipoxin-treated group. This change alone may be sufficient to explain the observed widespread improvement in BBB function that was seen in IHC preparations.

Our results suggest that inflammation induces changes in the physical properties of BVEC luminal surface membranes that mediate their flattening, and that these changes are accompanied by increased BBB permeability. Whether or not these changes in BBB permeability are due to impaired function of tight junction proteins or changes in the physical properties of the surface membranes remains to be determined. We propose that this inflammation-induced increase in BBB permeability results in a plasma influx into the brain parenchyma that disrupts brain homeostasis and neuronal activity, triggering POD. In the elderly, if left unresolved, it can lead to

postoperative cognitive decline (POCD) and perhaps be a trigger for later dementia. Furthermore, our results suggest that administration of Lipoxin after an inflammatory insult could help alleviate the symptoms normally caused by inflammation. We propose that Lipoxin should be administered to post-surgical patients, as this may curtail the effects of inflammation on the BBB and therefore reduce or prevent the incidence of POD in patients post-surgery.

The results of our study agree with Liu et al., who found that Lipoxin and BML-111, a lipoxin receptor agonist, reduce inflammation and have protective effects in LPS-induced keratinocytes and psoriasiform dermatitis (a psoriasis mimic) in mice [146]. The results of our study also agree with Guo et al., who found that Lipoxin reduces inflammation after a subarachnoid hemorrhage [147]. Our results also agree with that of Lin et al., who found that Lipoxin alleviates the symptoms of preeclampsia in rats exposed to the endotoxin LPS [148], and with Conte et al., who demonstrated that Lipoxin exerts an anti-inflammatory effect on zymosan-induced arthritis [149]. Finally, the results of our study also agree with Wu et al., who found that Lipoxin improves BBB integrity and function after focal ischemic stroke by reducing matrix metalloproteinase (MMP)-9 expression [150].

A major strength of this study is the use of SEM to directly examine the effects of LPS and Lipoxin on the brain endothelium and the physical structure of the BBB. To our knowledge, this approach has not been used elsewhere. The main limitation of this study is the small sample size of rats used here, due to the cost associated with

housing and providing for these animals. That being said, there was an easily discernable pattern of effects of LPS and Lipoxin on the BBB. However, additional studies using larger numbers of rats would be helpful in drawing further conclusions.

In conclusion, the data presented here show that administration of LPS to rats causes BBB disruption, as evidenced by the presence of IgG in the brain parenchyma, which we used as a biomarker of vascular leak. It is clear that LPS directly alters the luminal surface morphologies of BVECs, particularly in regions of BBB-associated tight junctions. Furthermore, our data show that treatment with Lipoxin after LPS insult causes a reduction in both the number of BBB-compromised vessels and the extent of their leak, suggesting that Lipoxin has a beneficial effect and allows for more rapid recovery from LPS-mediated BBB breach. Based on these findings, we propose that LPS disrupts the BBB, leading to an increase in BBB permeability. This allows an influx of plasma components such as IgG into the brain parenchyma, which compromises brain homeostasis and proper neuronal functions. Binding of IgG to neurons may further exacerbate neuronal dysfunction and contribute to the emergence of symptoms associated with POD. We suggest that failure to completely restore BBB function following surgery could lead to postoperative cognitive decline (POCD) in the short-term and, if unresolved, may favor the later development of dementia in the long-term. Therefore, maintenance of proper BBB function is crucial for preventing the occurrence and escalation of POD. The findings of this study suggest that administration of Lipoxin to post-surgical patients may aid in restoring proper BBB function and help prevent the incidence of POD.

FIGURES

Table 1: List of Animals Used in this Study

Identification Number	Age	DOB	DOE	Treatment
Lipoxin Rat 1	~20 months	11/28/2015	8/2/2017	5mg/kg LPS Only (24hr)
Lipoxin Rat 2	~20 months	11/28/2015	8/2/2017	5mg/kg LPS + Lipoxin (24hr)
Lipoxin Rat 3	~20 months	11/28/2015	8/4/2017	5mg/kg LPS Only (72hr)
Lipoxin Rat 4	~20 months	11/28/2015	8/4/2017	5mg/kg LPS + Lipoxin (72hr)
Lipoxin Rat 5	~7 months	1/24/2017	8/15/2017	10mg/kg LPS Only (24hr)
Lipoxin Rat 6	~7 months	1/24/2017	8/15/2017	10mg/kg LPS + Lipoxin (24hr)
Lipoxin Rat 7	~7 months	1/24/2017	8/17/2017	10mg/kg LPS Only (72hr)
Lipoxin Rat 8	~7 months	1/24/2017	8/17/2017	10mg/kg LPS + Lipoxin (72hr)
Lipoxin Rat 9	~7 months	1/15/2017	8/29/2017	15mg/kg LPS Only (24hr)
Lipoxin Rat 10	~7 months	1/15/2017	8/29/2017	15mg/kg LPS + Lipoxin (24hr)
Lipoxin Rat 11	~7 months	12/21/2016	8/31/2017	15mg/kg LPS Only (72hr)
Lipoxin Rat 12	~7 months	1/15/2017	8/31/2017	15mg/kg LPS + Lipoxin (72hr)
Lipoxin Rat 13	~22 months	11/28/2015	9/22/2017	10mg/kg LPS Only (96hr)
Lipoxin Rat 14	~22 months	11/28/2015	9/29/2017	10mg/kg LPS + Lipoxin (96hr)
Lipoxin Rat 15	~22 months	11/28/2015	9/28/2017	10mg/kg LPS + Lipoxin (96hr)
Lipoxin Rat 16	~28 months	5/8/2015	9/29/2017	10mg/kg LPS + Lipoxin (96hr)
Lipoxin Rat 17	~8 months	1/24/2017	10/6/2017	10mg/kg LPS Only (96hr)
Lipoxin Rat 18	~8 months	1/15/2017	10/6/2017	10mg/kg LPS Only (96hr)
Lipoxin Rat 19	~8 months	1/15/2017	10/6/2017	10mg/kg LPS Only (96hr)
Lipoxin Rat 20	~9 months	12/21/2016	10/6/2017	10mg/kg LPS Only (96hr)
Lipoxin Rat 21	~9 months	12/21/2016	10/6/2017	10mg/kg LPS Only (96hr)
Lipoxin Rat 22	~8 months	1/24/2017	10/13/2017	10mg/kg LPS + Lipoxin (96hr)
Lipoxin Rat 23	~8 months	1/24/2017	10/13/2017	10mg/kg LPS + Lipoxin (96hr)
Lipoxin Rat 24	~8 months	1/24/2017	10/13/2017	10mg/kg LPS + Lipoxin (96hr)
Lipoxin Rat 25	~8 months	1/24/2017	10/13/2017	10mg/kg LPS + Lipoxin (96hr)
Lipoxin Rat 26	~8 months	1/24/2017	10/13/2017	10mg/kg LPS + Lipoxin (96hr)
Lipoxin Rat 27	~12 months	3/12/2017	3/23/2018	15mg/kg LPS Only (96hr)
Lipoxin Rat 28	~12 months	3/12/2017	3/23/2018	15mg/kg LPS Only (96hr)
Lipoxin Rat 29	~14 months	1/24/2017	3/23/2018	15mg/kg LPS Only (96hr)
Lipoxin Rat 30	~12 months	3/12/2017	3/23/2018	15mg/kg LPS Only (96hr)
Lipoxin Rat 31	~12 months	3/12/2017	3/30/2018	15mg/kg LPS + Lipoxin (96hr)
Lipoxin Rat 32	~12 months	3/12/2017	3/30/2018	15mg/kg LPS + Lipoxin (96hr)
Lipoxin Rat 33	~12 months	3/12/2017	3/28/2018	15mg/kg LPS + Lipoxin (96hr)

This is a comprehensive list of the animals used in this study. DOB - Date of Birth; DOE - Date of Expiration; LPS - Lipopolysaccharides.

Figure 1: Immunohistochemistry of Rat Brains Was Used to Examine the Effects of 15mg/kg LPS on BBB Permeability

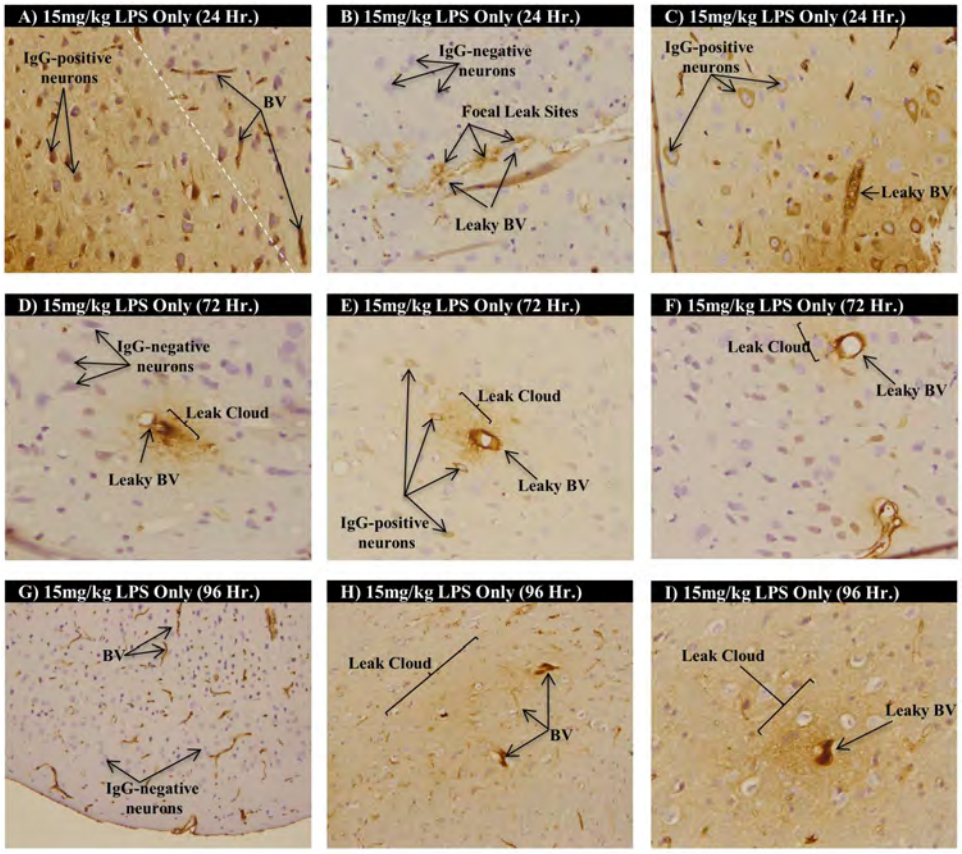

Histological sections of the cerebral cortex of rats that were immunostained to detect interstitial IgG as a result of BBB compromise. These sections reveal that rats treated with LPS show leaks in the BBB (**Fig. 1**). These leaks result in an influx of plasma into the brain parenchyma (**Fig. 1A-F, H-I**). Leaks were most prominent in association with small arterioles, most likely because they, unlike their companion venules, are under pressure (**Fig. 1C-F**). We found that the leaked IgG often has affinity for the surfaces of neurons, with an obvious preference for pyramidal neurons (**Fig. 1A, C, E-F**). BBB leaks were most conspicuous at 24 hours after exposure (**Fig. 1A-C**). Glial cells, astrocytes, and microglia were only very rarely IgG-immunopositive. At both 72 hours (**Fig. 1D-F**) and 96 hours (**Fig. 1G-I**) after LPS exposure, BBB leaks appeared to become less severe, suggesting that many blood vessels were able to recover their normal BBB function. BV - blood vessel; IgG - Immunoglobulin G.

Figure 2: Immunohistochemistry of Rat Brains Was Used to Examine the Effects of 10mg/kg LPS on BBB Permeability

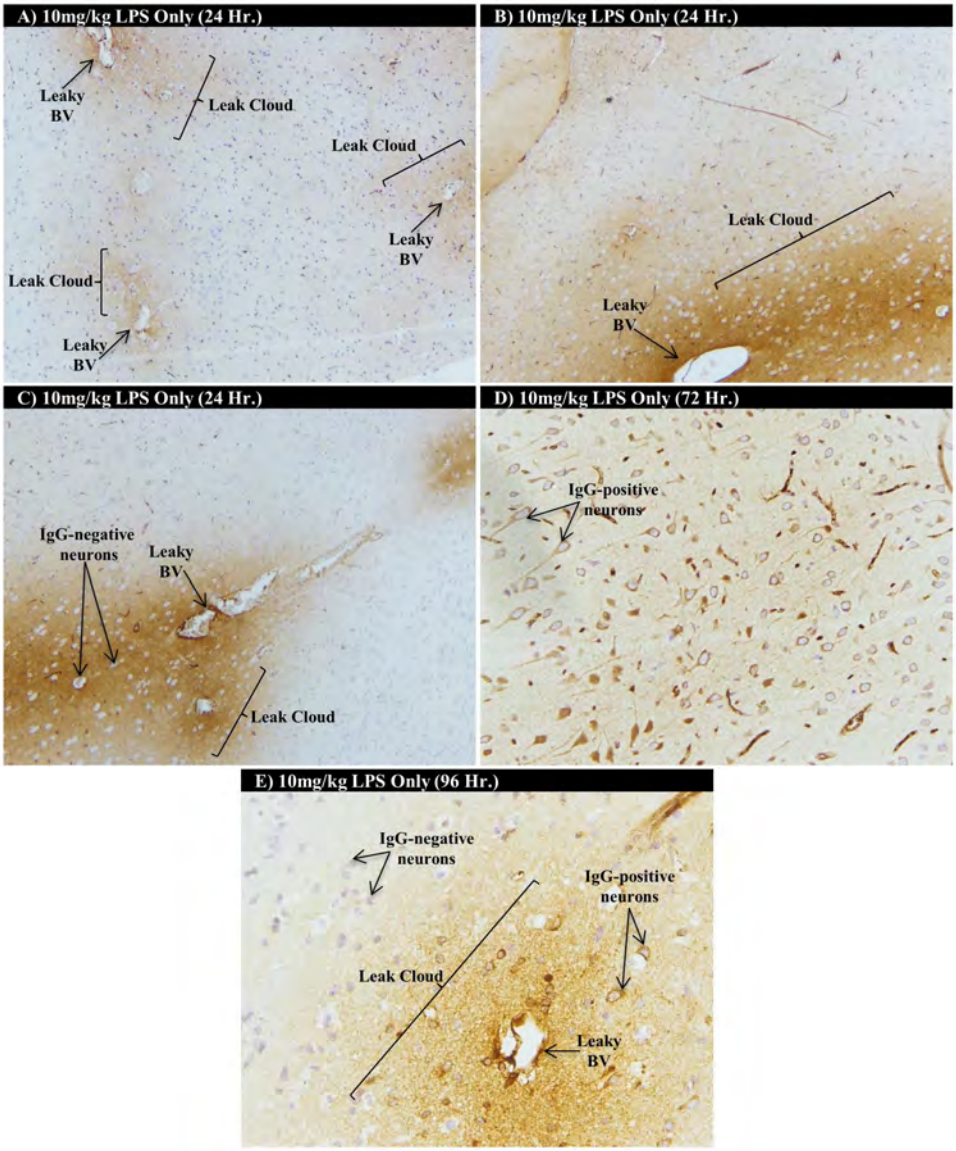

Histological sections of the cerebral cortex of rats that were immunostained to detect interstitial IgG as a result of BBB compromise. These sections reveal that reduction of the dose of LPS from 15mg/kg (**Fig. 1**) to 10mg/kg (**Fig. 2**) also results in leaks of a similar extent to those in animals treated with 15mg/kg LPS (**Fig. 1**), with the difference between the two being primarily that the lower dose results in less vessels being affected (compare **Fig. 1** with **Fig. 2**). BV - blood vessel; IgG - Immunoglobulin G.

Figure 3: Immunohistochemistry of Rat Brains Was Used to Examine the Effects of Lipoxin on BBB Permeability following an LPS Injection

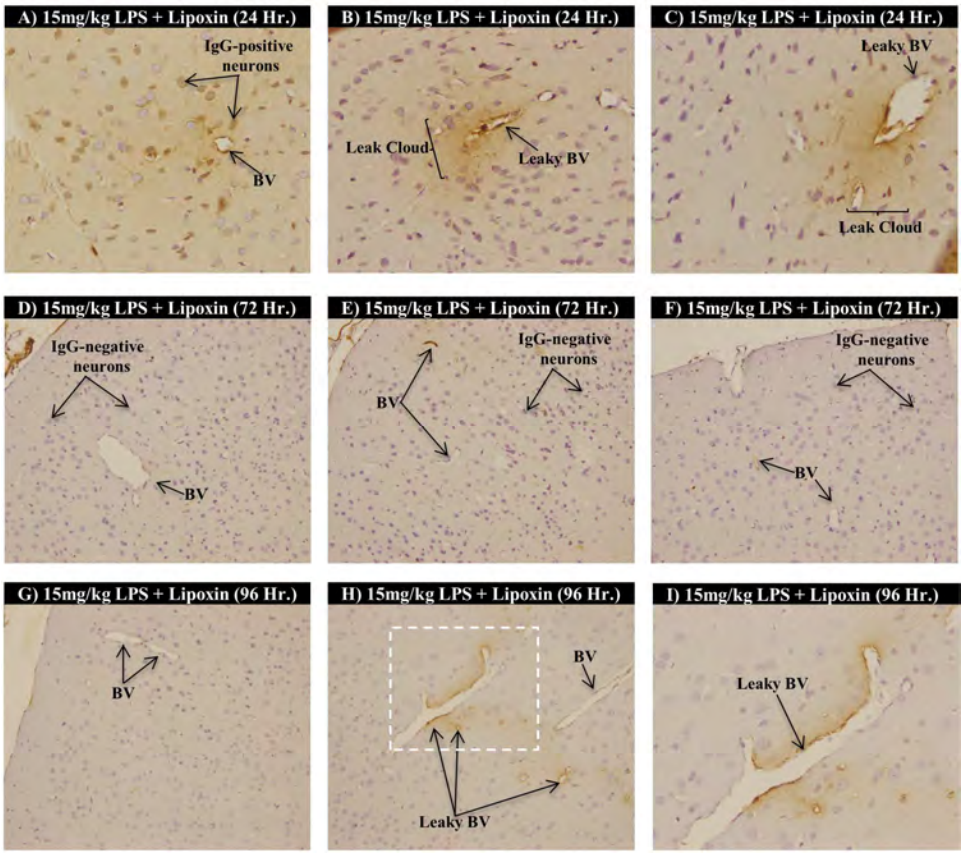

Histological sections of the cerebral cortex of rats that were immunostained to detect interstitial IgG as a result of BBB compromise. These sections reveal that treatment with 5µg/kg Lipoxin within 3 hours of LPS insult leads to an overall reduction in BBB leak (compare **Fig. 3** with **Fig.1** and **Fig. 2**). At 24 hours after LPS insult and Lipoxin treatment, the number of BBB-compromised vessels was reduced as was the extent of their leak evident in the tissue sections, suggesting that Lipoxin allows for more rapid recovery from LPS-mediated BBB breaches (**Fig. 3A-C**). At 72 hours and 96 hours after LPS insult and Lipoxin treatment, blood vessels showing BBB leaks were only rarely observed, suggesting that Lipoxin may promote faster functional recovery of the BBB in these blood vessels (**Fig. 3D-I**). BV - blood vessel; IgG - Immunoglobulin G.

Figure 4: Immunohistochemistry Revealed These Interesting Features in Animals Treated with LPS + Lipoxin for 24 Hours

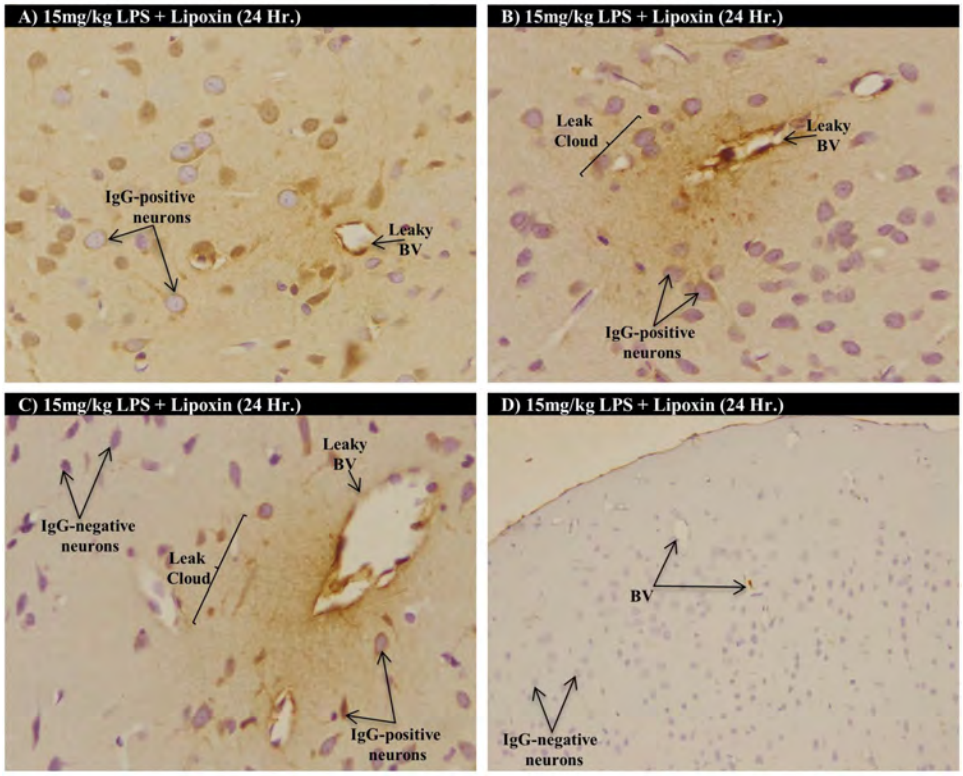

Histological sections of the cerebral cortex of rats that were immunostained to detect interstitial IgG as a result of BBB compromise. These sections reveal that treatment with 5µg/kg Lipoxin within 3 hours of LPS insult leads to an overall reduction in BBB leak (compare **Fig. 4** with **Fig.1** and **Fig. 2**). At 24 hours after LPS insult and Lipoxin treatment, the number of BBB-compromised vessels was reduced as was the extent of their leak evident in the tissue sections, suggesting that Lipoxin allows for more rapid recovery from LPS-mediated BBB breaches (**Fig. 4A-D**). BV - blood vessel; IgG - Immunoglobulin G.

Figure 5: Immunohistochemistry Revealed These Interesting Features in Animals Treated with LPS + Lipoxin for 72 Hours

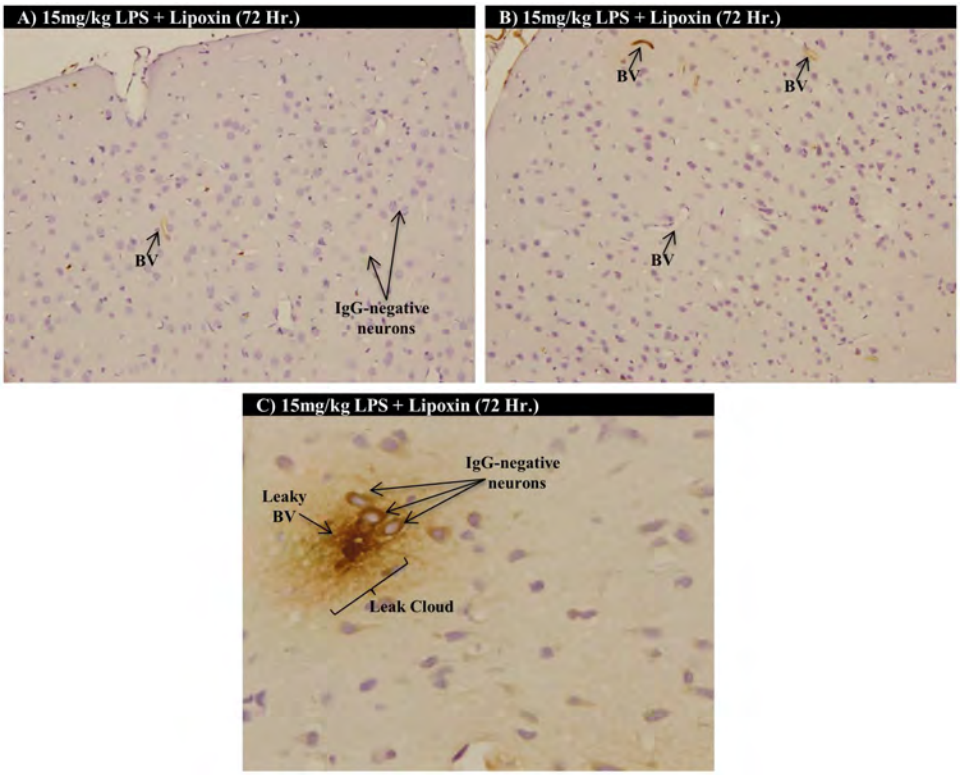

Histological sections of the cerebral cortex of rats that were immunostained to detect interstitial IgG as a result of BBB compromise. These sections reveal that treatment with 5µg/kg Lipoxin within 3 hours of LPS insult leads to an overall reduction in BBB leak (compare **Fig. 5** with **Fig.1** and **Fig. 2**). At 72 hours after LPS insult and Lipoxin treatment, blood vessels showing BBB leaks were only rarely observed, suggesting that Lipoxin may promote faster functional recovery of the BBB in these blood vessels (**Fig. 5A-C**). BV - blood vessel; IgG - Immunoglobulin G.

Figure 6: SEM Was Used to Examine BBB Morphology in Control Rat Brains

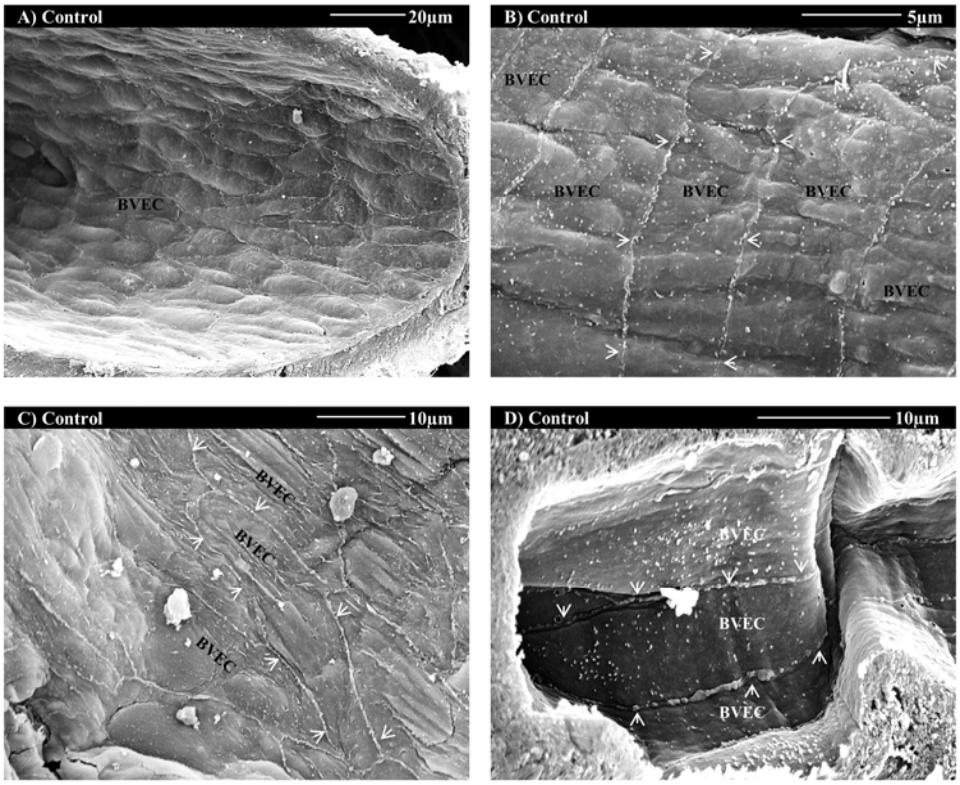

Scanning electron microscopic images of sections of age-matched control (untreated) rat brains. SEM was used to examine the luminal surfaces of adjacent BVECs, including the tight junctional contacts at BVEC cell margins that contribute to the BBB, in longitudinal, oblique, and cross-sectional profiles. In untreated control brains, BVECs showed flattened luminal surfaces and were oriented parallel to the long axis of the vessel. Nuclei were often found to bulge upwards slightly and project into the lumen (**Fig. 6A**). All along the interface between adjacent elongated BVECs, prominent sheet-like cytoplasmic extensions (here referred to as contact flaps), which contain extensive tight junctions to block paracellular plasma leak into the brain, project upwards into the lumen and run parallel to the direction of blood flow. These contact flaps occur at adjacent cell margins, where the tight junctions are known to provide the initial seal for the BBB (**Fig. 6B-D**). In these healthy animals, BVECs tend to be roughly the same size in that each cell seems to cover a similar surface area of the luminal epithelium. BVEC - brain vascular endothelial cell.

Figure 7: SEM of Rat Brains Was Used to Examine the Effects of LPS on BBB Morphology

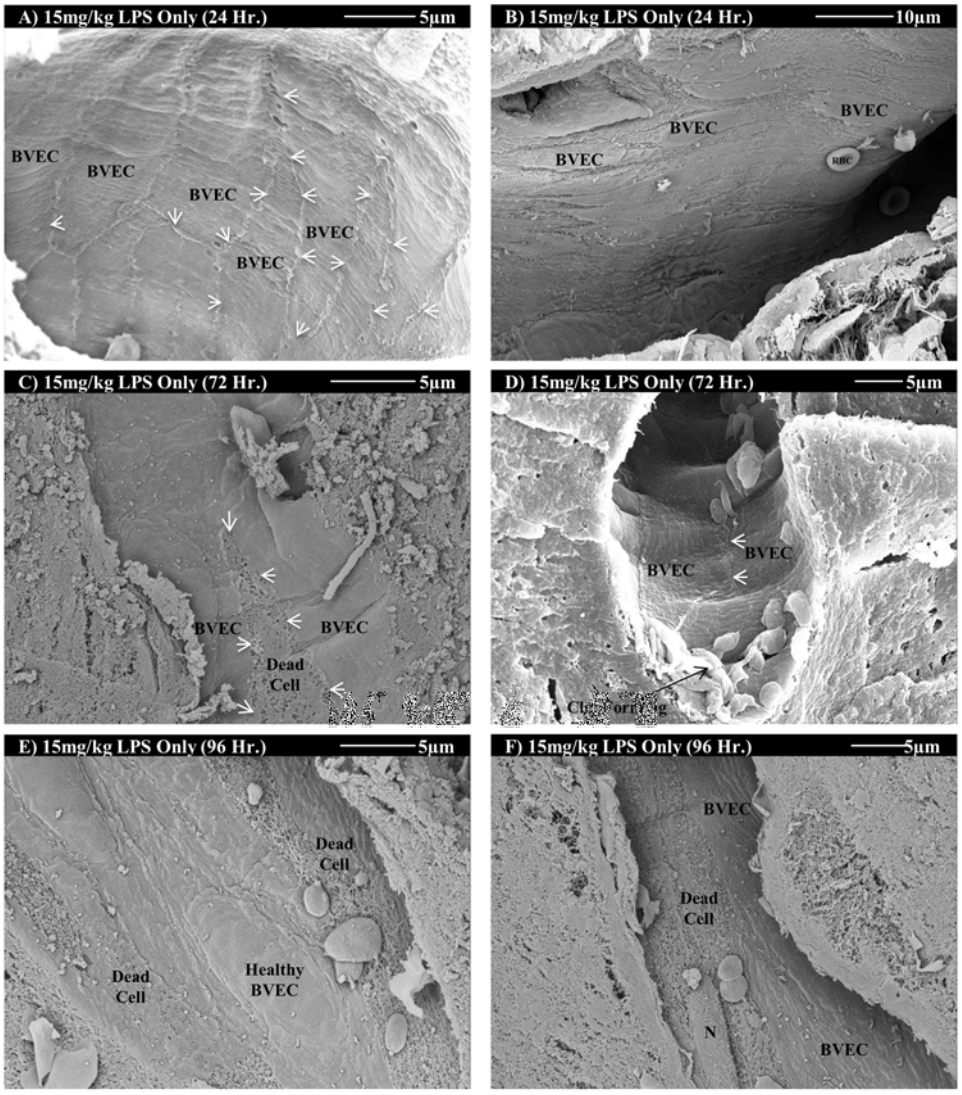

Figure 7: SEM of Rat Brains Was Used to Examine the Effects of LPS on BBB Morphology.

Scanning electron microscopy was used to examine the brains of rats that were exposed to 15mg/kg LPS. We examined the luminal surfaces of adjacent BVECs, including the tight junctional contacts at BVEC cell margins that contribute to the BBB, in longitudinal, oblique, and cross-sectional profiles. At 24 hours after LPS insult, LPS was found to cause a marked flattening of the luminal surfaces of BVECs, often with the marginal contact flaps flattened against the luminal surface (**Fig. 7A-B**). Microvilli were far less abundant than usual, pointing to the fact that exposure of these cells to LPS induces these changes to the cell surface. At 72 hours after LPS insult, dead BVECs were detected in the luminal lining (**Fig. 7C, E-F**). Nuclei are often stripped off by the shear forces of the rapid blood flow, but sometimes remain (**Fig. 7F**). Frequently, regions of the blood vessels containing dead BVECs are seeding sites for forming blood clots or attachment points for individual platelets (**Fig. 7D-F**). At 96 hours after LPS insult, dead BVECs were most numerous, especially in regions of increased turbulence and shear force, such as sites of blood vessel bifurcation (**Fig. 7E-F**). BVEC - brain vascular endothelial cell; RBC - red blood cell.

Figure 8: SEM Revealed These Interesting Features in Animals Treated with 15mg/kg LPS Only

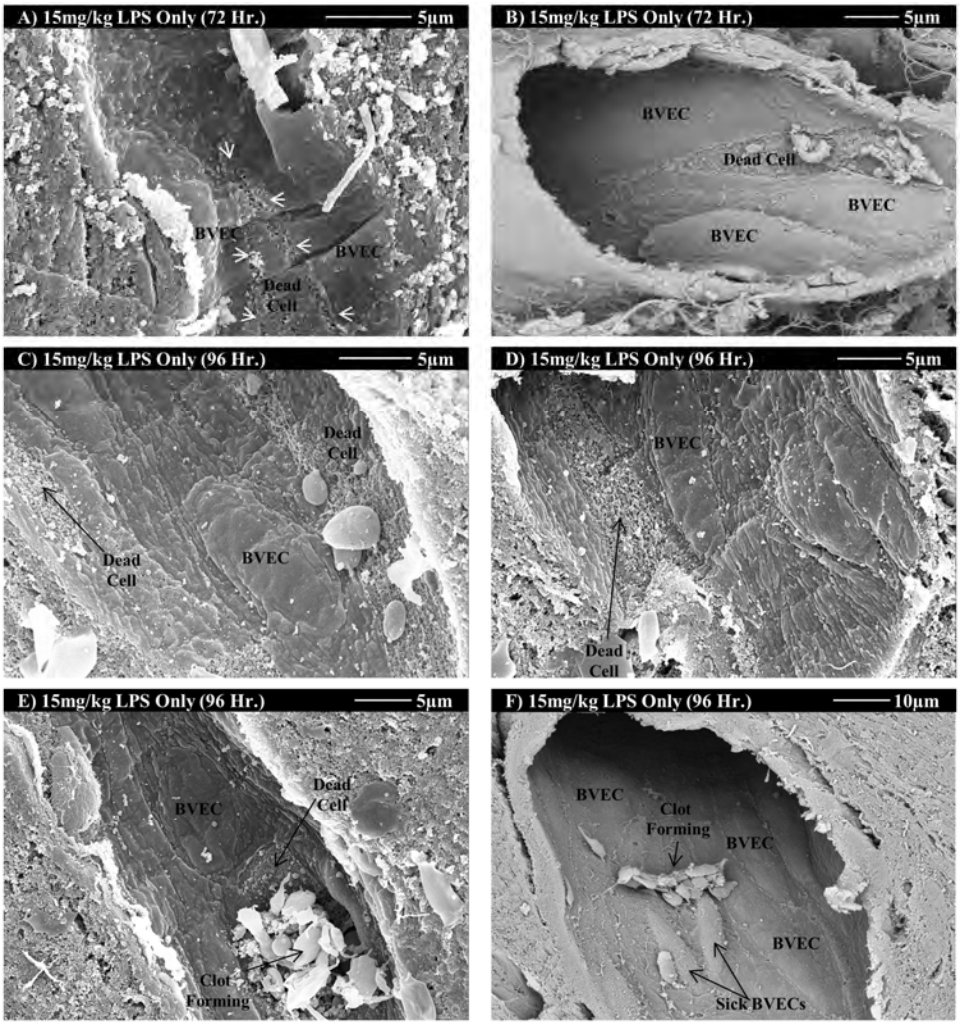

Figure 8: SEM Revealed These Interesting Features in Animals Treated with 15mg/kg LPS Only.

Scanning electron microscopy was used to examine the brains of rats that were exposed to 15mg/kg LPS. We examined the luminal surfaces of adjacent BVECs, including the tight junctional contacts at BVEC cell margins that contribute to the BBB, in longitudinal, oblique, and cross-sectional profiles. At 72 hours after LPS insult, dead BVECs were detected in the luminal lining (**Fig. 8A-B**). Cell remnants persist that contain a tangled web of cytoskeletal fibers with entrapped organelles (**Fig. 8B**). Frequently, regions of the blood vessels containing dead BVECs are seeding sites for forming blood clots or attachment points for individual platelets (**Fig. 8C**). At 96 hours after LPS insult, dead BVECs were most numerous as were clots, especially in regions of increased turbulence and shear force, such as sites of blood vessel bifurcation (**Fig. 8D-F**). BVEC - brain vascular endothelial cell.

Figure 9: SEM of Rat Brains Was Used to Examine the Effects of Lipoxin on BBB Morphology following an LPS Injection

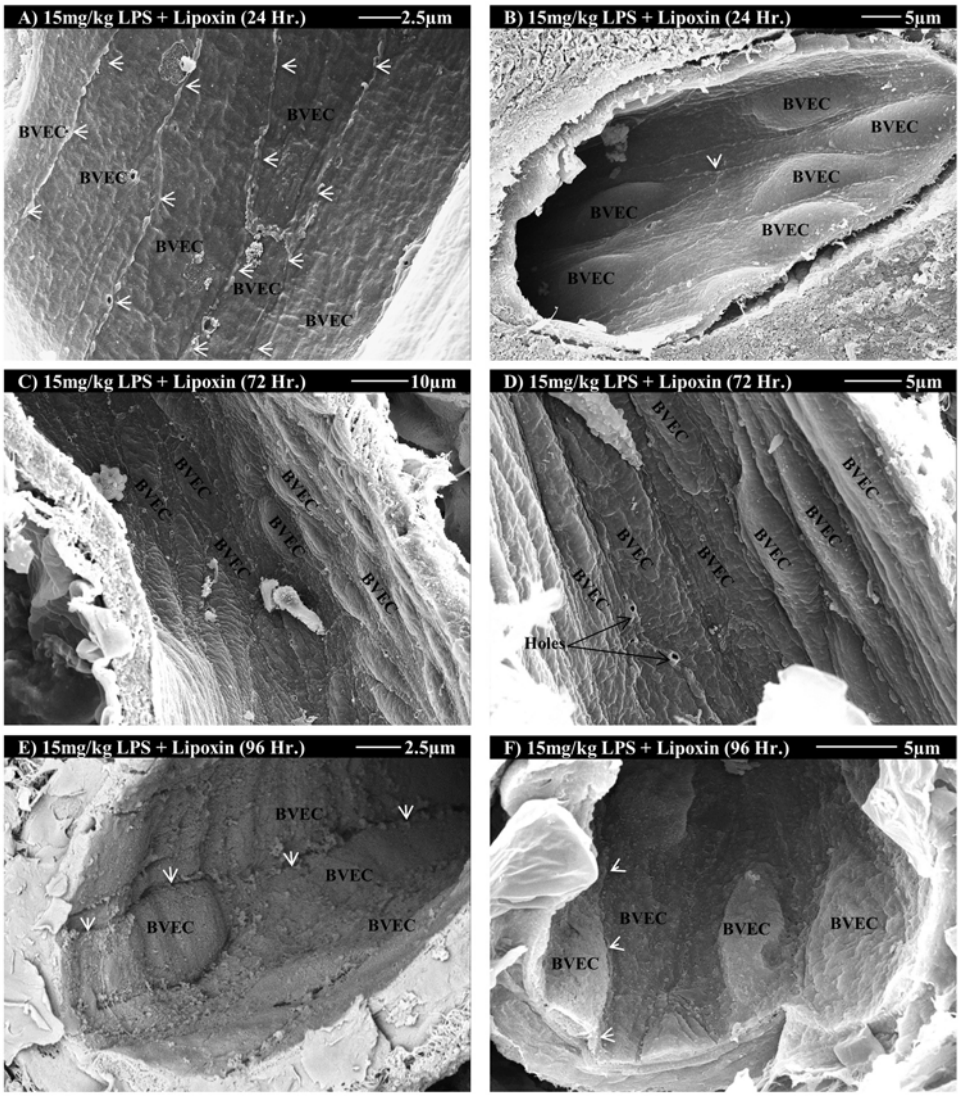

Figure 9: SEM of Rat Brains Was Used to Examine the Effects of Lipoxin on BBB Morphology following an LPS Injection.

Scanning electron microscopy was used to examine the brains of rats that were treated with 5µg/kg Lipoxin after exposure to 15mg/kg LPS. We examined the luminal surfaces of adjacent BVECs, including the tight junctional contacts at BVEC cell margins that contribute to the BBB, in longitudinal, oblique, and cross-sectional profiles. At 24 hours, BVEC luminal surfaces still showed a similar degree of flattening as was observed in the LPS-only group, with fewer microvilli and marginal contact flaps flattened against the luminal surface compared to untreated controls (**Fig. 9A-B**). At 72 hours and 96 hours, the most conspicuous difference between the luminal surfaces of BVECs in LPS-only and LPS + Lipoxin-treated was the nearly complete lack of dead BVECs in the LPS + Lipoxin-treated group. This change alone may be sufficient to explain the observed widespread improvement in BBB function as evidenced in IHC preparations (**Fig. 9C-F**). BVEC - brain vascular endothelial cell.

Figure 10: SEM Revealed These Interesting Features in Animals Treated with Lipoxin following an LPS Injection

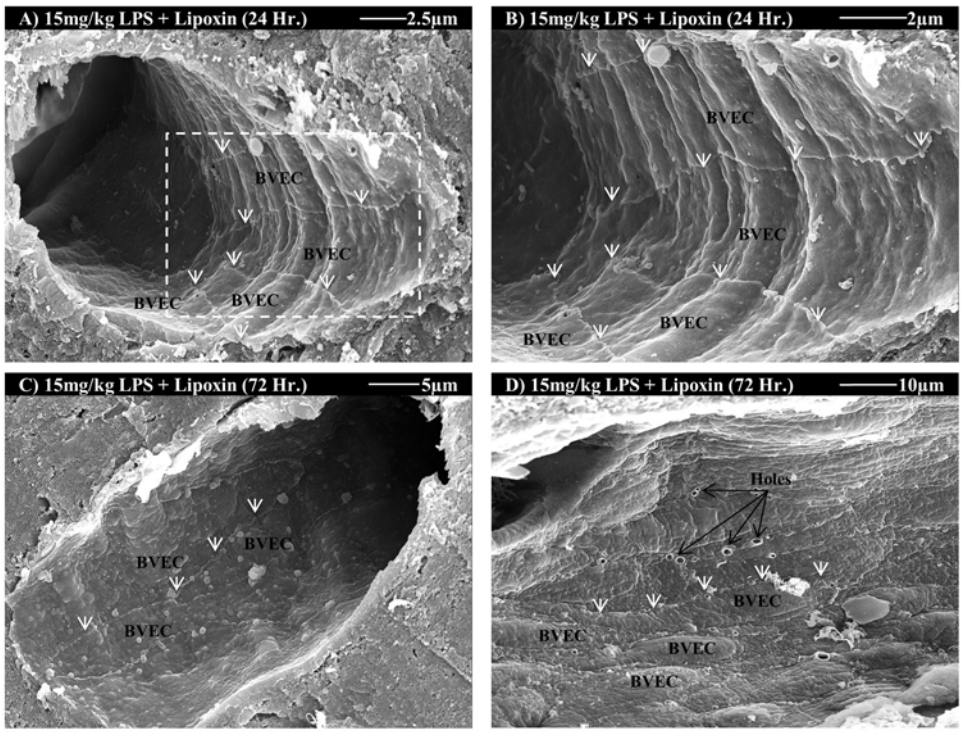

Scanning electron microscopy was used to examine the brains of rats that were treated with 5µg/kg Lipoxin after exposure to 15mg/kg LPS. We examined the luminal surfaces of adjacent BVECs, including the tight junctional contacts at BVEC cell margins that contribute to the BBB, in longitudinal, oblique, and cross-sectional profiles. At 24 hours, BVEC luminal surfaces still showed a similar degree of flattening as was observed in the LPS-only group, with fewer microvilli and marginal contact flaps flattened against the luminal surface compared to untreated controls (**Fig. 10A-B**). At 96 hours, the most conspicuous difference between the luminal surfaces of BVECs in LPS-only and LPS + Lipoxin-treated was the nearly complete lack of dead BVECs in the LPS + Lipoxin-treated group. This change alone may be sufficient to explain the observed widespread improvement in BBB function as evidenced in IHC preparations (**Fig. 10C-D**). BVEC - brain vascular endothelial cell.

CHAPTER VII:

Conclusion

The research conducted over the course of this study has led to a number of important findings. Preliminary research conducted between 2013 when I first joined the lab and 2015 revealed the following results:

1. Inhalation anesthetics increase BBB permeability in the rat.
2. Sevoflurane is more disruptive than Isoflurane to BBB functional integrity.
3. Aging and exposure to anesthesia have a synergistic effect on increasing BBB permeability.
4. Sevoflurane and Isoflurane induce dramatic structural changes in the luminal surfaces of BVECs that may be linked to BBB compromise.
5. Exposure to Sevoflurane and Isoflurane can be toxic to BVECs.
6. Vascular integrity and surface morphology of BVECs failed to recover within 24 hours of anesthetic treatment.

The initial findings led us to conduct another study which revealed the following results:

1. Sevoflurane (and Isoflurane to a lesser degree) increases BBB permeability in pre-adolescent and elderly rats.
2. Age-dependent changes occur in the luminal surface topography of brain vascular endothelial cells associated with development and maintenance of the

BBB.

3. Sevoflurane and Isoflurane induce changes in BVEC luminal surface topography that may be linked to increased BBB permeability.

We then conducted experiments using a human brain endothelial cell line (the hCMEC/D3 cell line), as we wanted to verify that human endothelial cells and the human BBB respond to anesthesia in a manner similar to that in rats. These *in vitro* experiments yielded the following results:

1. Immunocytochemistry and Western Blot verify that hCMEC/D3 cells express BBB-relevant tight junction proteins.
2. TEER decreases and Permeability increases after hCMEC/D3 cells are exposed to anesthesia.
3. There is no change in distribution or expression of the tight junction-associated scaffolding protein ZO-1 in hCMEC/D3 cells exposed to Isoflurane, Sevoflurane, or Sevoflurane + DMSO.
4. Addition of DMSO or floating cells to the cell culture medium did not aid the transfer of the inhalation anesthetics from the air to the cell monolayer.
5. Cell contractility was detected after exposure to Pertussis toxin.
6. hCMEC/D3 cells express the Histamine H1 receptor, and both Histamine and Acetaminophen induce contraction in hCMEC/D3 cells.

It has been speculated that inflammation of the BBB may be a mechanism of POD, as inflammatory conditions such as sepsis and wound infection are major causes of

delirium [44]. Therefore, we examined the effects of inflammation on the BBB by using LPS injections to induce BBB disruption. Furthermore, we performed experiments using the SPM Lipoxin to see if Lipoxin injections could reduce or resolve inflammation induced by LPS. The experiments yielded the following results:

1. LPS Injections caused an increase in BBB permeability, as evidenced by immunostaining of leaked IgG in rat brain tissue.
2. Lipoxin treatment after LPS insult causes a reduction in both the number of BBB-compromised vessels and the extent of their leak, suggesting that Lipoxin has a beneficial effect and allows for more rapid recovery from LPS-mediated BBB breaches.
3. LPS induces a number of luminal surface changes in rat BVECs, as shown by scanning electron microscopy.
4. Lipoxin restored the luminal surfaces of rat BVECs to normal, and in particular prevented BVEC death or loss, as shown by scanning electron microscopy.

Postoperative Delirium is a prevalent and serious form of delirium. As mentioned previously, POD is one of the most common postoperative complications faced by elderly patients undergoing surgery. Doctors know that exposure to certain anesthetics and drugs can cause one to develop POD, but they have been unable to explain how anesthetics or drugs could cause this. Therefore, we decided to examine the mechanism by which anesthesia induces POD in surgical patients.

We hypothesized that POD must be caused by a temporary, anesthesia or drug-

induced breakdown of the BBB, as BBB disruption and a subsequent increase in BBB permeability have been implicated in numerous neurological diseases, including cerebral ischemia, brain trauma, tumors, and neurodegenerative disorders [22].

Immunohistochemistry was performed on control and anesthesia-treated rat brains, and comparison of these brains revealed that exposure to anesthesia, particularly Sevoflurane, causes an increase in BBB permeability. We noticed that this increase in BBB permeability was exacerbated in the young and elderly. We next sought to understand how anesthesia could increase BBB permeability. We used scanning electron microscopy to examine brain blood vessels and their constituent brain vascular endothelial cells directly. Using this unique approach to examine the brain allowed us to see directly the effects that anesthesia has on the brain endothelium. By comparing control and anesthesia-treated rat brains, we discovered that Sevoflurane and Isoflurane induce changes in BVEC luminal surface topography. Furthermore, by comparing pre-adolescent, middle-age, and elderly rat brains, we discovered that there are age-related changes in the luminal surface topography of brain vascular endothelial cells. These changes include profound flattening of the luminal surfaces of the BVECs, loss of the prominent BBB-associated tight junction ridges, loss of microvilli, and the appearance of holes at cell borders. We believe that these anesthesia-associated changes in the luminal surfaces of the BVECs are linked to the increase in BBB permeability revealed by immunohistochemistry. Also, we believe that the luminal surface changes seen in the young and elderly are what make them so susceptible to chemical insult, such as exposure to certain anesthetics and drugs.

We propose that this anesthesia-induced increase in BBB permeability results in a large plasma influx into the brain parenchyma that disrupts brain homeostasis and neuronal activity, triggering POD initially and favoring postoperative cognitive decline (POCD) and even dementia. Pre-adolescents are most vulnerable to this effect because the brains of the very young are engaged in a period of exceptionally rapid growth and neurogenesis accompanied by extensive neovascularization and BBB formation. The elderly are vulnerable because the number of BVECs in brain blood vessels declines with age, and the remaining cells are forced to spread out and increase their surface area, which renders them more susceptible to potentially toxic effects of the anesthetic.

Hopefully, the findings presented here greatly benefit the medical field, and anesthesiologists and other doctors take this data into account when planning surgeries. Sevoflurane is currently the favored general anesthetic because it is the fastest acting anesthetic. Unfortunately, we now know that Sevoflurane has a direct negative effect on BVEC membranes which favors subsequent development of POD. However, not all anesthetics will have the same negative effects on the BBB. Anesthesiologists must now work to identify anesthetics that are slower acting as well as more favorable to maintaining BBB integrity during the surgical procedure and afterwards. This would be a major breakthrough for the medical field, as using less harmful anesthetics will lead to a decrease in the incidence of delirium. A decrease in the incidence of delirium will mean shorter hospital stays and therefore decreased hospital costs, better long-term cognitive outlooks, and lower mortality rates.

REFERENCES:

1. Horacek, R., et al., *Delirium in surgery intensive care unit.* Act Nerv Super Rediviva, 2011. **53**(3): p. 121-132.

2. Gross, A.L., et al., *Delirium and Long-term Cognitive Trajectory Among Persons With Dementia.* Arch Intern Med, 2012. **172**(17): p. 1324-31.

3. Vasilevskis, E.E. and E.W. Ely, *The Danger of Delirium: Comment on "Delirium and Long-term Cognitive Trajectory Among Persons With Dementia".* Arch Intern Med, 2012. **172**(17): p. 1331-2.

4. American Psychiatric Association, *Diagnostic and Statistical Manual of Mental Disorders (Fifth Edition)*. 2013, Washington, DC: American Psychiatric Publishing.

5. Harrington, C.J. and K. Vardi, *Delirium: presentation, epidemiology, and diagnostic evaluation (part 1).* R I Med J (2013), 2014. **97**(6): p. 18-23.

6. Brooks, P., et al., *Developing a strategy to identify and treat older patients with postoperative delirium.* AORN J, 2014. **99**(2): p. 257-73; quiz 274-6.

7. Ellard, L., et al., *Type of anesthesia and postoperative delirium after vascular surgery.* J Cardiothorac Vasc Anesth, 2014. **28**(3): p. 458-61.

8. Khan, E., *An examination of the blood-brain barrier in health and disease.* Br J Nurs, 2005. **14**(9): p. 509-13.

9. Grover, S. and N. Kate, *Assessment scales for delirium: A review.* World J Psychiatry, 2012. **2**(4): p. 58-70.

10. Attard, A., G. Ranjith, and D. Taylor, *Delirium and its treatment.* CNS Drugs, 2008. **22**(8): p. 631-44.

11. Alagiakrishnan, K. *Delirium: Overview*. 2014 [cited May 26, 2015]; Available from: http://emedicine.medscape.com/article/288890-overview#showall.

12. Breitbart, W. and Y. Alici-Evcimen, *Why off-label antipsychotics remain first-choice drugs for delirium.* Current Psychiatry, 2007. **6**(10): p. 49-63.

13. Katznelson, R., et al., *Preoperative use of statins is associated with reduced early delirium rates after cardiac surgery.* Anesthesiology, 2009. **110**(1): p. 67-73.

14. Page, V.J., et al., *Statin use and risk of delirium in the critically ill.* Am J Respir Crit Care Med, 2014. **189**(6): p. 666-73.

15. Morandi, A., et al., *Statins and delirium during critical illness: a multicenter, prospective cohort study.* Crit Care Med, 2014. **42**(8): p. 1899-909.

16. Xie, Z., et al., *Preoperative cerebrospinal fluid beta-Amyloid/Tau ratio and postoperative delirium.* Ann Clin Transl Neurol, 2014. **1**(5): p. 319-328.

17. *Census Bureau Reports World's Older Population Projected to Triple by 2050*. 2009 [cited June 18, 2014]; Available from: http://www.census.gov/newsroom/releases/archives/international_population/cb09-97.html.

18. Leslie, D.L., et al., *One-year health care costs associated with delirium in the elderly population.* Arch Intern Med, 2008. **168**(1): p. 27-32.

19. Sa-Pereira, I., D. Brites, and M.A. Brito, *Neurovascular unit: a focus on pericytes.* Mol Neurobiol, 2012. **45**(2): p. 327-47.

20. Abbott, N.J., et al., *Structure and function of the blood-brain barrier.* Neurobiol Dis, 2010. **37**(1): p. 13-25.

21. Ben-Zvi, A., et al., *Mfsd2a is critical for the formation and function of the blood-brain barrier.* Nature, 2014. **509**(7501): p. 507-11.

22. Wilhelm, I., C. Fazakas, and I.A. Krizbai, *In vitro models of the blood-brain barrier.* Acta Neurobiol Exp (Wars), 2011. **71**(1): p. 113-28.

23. Jones, E.V. and D.S. Bouvier, *Astrocyte-secreted matricellular proteins in CNS remodelling during development and disease.* Neural Plast, 2014. **2014**: p. 321209.

24. Bicker, J., et al., *Blood-brain barrier models and their relevance for a successful development of CNS drug delivery systems: a review.* Eur J Pharm Biopharm, 2014. **87**(3): p. 409-32.

25. Correale, J. and A. Villa, *Cellular elements of the blood-brain barrier.* Neurochem Res, 2009. **34**(12): p. 2067-77.

26. He, Y., et al., *Cell-culture models of the blood-brain barrier.* Stroke, 2014. **45**(8): p. 2514-26.

27. Liu, S., et al., *The role of pericytes in blood-brain barrier function and stroke.* Curr Pharm Des, 2012. **18**(25): p. 3653-62.

28. Afonso, P.V., et al., *Human blood-brain barrier disruption by retroviral-infected lymphocytes: role of myosin light chain kinase in endothelial tight-junction disorganization.* J Immunol, 2007. **179**(4): p. 2576-83.

29. Abbott, N.J., L. Ronnback, and E. Hansson, *Astrocyte-endothelial interactions at the blood-brain barrier.* Nat Rev Neurosci, 2006. **7**(1): p. 41-53.

30. Petty, M.A. and E.H. Lo, *Junctional complexes of the blood-brain barrier: permeability changes in neuroinflammation.* Prog Neurobiol, 2002. **68**(5): p. 311-23.

31. Campbell, H.K., J.L. Maiers, and K.A. DeMali, *Interplay between tight junctions & adherens junctions.* Experimental cell research, 2017. **358**(1): p. 39-44.

32. Wolburg, H. and A. Lippoldt, *Tight junctions of the blood-brain barrier: development, composition and regulation.* Vascul Pharmacol, 2002. **38**(6): p. 323-37.

33. Wilhelm, I. and I.A. Krizbai, *In vitro models of the blood-brain barrier for the study of drug delivery to the brain.* Mol Pharm, 2014. **11**(7): p. 1949-63.

34. Ruffer, C. and V. Gerke, *The C-terminal cytoplasmic tail of claudins 1 and 5 but not its PDZ-binding motif is required for apical localization at epithelial and endothelial tight junctions.* Eur J Cell Biol, 2004. **83**(4): p. 135-44.

35. Schreibelt, G., et al., *Reactive oxygen species alter brain endothelial tight junction dynamics via RhoA, PI3 kinase, and PKB signaling.* FASEB J, 2007. **21**(13): p. 3666-76.

36. Kluger, M.S., et al., *Claudin-5 controls intercellular barriers of human dermal microvascular but not human umbilical vein endothelial cells.* Arterioscler Thromb Vasc Biol, 2013. **33**(3): p. 489-500.

37. Haseloff, R.F., et al., *Transmembrane proteins of the tight junctions at the blood-brain barrier: structural and functional aspects.* Semin Cell Dev Biol, 2015. **38**: p. 16-25.

38. Indra, I., et al., *The adherens junction: a mosaic of cadherin and nectin clusters bundled by actin filaments.* The Journal of investigative dermatology, 2013. **133**(11): p. 2546-2554.

39. Durán, W.N., F.A. Sánchez, and J.W. Breslin, *Chapter 4 - Microcirculatory Exchange Function*, in *Microcirculation (Second Edition)*, R.F. Tuma, W.N. Durán, and K. Ley, Editors. 2008, Academic Press: San Diego. p. 81-124.

40. Hartsock, A. and W.J. Nelson, *Adherens and tight junctions: structure, function and connections to the actin cytoskeleton.* Biochimica et biophysica acta, 2008. **1778**(3): p. 660-669.

41. Dejana, E., F. Orsenigo, and M.G. Lampugnani, *The role of adherens junctions and VE-cadherin in the control of vascular permeability.* Journal of Cell Science, 2008. **121**(13): p. 2115.

42. Rikitake, Y., K. Mandai, and Y. Takai, *The role of nectins in different types of cell–cell adhesion.* Journal of Cell Science, 2012. **125**(16): p. 3713.

43. Dias, M.C., et al., *Structure and Junctional Complexes of Endothelial, Epithelial and Glial Brain Barriers.* Int J Mol Sci, 2019. **20**(21).

44. Mietani, K., et al., *Dysfunction of the blood-brain barrier in postoperative delirium patients, referring to the axonal damage biomarker phosphorylated neurofilament heavy subunit.* PLOS ONE, 2019. **14**(10): p. e0222721.

45. Acharya, N.K., et al., *Sevoflurane and Isoflurane induce structural changes in brain vascular endothelial cells and increase blood-brain barrier permeability: Possible link to postoperative delirium and cognitive decline.* Brain Res, 2015. **1620**: p. 29-41.

46. Yang, S., et al., *Anesthesia and Surgery Impair Blood-Brain Barrier and Cognitive Function in Mice.* Frontiers in Immunology, 2017. **8**(902).

47. Kim, K.S., *Mechanisms of microbial traversal of the blood-brain barrier.* Nature reviews. Microbiology, 2008. **6**(8): p. 625-634.

48. Poller, B., *Evaluation of the hCMEC/D3 cell line, a new "in vitro" model of the human blood-brain barrier for transport and gene regulation studies*. 2009, University of Basel.

49. Brown, E.N., R. Lydic, and N.D. Schiff, *General anesthesia, sleep, and coma.* N Engl J Med, 2010. **363**(27): p. 2638-50.

50. Nadelson, M.R., R.D. Sanders, and M.S. Avidan, *Perioperative cognitive trajectory in adults.* Br J Anaesth, 2014. **112**(3): p. 440-51.

51. Ansaloni, L., et al., *Risk factors and incidence of postoperative delirium in elderly patients after elective and emergency surgery.* Br J Surg, 2010. **97**(2): p. 273-80.

52. Inouye, S.K., R.G.J. Westendorp, and J.S. Saczynski, *Delirium in elderly people.* The Lancet, 2014. **383**(9920): p. 911-922.

53. Neufeld, K.J., et al., *Outcomes of early delirium diagnosis after general anesthesia in the elderly.* Anesth Analg, 2013. **117**(2): p. 471-8.

54. Rudolph, J.L. and E.R. Marcantonio, *Postoperative Delirium: Acute change with long-term implications.* Anesthesia and Analgesia, 2011. **112**(5): p. 1202-1211.

55. Howden, L. and J. Meyer, *Age and Sex Composition: 2010.* 2010 Census Briefs, 2011: p. 1-15.

56. Brown, E.N. and P.L. Purdon, *The aging brain and anesthesia.* Curr Opin Anaesthesiol, 2013. **26**(4): p. 414-9.

57. Neufeld, K.J. and C. Thomas, *Delirium: definition, epidemiology, and diagnosis.* J Clin Neurophysiol, 2013. **30**(5): p. 438-42.

58. Bedford, P.D., *Adverse cerebral effects of anaesthesia on old people.* Lancet, 1955. **269**(6884): p. 259-63.

59. Burns, A., A. Gallagley, and J. Byrne, *Delirium.* J Neurol Neurosurg Psychiatry, 2004. **75**(3): p. 362-7.

60. Strom, C., L.S. Rasmussen, and F.E. Sieber, *Should general anaesthesia be avoided in the elderly?* Anaesthesia, 2014. **69 Suppl 1**: p. 35-44.

61. van Munster, B.C. and S.E. de Rooij, *Delirium: a synthesis of current knowledge.* Clin Med (Lond), 2014. **14**(2): p. 192-5.

62. Maldonado, J.R., *Neuropathogenesis of delirium: review of current etiologic theories and common pathways.* Am J Geriatr Psychiatry, 2013. **21**(12): p. 1190-222.

63. Clifford, P.M., et al., *α7 nicotinic acetylcholine receptor expression by vascular smooth muscle cells facilitates the deposition of Aβ peptides and promotes cerebrovascular amyloid angiopathy.* Brain Research, 2008. **1234**: p. 158-171.

64. Kalaria, R.N., *Vascular basis for brain degeneration: faltering controls and risk factors for dementia.* Nutrition Reviews, 2010. **68**(suppl_2): p. S74-S87.

65. Rouhl, R.P.W., et al., *Vascular inflammation in cerebral small vessel disease.* Neurobiology of Aging, 2012. **33**(8): p. 1800-1806.

66. Vasilevko, V., et al., *Aging and cerebrovascular dysfunction: contribution of hypertension, cerebral amyloid angiopathy, and immunotherapy.* Ann N Y Acad Sci, 2010. **1207**: p. 58-70.

67. Zlokovic, B.V., *The blood-brain barrier in health and chronic neurodegenerative disorders.* Neuron, 2008. **57**(2): p. 178-201.

68. Nagele, R.G., et al., *Brain-reactive autoantibodies prevalent in human sera increase intraneuronal amyloid-beta(1-42) deposition.* J Alzheimers Dis, 2011. **25**(4): p. 605-22.

69. Acharya, N.K., et al., *Diabetes and hypercholesterolemia increase blood-brain barrier permeability and brain amyloid deposition: beneficial effects of the LpPLA2 inhibitor darapladib.* J Alzheimers Dis, 2013. **35**(1): p. 179-98.

70. Jin, A.Y., et al., *Reduced blood brain barrier breakdown in P-selectin deficient mice following transient ischemic stroke: a future therapeutic target for treatment of stroke.* BMC Neurosci, 2010. **11**: p. 12.

71. Kuang, F., et al., *Extravasation of blood-borne immunoglobulin G through blood-brain barrier during adrenaline-induced transient hypertension in the rat.* Int J Neurosci, 2004. **114**(6): p. 575-91.

72. Iida, H., et al., *Isoflurane and sevoflurane induce vasodilation of cerebral vessels via ATP-sensitive K+ channel activation.* Anesthesiology, 1998. **89**(4): p. 954-960.

73. Sahu, D.K., V. Kaul, and R. Parampill, *Comparison of isoflurane and sevoflurane in anaesthesia for day care surgeries using classical laryngeal mask airway.* Indian J Anaesth, 2011. **55**(4): p. 364-9.

74. Scholz, J., et al., *Comparison of Sevoflurane and Isoflurane in Ambulatory Surgery. Results of a multicenter study.* Anaesthesist, 1996. **45 Suppl 1**: p. S63-70.

75. Lossinsky, A.S., A.W. Vorbrodt, and H.M. Wisniewski, *Scanning and transmission electron microscopic studies of microvascular pathology in the osmotically impaired blood-brain barrier.* Journal of Neurocytology, 1995. **24**(10): p. 795-806.

76. Hazama, F., T. Ozaki, and S. Amano, *Scanning electron microscopic study of endothelial cells of cerebral arteries from spontaneously hypertensive rats.* Stroke, 1979. **10**(3): p. 245-52.

77. Kaneko, Y., et al., *Cell therapy for stroke: emphasis on optimizing safety and efficacy profile of endothelial progenitor cells.* Current pharmaceutical design, 2012. **18**(25): p. 3731-3734.

78. Peplow, P., *Growth factor- and cytokine-stimulated endothelial progenitor cells in post-ischemic cerebral neovascularization.* Neural Regeneration Research, 2014. **9**(15): p. 1425-1429.

79. Wei, H., et al., *Circulating endothelial progenitor cells in traumatic brain injury: an emerging therapeutic target?* Chinese Journal of Traumatology (English Edition), 2010. **13**(5): p. 316-318.

80. Tetrault, S., et al., *Opening of the blood-brain barrier during isoflurane anaesthesia.* Eur J Neurosci, 2008. **28**(7): p. 1330-41.

81. Hu, N., et al., *Involvement of the blood-brain barrier opening in cognitive decline in aged rats following orthopedic surgery and high concentration of sevoflurane inhalation.* Brain Res, 2014. **1551**: p. 13-24.

82. Dzenko, K.A., et al., *CCR2 expression by brain microvascular endothelial cells is critical for macrophage transendothelial migration in response to CCL2.* Microvascular Research, 2005. **70**(1): p. 53-64.

83. Thal, S.C., et al., *Volatile anesthetics influence blood-brain barrier integrity by modulation of tight junction protein expression in traumatic brain injury.* PLoS One, 2012. **7**(12): p. e50752.

84. Popescu, B.O., et al., *Blood-brain barrier alterations in ageing and dementia.* Journal of the Neurological Sciences, 2009. **283**(1): p. 99-106.

85. Shah, G.N. and A.D. Mooradian, *Age-related changes in the blood-brain barrier.* Exp Gerontol, 1997. **32**(4-5): p. 501-19.

86. Zeevi, N., et al., *The blood-brain barrier: geriatric relevance of a critical brain-body interface.* J Am Geriatr Soc, 2010. **58**(9): p. 1749-57.

87. Michalak, Z., et al., *IgG leakage may contribute to neuronal dysfunction in drug-refractory epilepsies with blood-brain barrier disruption.* Journal of Neuropathology and Experimental Neurology, 2012. **71**(9): p. 826-838.

88. Cristelo, D., et al., *Quality of recovery in elderly patients with postoperative delirium.* Saudi J Anaesth, 2019. **13**(4): p. 285-289.

89. Daiello, L.A., et al., *Postoperative Delirium and Postoperative Cognitive Dysfunction: Overlap and Divergence.* Anesthesiology, 2019. **131**(3): p. 477-491.

90. Ahn, E.J., et al., *Comparison of general anaesthesia and regional anaesthesia in terms of mortality and complications in elderly patients with hip fracture: a nationwide population-based study.* BMJ Open, 2019. **9**(9): p. e029245.

91. Hu, N., et al., *The role of the Wnt/beta-catenin-Annexin A1 pathway in the process of sevoflurane-induced cognitive dysfunction.* J Neurochem, 2016. **137**(2): p. 240-52.

92. Vutskits, L. and Z. Xie, *Lasting impact of general anaesthesia on the brain: mechanisms and relevance.* Nat Rev Neurosci, 2016. **17**(11): p. 705-717.

93. Jevtovic-Todorovic, V., *General Anesthetics and Neurotoxicity: How Much Do We Know?* Anesthesiol Clin, 2016. **34**(3): p. 439-51.

94. Eckenhoff, J.E., *Relationship of anesthesia to postoperative personality changes in children.* AMA Am J Dis Child, 1953. **86**(5): p. 587-91.

95. Andropoulos, D.B. and M.F. Greene, *Anesthesia and Developing Brains - Implications of the FDA Warning.* N Engl J Med, 2017. **376**(10): p. 905-907.

96. Wang, C. and W. Slikker, Jr., *Strategies and experimental models for evaluating anesthetics: effects on the developing nervous system.* Anesth Analg, 2008. **106**(6): p. 1643-58.

97. Walkden, G.J., A.E. Pickering, and H. Gill, *Assessing Long-term Neurodevelopmental Outcome Following General Anesthesia in Early Childhood: Challenges and Opportunities.* Anesth Analg, 2019. **128**(4): p. 681-694.

98. Bellinger, D.C. and J. Calderon, *Neurotoxicity of general anesthetics in children: evidence and uncertainties.* Curr Opin Pediatr, 2019. **31**(2): p. 267-273.

99. Berns, M., et al., *Effects of sevoflurane on primary neuronal cultures of embryonic rats.* Eur J Anaesthesiol, 2009. **26**(7): p. 597-602.

100. Semple, B.D., et al., *Brain development in rodents and humans: Identifying benchmarks of maturation and vulnerability to injury across species.* Prog Neurobiol, 2013. **106-107**: p. 1-16.

101. Franken, A., D. Sebbens, and J. Mensik, *Pediatric Delirium: Early Identification of Barriers to Optimize Success of Screening and Prevention.* J Pediatr Health Care, 2018.

102. Chandler, J.R., et al., *Emergence delirium in children: a randomized trial to compare total intravenous anesthesia with propofol and remifentanil to inhalational sevoflurane anesthesia.* Paediatr Anaesth, 2013. **23**(4): p. 309-15.

103. Costi, D., et al., *Effects of sevoflurane versus other general anaesthesia on emergence agitation in children.* Cochrane Database Syst Rev, 2014(9): p. 1-210.

104. Akeju, O., et al., *Age-dependency of sevoflurane-induced electroencephalogram dynamics in children.* Br J Anaesth, 2015. **115 Suppl 1**: p. i66-i76.

105. Sanders, R.D., et al., *Impact of anaesthetics and surgery on neurodevelopment: an update.* Br J Anaesth, 2013. **110 Suppl 1**: p. i53-72.

106. Kain, Z.N., et al., *Preoperative anxiety and emergence delirium and postoperative maladaptive behaviors.* Anesth Analg, 2004. **99**(6): p. 1648-54.

107. Lunardi, N., et al., *General anesthesia causes long-lasting disturbances in the ultrastructural properties of developing synapses in young rats.* Neurotox Res, 2010. **17**(2): p. 179-88.

108. Almutairi, M.M., et al., *Factors controlling permeability of the blood-brain barrier.* Cell Mol Life Sci, 2016. **73**(1): p. 57-77.

109. Ballabh, P., A. Braun, and M. Nedergaard, *The blood-brain barrier: an overview: structure, regulation, and clinical implications.* Neurobiol Dis, 2004. **16**(1): p. 1-13.

110. Adriani, G., et al., *Modeling the Blood-Brain Barrier in a 3D triple co-culture microfluidic system.* Conf Proc IEEE Eng Med Biol Soc, 2015. **2015**: p. 338-41.

111. Mooradian, A.D., *Effect of aging on the blood-brain barrier.* Neurobiol Aging, 1988. **9**(1): p. 31-9.

112. Burns, E.M., T.W. Kruckeberg, and P.K. Gaetano, *Changes with age in cerebral capillary morphology.* Neurobiology of Aging, 1981. **2**(4): p. 285-291.

113. Hicks, P., et al., *Age-related changes in rat brain capillaries.* Neurobiology of Aging, 1983. **4**(1): p. 69-75.

114. Acharya, N.K., et al., *Retinal pathology is associated with increased blood-retina barrier permeability in a diabetic and hypercholesterolaemic pig model: Beneficial effects of the LpPLA2 inhibitor Darapladib.* Diab Vasc Dis Res, 2017. **14**(3): p. 200-213.

115. Aurini, L. and P.F. White, *Anesthesia for the elderly outpatient.* Curr Opin Anaesthesiol, 2014. **27**(6): p. 563-75.

116. Disma, N., et al., *Anesthesia and the developing brain: A way forward for laboratory and clinical research.* Paediatr Anaesth, 2018. **28**(9): p. 758-763.

117. Rundshagen, I., *Postoperative cognitive dysfunction.* Deutsches Arzteblatt international, 2014. **111**(8): p. 119-125.

118. Bors, L., et al., *Age-dependent changes at the blood-brain barrier. A Comparative structural and functional study in young adult and middle aged rats.* Brain Res Bull, 2018. **139**: p. 269-277.

119. Erdő, F., L. Denes, and E. de Lange, *Age-associated physiological and pathological changes at the blood-brain barrier: A review.* Journal of cerebral blood flow and metabolism : official journal of the International Society of Cerebral Blood Flow and Metabolism, 2017. **37**(1): p. 4-24.

120. Erickson, M.A. and W.A. Banks, *Age-Associated Changes in the Immune System and Blood–Brain Barrier Functions.* International journal of molecular sciences, 2019. **20**(7): p. 1632.

121. Montagne, A., et al., *Blood-brain barrier breakdown in the aging human hippocampus.* Neuron, 2015. **85**(2): p. 296-302.

122. Bar, T., *Morphometric evaluation of capillaries in different laminae of rat cerebral cortex by automatic image analysis: changes during development and aging.* Adv Neurol, 1978. **20**: p. 1-9.

123. Lee, P., et al., *Effects of aging on blood brain barrier and matrix metalloproteases following controlled cortical impact in mice.* Experimental neurology, 2012. **234**(1): p. 50-61.

124. Weksler, B.B., et al., *Blood-brain barrier-specific properties of a human adult brain endothelial cell line.* FASEB J, 2005. **19**(13): p. 1872-4.

125. Poller, B., et al., *The human brain endothelial cell line hCMEC/D3 as a human blood-brain barrier model for drug transport studies.* J Neurochem, 2008. **107**(5): p. 1358-68.

126. Vu, K., et al., *Immortalized human brain endothelial cell line HCMEC/D3 as a model of the blood-brain barrier facilitates in vitro studies of central nervous system infection by Cryptococcus neoformans.* Eukaryot Cell, 2009. **8**(11): p. 1803-7.

127. Weksler, B., I.A. Romero, and P.O. Couraud, *The hCMEC/D3 cell line as a model of the human blood brain barrier.* Fluids Barriers CNS, 2013. **10**(1): p. 16.

128. Eigenmann, D.E., et al., *Comparative study of four immortalized human brain capillary endothelial cell lines, hCMEC/D3, hBMEC, TY10, and BB19, and optimization of culture conditions, for an in vitro blood-brain barrier model for drug permeability studies.* Fluids Barriers CNS, 2013. **10**(1): p. 33.

129. Kugler, S., et al., *Pertussis toxin transiently affects barrier integrity, organelle organization and transmigration of monocytes in a human brain*

microvascular endothelial cell barrier model. Cell Microbiol, 2007. **9**(3): p. 619-32.

130. Schellenberg, A.E., et al., *Blood-brain barrier disruption in CCL2 transgenic mice during pertussis toxin-induced brain inflammation.* Fluids Barriers CNS, 2012. **9**(1): p. 10.

131. Haddad-Tóvolli, R., et al., *Development and Function of the Blood-Brain Barrier in the Context of Metabolic Control.* Frontiers in neuroscience, 2017. **11**: p. 224-224.

132. Banks, W.A., et al., *Lipopolysaccharide-induced blood-brain barrier disruption: roles of cyclooxygenase, oxidative stress, neuroinflammation, and elements of the neurovascular unit.* J Neuroinflammation, 2015. **12**: p. 223.

133. Abdulkhaleq, L.A., et al., *The crucial roles of inflammatory mediators in inflammation: A review.* Veterinary world, 2018. **11**(5): p. 627-635.

134. Montero-Melendez, T., *May Inflammation Be With You!* Frontiers for Young Minds, 2018. **6**(51).

135. Chen, L., et al., *Inflammatory responses and inflammation-associated diseases in organs.* Oncotarget, 2018. **9**(6): p. 7204-7218.

136. Bannenberg, G. and C.N. Serhan, *Specialized pro-resolving lipid mediators in the inflammatory response: An update.* Biochim Biophys Acta, 2010. **1801**(12): p. 1260-73.

137. Sherwood, E.R. and T. Toliver-Kinsky, *Mechanisms of the inflammatory response.* Best Practice & Research Clinical Anaesthesiology, 2004. **18**(3): p. 385-405.

138. Serhan, C.N., et al., *Novel anti-inflammatory--pro-resolving mediators and their receptors.* Current topics in medicinal chemistry, 2011. **11**(6): p. 629-647.

139. Tang, S., et al., *Maresins: Specialized Proresolving Lipid Mediators and Their Potential Role in Inflammatory-Related Diseases.* Mediators Inflamm, 2018. **2018**: p. 2380319.

140. Sugimoto, M.A., et al., *Resolution of Inflammation: What Controls Its Onset?* Frontiers in Immunology, 2016. **7**(160).

141. Bisicchia, E., et al., *Resolvin D1 Halts Remote Neuroinflammation and Improves Functional Recovery after Focal Brain Damage Via ALX/FPR2 Receptor-Regulated MicroRNAs.* Mol Neurobiol, 2018.

142. Perretti, M., et al., *Resolution Pharmacology: Opportunities for Therapeutic Innovation in Inflammation.* Trends Pharmacol Sci, 2015. **36**(11): p. 737-755.

143. Ortega-Gomez, A., M. Perretti, and O. Soehnlein, *Resolution of inflammation: an integrated view.* EMBO Mol Med, 2013. **5**(5): p. 661-74.

144. Serhan, C.N., et al., *Protectins and maresins: New pro-resolving families of mediators in acute inflammation and resolution bioactive metabolome.* Biochim Biophys Acta, 2015. **1851**(4): p. 397-413.

145. Terrando, N., et al., *Aspirin-triggered resolvin D1 prevents surgery-induced cognitive decline.* FASEB J, 2013. **27**(9): p. 3564-71.

146. Liu, X., et al., *Lipoxin A4 and its analog suppress inflammation by modulating HMGB1 translocation and expression in psoriasis.* Sci Rep, 2017. **7**(1): p. 7100.

147. Guo, Z., et al., *Lipoxin A4 Reduces Inflammation Through Formyl Peptide Receptor 2/p38 MAPK Signaling Pathway in Subarachnoid Hemorrhage Rats.* Stroke, 2016. **47**(2): p. 490-7.

148. Lin, F., et al., *Treatment of Lipoxin A4 and its analogue on low-dose endotoxin induced preeclampsia in rat and possible mechanisms.* Reproductive Toxicology, 2012. **34**(4): p. 677-685.

149. Conte, F.P., et al., *Lipoxin A(4) attenuates zymosan-induced arthritis by modulating endothelin-1 and its effects.* British journal of pharmacology, 2010. **161**(4): p. 911-924.

150. Wu, Y., et al., *A lipoxin A4 analog ameliorates blood-brain barrier dysfunction and reduces MMP-9 expression in a rat model of focal cerebral ischemia-reperfusion injury.* J Mol Neurosci, 2012. **46**(3): p. 483-91.

ABBREVIATIONS LIST:

1°-Ab = Primary Antibody

2°-Ab = Secondary Antibody

Ab = Antibody

Aβ = Amyloid Beta

AD = Alzheimer's Disease

AJ = Adherens Junction

AZT = Azidothymidine

BBB = Blood-Brain Barrier

BSA = Bovine Serum Albumin

BV = Blood Vessel

BVEC = Brain Vascular Endothelial Cell

CAM = Confusion Assessment Method

CAM-ICU = Confusion Assessment Method for the Intensive Care Unit

CNS = Central Nervous System

CSF = Cerebrospinal Fluid

dBVECs = Dying or Dead Brain Vascular Endothelial Cells

DDS = Delirium Detection Score

DM = Diabetes Mellitus

DMSO = Dimethyl Sulfoxide

DOSS = Delirium Observation Screening Scale

DRS-R-98 = Delirium Rating Scale-Revised Version

DSI = Delirium Symptom Interview

DSM-5 = Diagnostic and Statistical Manual of Mental Disorders, 5th edition

EBM-2 = Endothelial Cell Basal Medium-2

ECL = Enhanced Chemiluminescence

ER = Endoplasmic Reticulum

FBS = Fetal Bovine Serum

FITC = Fluorescein Isothiocyanate

hCMEC/d3 = Human Cerebral Microvascular Endothelial Cells

IA = Inhaled Anesthetic

IACUC = Institutional Animal Care and Use Committee

ICC = Immunocytochemistry

ICDSC = Intensive Care Delirium Screening Checklist

ICU = Intensive Care Unit

IF = Immunofluorescence

IFNγ = Interferon Gamma, also known as Type II Interferon

Ig = Immunoglobulin

IgG = Immunoglobulin Isotype G

IHC = Immunohistochemistry

IP = Intraperitoneal

IRB = Institutional Review Board

IV = Intravenous

JAM = Junctional Adhesion Molecule

MAC = Minimum Alveolar Concentration

MDAS = Memorial Delirium Assessment Scale

MS = Multiple Sclerosis

N-Cadherin = Neuronal Cadherin

Nu-DESC = Nursing Delirium Screening Scale

NVU = Neurovascular Unit

PBS = Phosphate-Buffered Saline

PBS-T = Phosphate-Buffered Saline containing 0.2% Tween 20

PD = Parkinson's Disease

PFA = Paraformaldehyde

PN = Pyramidal Neuron

POCD = Postoperative Cognitive Decline

POD = Postoperative Delirium

RBC = Red Blood Cell

RITC = Rhodamine B Isothiocyanate

SEM = Scanning Electron Microscopy

TBI = Traumatic Brain Injury

TEER = Transendothelial Electrical Resistance

TEM = Transmission Electron Microscopy

TJ = Tight Junction

TNF-α = Tumor Necrosis Factor α

VE-Cadherin = Vascular Endothelial Cadherin

VEGF = Vascular Endothelial Growth Factor

ZO = Zonnula Occludens

ATTRIBUTIONS:

Chapter I: Introduction

Figure 1. This figure was taken from [47]:

Kim, K.S. *Mechanisms of microbial traversal of the blood-brain barrier.* Nature reviews. Microbiology, 2008. **6**(8): p. 625-634.

Figure 2. GAG & RGN were responsible for creating this figure.

Figure 3. This figure was taken from [29] and [48]:

Abbott, N.J., L. Ronnback, and E. Hansson, *Astrocyte-endothelial interactions at the blood-brain barrier.* Nat Rev Neurosci, 2006. **7**(1): p. 41-53.

Poller, B., *Evaluation of the hCMEC/D3 cell line, a new "in vitro" model of the human blood-brain barrier for transport and gene regulation studies*. 2009, University of Basel.

Figure 4. This figure was taken from [21]:

Ben-Zvi, A., et al., *Mfsd2a is critical for the formation and function of the blood-brain barrier.* Nature, 2014. 509(7501): p. 507-11.

Figure 5. This figure was taken from [29]:

Abbott, N.J., L. Ronnback, and E. Hansson, *Astrocyte-endothelial interactions at the blood-brain barrier.* Nat Rev Neurosci, 2006. **7**(1): p. 41-53.

Figure 6. This figure was taken from [19]:

Sa-Pereira, I., D. Brites, and M.A. Brito, *Neurovascular unit: a focus on pericytes.* Mol Neurobiol, 2012. **45**(2): p. 327-47.

Figure 7. This figure was taken from [43]:

Dias, M.C., et al., *Structure and Junctional Complexes of Endothelial, Epithelial and Glial Brain Barriers.* Int J Mol Sci, 2019. **20**(21).

Figure 8. This figure was taken from [42]:

Rikitake, Y., K. Mandai, and Y. Takai, *The role of nectins in different types of cell–cell adhesion.* Journal of Cell Science, 2012. **125**(16): p. 3713.

Figure 9. We wish to thank Amanda S. Almon, M.F.A. C.M.I. from the Department of Art at the College of Communication and Creative Arts of Rowan University for the creation of **Figure 3**, which was used in [45]:

> Acharya, N.K., et al. *Sevoflurane and Isoflurane induce structural changes in brain vascular endothelial cells and increase blood-brain barrier permeability: Possible link to postoperative delirium and cognitive decline.* Brain Res, 2015. **1620**: p. 29-41.

Chapter II: Rationale

***No Attributions**

Chapter III: Sevoflurane and Isoflurane Induce Structural Changes in Brain Vascular Endothelial Cells and Increase Blood-Brain Barrier Permeability: Possible Link to Postoperative Delirium and Cognitive Decline

Journal

Published in Brain Research, Volume 1620, Pages 29-41, on September 16, 2015.

PMID: 25960348.

Authors

Nimish K. Acharya[1,3], Eric L. Goldwaser[1,2,], Martin M. Forsberg[3], **George A. Godsey**[1,2], Cristina A. Johnson[1,2], Abhirup Sarkar[1,2], Cassandra A. DeMarshall[1,2], Mary C. Kosciuk[1,3], Jacqueline M. Dash[2,3], Caitlin P. Hale[3], Douglas M. Leonard[4], Denah M. Appelt[5], Robert G. Nagele[1,3].

Affiliations

[1]Biomarker Discovery Center, New Jersey Institute for Successful Aging, Rowan University School of Osteopathic Medicine, Stratford, NJ 08084, USA
[2]Graduate School of Biomedical Sciences, Rowan University, Stratford, NJ 08084, USA
[3]Department of Geriatrics and Gerontology, Rowan University School of Osteopathic Medicine, Stratford, NJ 08084
[4]Department of Psychiatry, Rowan University School of Osteopathic Medicine, Stratford, NJ 08084, USA
[5]Philadelphia College of Osteopathic Medicine, Philadelphia, PA 19131, USA

Funding Disclosure
The authors wish to thank the Osteopathic Heritage Foundation (OHF) for supporting this project.

Figure 1. ELG, NKA, GAG, AS, MCK, JMD, CPH, CAJ, and CAD helped to harvest, process, and image tissue from animals.

Figure 2. ELG, NKA, GAG, AS, and CAD helped to harvest, process, and image tissue from animals.

Figure 3. ELG, NKA, GAG, AS, and CAD helped in the making of this graph.

Figure 4. ELG, NKA, GAG, AS, and CAD helped to harvest, process, and image tissue with help from DA.

Figure 5. ELG, NKA, GAG, AS, and CAD helped to harvest, process, and image tissue with help from DA.

Figure 6. ELG, NKA, GAG, AS, and CAD helped to harvest, process, and image tissue with help from DA.

Figure 7. We wish to thank Amanda S. Almon, M.F.A. C.M.I. from the Department of Art at the College of Communication and Creative Arts of Rowan University for the creation of **Figure 7.**

Chapter IV: The Heightened Vulnerability of the Pre-Adolescent & Elderly Populations to Anesthesia-Triggered Delirium is Linked to Increased Blood-Brain Barrier Permeability

Journal

This manuscript has been submitted for publication.

Authors

George A. Godsey[1,2]; Hana Choi[1]; Nimish K. Acharya, Ph.D.[3]; Mary C. Kosciuk, Ph.D.[2,3]; Robert G. Nagele, Ph.D.[2,3,4].

Affiliations

[1]Graduate School of Biomedical Sciences, Rowan University, Stratford, New Jersey, USA

[2]Biomarker Discovery Center, New Jersey Institute for Successful Aging, Rowan University School of Osteopathic Medicine, Stratford, New Jersey, USA

[3]Department of Geriatrics and Gerontology, Rowan University School of Osteopathic Medicine, Stratford, New Jersey, USA

[4]Durin Technologies, Inc., Mullica Hill, New Jersey, USA

Funding Disclosure

The authors wish to thank the Osteopathic Heritage Foundation for supporting this project.

Table 1. GAG & RGN were responsible for creating this table.

Figure 1. GAG & RGN were responsible for creating this figure.

Figure 2. GAG & RGN were responsible for creating this figure.

Figure 3. GAG & RGN were responsible for creating this figure.

Figure 4. GAG & RGN were responsible for creating this figure.

Figure 5. We wish to thank Amanda S. Almon, M.F.A. C.M.I. from the Department of Art at the College of Communication and Creative Arts of Rowan University for the creation of **Figure 5**.

Chapter V: Effects of Anesthetics and Select Agents on the Barrier Function of Human Brain Vascular Endothelial Cells *In Vitro*

Journal

This data has not been published.

Figure 1. GAG & RGN were responsible for creating this figure.

Figure 2. This figure was taken and modified from [33]:

> Wilhelm, I. and I.A. Krizbai, *In vitro models of the blood-brain barrier for the study of drug delivery to the brain.* Mol Pharm, 2014. **11**(7): p. 1949-63.

Figure 3. GAG & RGN were responsible for creating this figure.

Figure 4. GAG & RGN were responsible for creating this figure.

Figure 5. GAG & RGN were responsible for creating this figure.

Figure 6. GAG & RGN were responsible for creating this figure.

Figure 7. GAG & RGN were responsible for creating this figure.

Figure 8. GAG & RGN were responsible for creating this figure.

Figure 9. GAG & RGN were responsible for creating this figure.

Figure 10. GAG & RGN were responsible for creating this figure.

Figure 11. GAG & RGN were responsible for creating this figure.

Figure 12. GAG & RGN were responsible for creating this figure.

Figure 13. GAG & RGN were responsible for creating this figure.

Figure 14. GAG & RGN were responsible for creating this figure.

Figure 15. GAG & RGN were responsible for creating this figure.

Chapter VI: Administration of Lipoxin after LPS Insult Reduces Inflammation and Blood-Brain Barrier Permeability in Rats

Journal

This manuscript is being prepared for publication.

Authors

George A. Godsey[1,2]; Hana Choi[1]; Nimish K. Acharya, Ph.D.[3]; Mary C. Kosciuk, Ph.D.[2,3]; Ana R. Rodriguez[4]; Jean Walker[4]; Bernd W. Spur[4]; Kingsley Yin[4]; Robert G. Nagele, Ph.D.[2,3,5].

Affiliations

[1]Graduate School of Biomedical Sciences, Rowan University, Stratford, New Jersey, USA

[2]Biomarker Discovery Center, New Jersey Institute for Successful Aging, Rowan University School of Osteopathic Medicine, Stratford, New Jersey, USA

[3]Department of Geriatrics and Gerontology, Rowan University School of Osteopathic Medicine, Stratford, New Jersey, USA

[4]Department of Cell Biology, Rowan University School of Osteopathic Medicine, Stratford, New Jersey, USA

[5]Durin Technologies, Inc., Mullica Hill, New Jersey, USA

Funding Disclosure

The authors wish to thank the Osteopathic Heritage Foundation for supporting this project.

Table 1. GAG & RGN were responsible for creating this table.

Figure 1. GAG & RGN were responsible for creating this figure.

Figure 2. GAG & RGN were responsible for creating this figure.

Figure 3. GAG & RGN were responsible for creating this figure.

Figure 4. GAG & RGN were responsible for creating this figure.

Figure 5. GAG & RGN were responsible for creating this figure.

Figure 6. GAG & RGN were responsible for creating this figure.

Figure 7. GAG & RGN were responsible for creating this figure.

Figure 8. GAG & RGN were responsible for creating this figure.

Figure 9. GAG & RGN were responsible for creating this figure.

Figure 10. GAG & RGN were responsible for creating this figure.

Chapter VII: Conclusions

***No Attributions**